AD_____

AWARD NUMBER: W81XWH-04-1-0912

TITLE: Therapy of Prostate Cancer Using a Human Antibody Targeting the Type 1 Insulin-Like Growth Factor Receptor (IGF-IR)

PRINCIPAL INVESTIGATOR: Stephen R. Plymate

CONTRACTING ORGANIZATION: University of Washington
Seattle, WA 98195

REPORT DATE: September 2009

TYPE OF REPORT: Final

PREPARED FOR: U.S. Army Medical Research and Materiel Command
Fort Detrick, Maryland 21702-5012

REPORT DOCUMENTATION PAGE

Form Approved
OMB No. 0704-0188

1. REPORT DATE 01/Sep*/2009*	2. REPORT TYPE Final *	3. DATES COVERED 30 NOV 2004 - 29 AUG 2009

4. TITLE AND SUBTITLE
Therapy of Prostate Cancer Using a Human Antibody Targeting

the Type 1 Insulin-Like Growth Factor Receptor(IGF-IR)

5a. CONTRACT NUMBER
W81XWH-04-1-0912

5b. GRANT NUMBER
PC040364

5c. PROGRAM ELEMENT NUMBER

6. AUTHOR(S)
Stephen R. Plymate
Email: splymate@u.washington.edu

5d. PROJECT NUMBER

5e. TASK NUMBER

5f. WORK UNIT NUMBER

7. PERFORMING ORGANIZATION NAME(S) AND ADDRESS(ES)

University of Washington
Office of Sponsored Programs
4333 Brooklyn Ave. NE
Box 359472
Seattle, WA 98195-9472

8. PERFORMING ORGANIZATION REPORT NUMBER

9. SPONSORING / MONITORING AGENCY NAME(S) AND ADDRESS(ES)
U.S.Army Medical Research and
Material Command
Fort Detrick, Maryland
21702-5012

10. SPONSOR/MONITOR'S ACRONYM(S)

11. SPONSOR/MONITOR'S REPORT NUMBER(S)

12. DISTRIBUTION / AVAILABILITY STATEMENT
Approved for Public Release:distribution unlimited

13. SUPPLEMENTARY NOTES

14. ABSTRACT: During this funding period we have shown that inhibition of the type 1 IGF receptor with a fully human monoclonal antibody can delay prostate cancer growth in intact and castrate human xenograft mouse models. Further IGF-IR inhibition of IGF-IR greatly enhanced the effects of castration and docetaxel on prostate cancer. There was a significant effect on prostate cancer when growing in bone, especially in combination with Docetaxel. There was no evidence of significant treatment toxicity. The results of these preclinical studies have led to phase 1 and 2 clinical trials in each instance.

15. SUBJECT TERMS
Prostate Cancer, IGF-IR, monoclonal antibody

16. SECURITY CLASSIFICATION OF:			17. LIMITATION OF ABSTRACT	18. NUMBER OF PAGES	19a. NAME OF RESPONSIBLE PERSON
a. REPORT U	b. ABSTRACT U	c. THIS PAGE U	UU	72	USAMRMC
					19b. TELEPHONE NUMBER *(include area code)*

Table of Contents

Page

Introduction…….…….…….. 4

Body…….. 4-6

Key Research Accomplishments…….…….. 7

Reportable Outcomes……. 7-8

Conclusion…… 9

Introduction: : The insulin-like growth factor (IGF) system has been demonstrated to be involved in the pathogenesis and progression of prostate cancer. Specifically, it has been demonstrated to be a target to inhibit prostate epithelial transformation, proliferation, migration and be anti-apoptotic. Others and we have demonstrated that inhibition of signaling through the type 1 IGF tyrosine kinase receptor (IGF-IR) will inhibit prostate cancer growth and metastasis. Further, in the Preliminary data presented in this study, we show that the IGF-IR remains as a viable target therapy in primary prostate cancer as well as prostate cancer that has metastasized to bone. We have also shown, that the human IGF-IR antibody, A12, effectively decreases the growth of human prostate cells and xenografts *in vitro* and *in vivo*. The effectiveness of A12 results not only in its ability to inhibit the IGF-ligand/IGF-IR interaction but also to target the IGF-IR for lysosomal degradation. In addition, treatment with anti-IGF-IR agents in multiple murine studies has not appeared to result in significant toxicity. We have selected for this proposal two areas of clinical treatment that would improve patient outcomes. These include: 1) prolongation of time to emergence of androgen-independent disease following castration and 2) effective therapy of bone metastases. Based on this background we propose the **hypothesis** that: inhibition of the IGF-1R will 1) significantly prolong the time to progression to androgen-independent (AI) disease following castration and 2) decrease growth of osseous prostate cancer metastases lesions while the LuCaP 35 line forms primarily osteolytic lesions. Thus we think that these two cell lines most accurately reflect human disease and are appropriate for this **pre-clinical** study. In order to study these issues we have used a variety of animal models and human prostate xenografts. The results of these studies have been published in high quality journal.

Body:

Task 1: To determine whether inhibition of IGF-IR signaling by administration of antagonistic IGF-IR antibody increases time to recurrence of LuCaP 35 CaP xenograft following castration.

1.1 Determine if IGF-IR inhibition soon after castration can prolong time to emergence of androgen-independent (AI) prostate cancer. Months 1-12 (120mice)

a. Grow stock of LuCaP 35 sc in SCID mice

b. Implant 120 SCID mice sc with LuCaP 35

c. When tumors reach 150-200mm^3 castrate mice.

d. At 7 and 14 days after castration begin antibody injection 3x week for 14 days following the initiation of therapy. Control animals will receive two weeks of vehicle beginning 7 days after castration.

e. Follow animals with tumor measurements and PSA. When control tumors recur, sacrifice 20 animals from each group. Evaluate tumors for apoptosis, cell cycle, IGGF-IR expression.

d. Collate data and evaluate efficacy. Determine if alternative time points needed. Prepare data for publication.

1.2 Determine effectiveness of IGF-IR inhibition following tumor regrowth after castration. Months 6-18 (40 mice)

a. Implant 60 SCID mice with LuCap 35 sc.

b.When tumors reach 150-200mm^3 castrate mice.

c. When tumors recur, begin therapy with IGF-IR antibody 3x week for 6 weeks in treatment group and vehicle only in control group.

d. At six week time point post initiation of therapy sacrifice mice and begin evaluation of treated and untreated tumors.

e. Evaluate data and prepare reports and publications.

Task 1 accomplishments: This task was completed and demonstrated that treatment of mice with IGF-IR hmab for 2 weeks beginning either 1 or two weeks after castration resulted in an increase in time to recurrence after castration that was > 5-fold that seen with castration alone. These results have been published : Plymate, SR Haugk, K Coleman, I Woodke, L Vessella, R Nelson, PS Montgomery, RB Ludwig ,DL and Wu, JD. An Antibody Targeting the Type 1 Insulin-like Growth Factor Receptor Enhances the Castration-Induced Response in Androgen-Dependent Prostate Cancer: Clinical Cancer Research Clin Cancer Res. 2007 Nov 1;13(21):6429-39; Wu, JD Haugk, K Woodke, L Nelson, P, Coleman, I Plymate, SR. 2006 Interaction of IGF signaling and the androgen receptor in prostate cancer progression. J

Cell Biochem. 99:392-401.These complete references are in the appendices. Finally, the results of this task have led to an NIH funded clinical trial using IGF-IR hmab and castration as neoadjuvant therapy.

Task **2**. Determine influence of IGF-IR inhibition on growth of osteoblastic and osteolytic prostate cancer bone metastases.

2.1 Determine efficancy of IGF-IR antibody therapy on progression of osteolytic and osteoblastic metastases: Months 18 – 30 (80 mice)

a. Establish osseous tumor implants in SCID mice with LuCaP 23.1 and LuCaP 35 prostate cancer xenografts.

b. When xenografts are established in bone based on a serum PSA of 5-10 ng/nl begin therapy with the IGF-IR antibody 3 x a week for six weeks i.p. or vehicle control.

c. Perform bone densitometry as indicated.

d. At six weeks sacrifice all animals. Remove bone lesions, prepare slides and evaluate histologically as indicated in the Plan of the proposal body.

e. Evaluate data and prepare manuscripts for publication.

2.2 Determine the effects of castration and IGF-IR inhibition on progression of osseous metastases: Months 24-36 (120 mice)

a. Establish osseous xenograpfts in SCID mice for LuCaP 23.1 and LuCaP 35 prostate cancer xenografts.

b. Castrate all animals when PSA levels are between 5 and 10 ng/ml. IGF-IR antibody or vehicle control administration i.p 3 x a week will be begun either 7 or 14 days after castration and treatment continued for 2 weeks.

c. When there is evidence of tumor regrowth in the control group following castration, based on an increase in PSA, all animals will be sacrificed. Dexa bone densitometry will be performed prior to sacrifice. Following sacrifice the bone will be removed and prepared for immunohistochemistry and histomorphometry as described.

e. Evaluate and prepare data for publication.

f. Plan human phase 2 protocols assuming animal toxicity and human phase 1 trials have been successfully completed.

Task 2 accomplishments: These two tasks have been accomplished and show that the combination of IGF-IR inhibition with a monoclonal antibody either alone or in combination with docetaxel significantly inhibits human xenograft growth in an interosseous position. These results have been reported: Wu, DD , Haugk, K Coleman, I Woodke, L Vessella, RL, Nelson, PS, Montgomery, RB Ludwig, DL and Plymate, SR Antibodies Targeting the Type 1 Insulin-like Growth Factor Receptor Enhance the Activity of Docetaxel Against Androgen-independent Human Prostate Cancer. 2006 Clinical Cancer Res. 12:6153-60. The results of the interosseus tumors with castration and IGF-IR hmab could not be done because of failure of the tumor model.

Work Accomplished specifically accomplished during the Nov 2007 to Nov 2008 period:

During this reporting period we were able to show that following androgen ablation that there was a significant increase in IGFBP-5 on cDNA microarray analysis and this was confirmed by protein expression on IHC and Western blot. Furthermore, we demonstrated that the increase in BP-5 increased prostate epithelial cell proliferation by enhancing the activity of IGF-I on IGF-IR and that this activity could be inhibited by A12. This data was published:

Xu, C., Graf, L.F., Fazli, L., Coleman, I.M., Mauldin, D.E., Nelson, P.S., Gleave, M., Plymate, S.R., Cox, M.E., Torok-Storb, B.J., Knudsen, B.S. (2007) regulation of global gene expression in the bone marrow microenvironment by androgen: androgen ablation increases insulin-like growth factor binding protein - 5 expression Prostate, 67, 1621-1629.

Modified SOW for period 11/08 to 08/09

1.2 Determine the effects of A12 on 2 LM subunit expressing M12 xenografts in SCID mice. Assuming a 90% tumor take rate we will use 12 animals/ group. 2 x 10^6 tumor cells will be injected sc.

Tumor volume will followed until the tumors have reached a volume of 200 mm^3 at which time A12 will be injected i.p. at a dose of 40 mg/kg for 4 weeks in treated groups or a similar amount of isotype IgG in the control group. Mice will be followed for 4 weeks with tumors measured weekly. Mice will be treated according to our University of Washington IACUC protocol and DOD approved protocols. At the end of the four week period of time mice will be euthanized, tumors harvested and portions processed for IHC, Western blot, flow cytometry, culture, and RNA analysis. If not enough tissue is available for each of these processes, culture, paraffin blocks, and RNA will have priority.

2.2 Determine the effects of castration and IGF-IR inhibition on progression of osseous metastases: Months 24-36 (120 mice)

a. Establish osseous xenografts in SCID mice for LuCaP 23.1 and LuCaP 35 prostate cancer xenografts.

b. Castrate all animals when PSA levels are between 5 and 10 ng/ml. IGF-IR antibody or vehicle control administration i.p 3 x a week will be begun either 7 or 14 days after castration and treatment continued for 2 weeks.

c. When there is evidence of tumor regrowth in the control group following castration, based on an increase in PSA, all animals will be sacrificed. Dexa bone densitometry will be performed prior to sacrifice. Following sacrifice the bone will be removed and prepared for immunohistochemistry and histomorphometry as described.

Task 1 Research accomplishments: During this funding period we were able to determine that alteration in laminin beta 2 production during cell senescence markedly enhance prostate cancer growth in the subcutaneous position of nude mice. Furthermore these cells increased their expression of IGF-IR and could be inhibited by antibodies to the IGF-IR, A12, and in vitro could be inhibited by antibodies to beta 1 integrin.

In additional studies we demonstrated that the alterations in extracellular matrices markedly altered androgen regulated gene expression of prostate cancer cells that are in contact with these matrices.

These results have been published in part in the following papers:

Eyman D, Damodarasamy M, Plymate SR, Reed MJ. CCL5 secreted by senescent aged fibroblasts induces proliferation of prostate epithelial cells and expression of genes that modulate angiogenesis.J Cell Physiol. 2009 Aug;220(2):376-81.PMID: 19360811

Sprenger CC, Drivdahl RH, Woodke LB, Eyman D, Reed MJ, Carter WG, Plymate SR.Senescence-induced alterations of laminin chain expression modulate tumorigenicity of prostate cancer cells. Neoplasia. 2008 Dec;10(12):1350-61.PMID: 19048114

2.2 Determine the effects of castration and IGF-IR inhibition on progression of osseous metastases: Months 24-36 (120 mice) Task 2 was completed for LuCap 23.1. However the model for LuCaP 35 failed to grow. Lucap 23.12 growth in bone was marked inhibited by A12 and castration.

Key Research Accomplishments:

- Human monoclonal antibodies directed against the IGF-IR used as a single agent inhibit human prostate cancer xenograft growth in a preclinical mouse model.
- Human monoclonal antibodies directed against the IGF-IR markedly enhance the effects of docetaxel on sc and intraosseous tumor growth.
- Human monoclonal antibodies directed against the IGF-IR markedly enhance the effects of castration on prostate cancer growth.

Reportable outcomes:

Papers:

Wu, DD , Haugk, K Coleman, I Woodke, L Vessella, RL, Nelson, PS, Montgomery, RB Ludwig, DL and Plymate, SR Antibodies Targeting the Type 1 Insulin-like Growth Factor Receptor Enhance the Activity of Docetaxel Against Androgen-independent Human Prostate Cancer. 2006 Clinical Cancer Res. 12:6153-60

Wu, JD Haugk, K Woodke, L Nelson, P, Coleman, I Plymate, SR. 2006
Interaction of IGF signaling and the androgen receptor in prostate cancer progression. J Cell Biochem. 99:392-401

Plymate, SR Haugk, K Coleman, I Woodke, L Vessella, R Nelson, PS Montgomery, RB Ludwig ,DL and Wu, JD. An Antibody Targeting the Type 1 Insulin-like Growth Factor Receptor Enhances the Castration-Induced Response in Androgen-Dependent Prostate Cancer: Clinical Cancer Research Clin Cancer Res. 2007 Nov 1;13(21):6429-39

Xu C, Graf LF, Fazli L, Coleman IM, Mauldin DE , Nelson PS, Gleave M, Plymate SR, Cox ME, Torok-Storb BJ, Knudsen BS. 2008 Regulation of Global Gene Expression in the Bone Marrow Microenvironment by Androgen: Androgen Ablation Increases Insulin-like Growth Factor Binding Protein - 5 Expression Prostate: 67:1621-9.

Bentov I, Narla G, Schayek H, Akita K, Plymate SR, Leroith D, Friedman SL, Werner H. Insulin-like growth factor-1 regulates KLF6 gene expression in a p53-dependent manner. Endocrinology. 2008 Jan 3; [Epub ahead of print]

Sprenger CC, Drivdahl RH, Woodke LB, Eyman D, Reed MJ, Carter WG, Plymate SR.Senescence-induced alterations of laminin chain expression modulate tumorigenicity of prostate cancer cells. Neoplasia. 2008 Dec;10(12):1350-61.PMID: 19048114

Schayek, H., Haugk, K., Sun, S., True, L.D., Plymate, S.R., Werner, H. 2009 Tumor suppressor BRCA1 is expressed in prostate cancer and controls insulin-like growth factor-I receptor (IGF-IR) gene transcription in an androgen receptor-dependent manner. Clin Cancer Res. 2009 Mar 1;15(5):1558-65. Epub 2009 Feb 17.PMID: 19223505

Eyman D, Damodarasamy M, Plymate SR, Reed MJ. CCL5 secreted by senescent aged fibroblasts induces proliferation of prostate epithelial cells and expression of genes that modulate angiogenesis.J Cell Physiol. 2009 Aug;220(2):376-81.PMID: 19360811

Sprenger CC, Haugk K, Sun S, Coleman I, Nelson PS, Vessella RL, Ludwig DL, Wu JD, Plymate SR.Transforming Growth Factor-{beta}-Stimulated Clone-22 Is an Androgen-Regulated Gene That Enhances Apoptosis in Prostate Cancer following Insulin-Like Growth Factor-I Receptor Inhibition. Clin Cancer Res. 2009 Dec 15;15(24):7634-7641. Epub .PMID: 19996218

Research Grants:
NIH-NCI PO1 CA 85859 - Project 3 07/01/2009 – 06/30/2014
Interaction of Androgens and IGF in Prostate Cancer Metastases.

This study is to determine the role of genes co-stimulated by IGF-1 and the androgen receptor in prostate cancer metastasis
Paul Lange, MD-Program Director
PI- S. Plymate 2.4 months%
Current year budget: $253,000

Veterans Affairs Merit Review 12/1/09-11/30/14
Mechanisms of Progression to Castrate Resistant Prostate Cancer
This study will determine have androgen receptor splice variants contribute to the progression of prostate cancer
PI-S. Plymate 2.4 mo
Current year budget $ 150,000

NIH-NCI U-54
Plymate –PI 3 mo
Prostate Tumor Microenvironment
2006-2011
$574,000/year –Direct costs

NIH- SPORE- Program –
Plymate PI Project 2 (2 months)
IGF-IR and Androgen Receptor in Prostate Cancer Progression
2007-2012
$168,000/yr-

Imclone Systems
Effects of Castration and IGF-IR Inhibition on Prostate Cancer
2009-2011
$140,000/yr

Conclusions:
Human monoclonal antibodies against the IGF-IR are effective as single agents in prostate cancer but are most effective when used in combination with chemotherapy or androgen ablation.

References: in text

Combined *In vivo* Effect of A12, a Type 1 Insulin-Like Growth Factor Receptor Antibody, and Docetaxel against Prostate Cancer Tumors

Jennifer D. Wu,[1] Kathy Haugk,[2] Ilsa Coleman,[3] Lillie Woodke,[1] Robert Vessella,[2,4] Peter Nelson,[3] R. Bruce Montgomery,[1] Dale L. Ludwig,[5] and Stephen R. Plymate[1,2]

Abstract

Purpose: A human type 1 insulin-like growth factor receptor antibody (A12) has been shown to effectively inhibit human xenograft tumor growth, including androgen-dependent and androgen-independent prostate tumors. Docetaxel, either as a single agent or combined with others, has shown a survival benefit in prostate cancer patients. Based on these data, we investigated the combined *in vivo* effect of A12 and docetaxel on human androgen-independent and osseous prostate tumor growth.

Experimental Design: To study human androgen-independent prostate cancer model, LuCaP35V tumors were implanted s.c. into castrated severe combined immunodeficient mice. When tumors reached about 100 mm^3, animals were treated with vehicle control docetaxel (10 or 20 mg/kg) and docetaxel in combination with A12 (40 μg/kg) for 4 weeks. To study human osseous prostate cancer model, LuCaP 23.1 tumors were implanted intratibiae. When serum prostate-specific antigen reached 5 to 10 ng/mL, treatments were initiated.

Results: A12 markedly augmented the inhibition of docetaxel on tumor growth. When docetaxel is combined with A12, the inhibition of tumor growth continued after treatment cessation, which was associated with continued apoptosis and decreased proliferation of tumor cells. Gene expression profiles indicated that the posttreatment suppression of tumor growth may be due to enhanced negative regulation of cell cycle progression – and/or cell survival – associated genes, some of which have been shown to induce resistance to docetaxel.

Conclusions: Our findings suggest that targeting type 1 insulin-like growth factor receptor can enhance the therapeutic effect of docetaxel on advanced prostate cancer. Our findings also suggest a potential mechanism to improve the treatment efficacy of docetaxel in prostate cancer.

Inhibition of type 1 insulin-like growth factor receptor (IGF-IR) signaling has been proposed as a potential means of optimizing anticancer therapy in a number of tumor systems (1–3). We have previously shown that interrupting the function of IGF-IR using the human IGF-IR monoclonal antibody A12 markedly decreases tumor size in human xenograft models of androgen-dependent and androgen-independent prostate cancer (4). In addition, blocking IGF-IR activation with A12 has been shown to induce cell cycle G_1 arrest in androgen-dependent prostate tumors and G_2-M arrest in androgen-independent prostate tumors (4). Therefore, inhibition of IGF-IR signaling with A12 might enhance or suppress the activity of cell cycle–specific chemotherapy if transition to cell cycle checkpoints is blocked. Because tumor recovery from radiation and chemotherapy involves activation of the IGF-IR, A12 may also be an attractive adjunct to these modalities (5).

Docetaxel, a member of the taxane family, is one of the newer potent anti–solid tumor agents currently undergoing extensive laboratory and clinical investigations (6). Docetaxel is a microtubulin active drug that causes cancer cells to arrest at the G_2-M cell cycle transition and ultimately to undergo apoptosis (7, 8). The antimitotic mechanisms of docetaxel are not fully understood; yet, studies have shown that docetaxel induces expression of tumor suppressor gene *p53* and cyclin-dependent kinase inhibitor p27/Kip-1 and phosphorylation of the antiapoptotic protein bcl-2 (9, 10). Clinical trials have shown that docetaxel has significant activity against androgen-independent prostate cancers (11, 12). It is the only drug to date shown to improve survival in patients with androgen-independent prostate cancer (13, 14). Although significant, the median gain in life expectancy in patients with androgen-independent prostate cancers treated with docetaxel is only 2 to 3 months (15). Some phase I studies have suggested that docetaxel in combination with other tumor-targeting cytotoxic

Authors' Affiliations: [1]Department of Medicine, University of Washington; [2]Veterans Affairs Puget Sound Health Care System; [3]Fred Hutchinson Cancer Research Center; [4]Departments of Urology and Immunology, University of Washington, Seattle, Washington; and [5]ImClone Systems, New York, New York

Received 2/23/06; revised 7/11/06; accepted 7/27/06.

Grant support: NIH grant PO1-CA85859 (S.R. Plymate), Veterans Affair Research Program (S.R. Plymate), Fred Hutchinson Cancer Research Center Consortium Grant (S.R. Plymate), DAMD17-03-2-033 (P.S. Nelson), Pacific Northwest Prostate Cancer Specialized Programs of Research Excellence (P.S. Nelson), and Department of Defense New Investigator's Award W81XWH-04-1-0577 (J.D. Wu), and NIH Temin Award 1K01CA116002 (J.D. Wu).

The costs of publication of this article were defrayed in part by the payment of page charges. This article must therefore be hereby marked *advertisement* in accordance with 18 U.S.C. Section 1734 solely to indicate this fact.

Requests for reprints: Jennifer D. Wu, Department of Medicine, University of Washington, Box 359625, Seattle, WA 98104. Phone: 206-341-5349; Fax: 206-341-5302; E-mail: wuj@u.washington.edu.

doi:10.1158/1078-0432.CCR-06-0443

agents, such as calcitriol, may extend life expectancy much further (12).

Because the IGF-IR signaling pathways are important in tumor growth and also are suggested as one of the possible mechanisms by which tumor cells can survive taxane treatment (5), we postulated that the IGF-IR would be a potential therapeutic target as combined therapy with docetaxel for advanced prostate cancer. In the current study, we tested whether the addition of the IGF-IR antibody A12 would augment or inhibit the activity of docetaxel using two established human prostate tumor xenograft models: the androgen-independent model LuCaP 35V and the osseous model LuCaP 23.1 (16).

Materials and Methods

Anti-IGF-IR antibody and docetaxel. A12 is a fully human antibody antagonist to the human IGF-IR. The generation and characterization of A12 has been previously described (3). Docetaxel was purchased from Aventis Pharmaceuticals (Bridgewater, NJ).

In vivo *study of AI LuCaP 35V tumors.* Tumor bits (20-30 mm^3) of human androgen-independent prostate tumor xenograft LuCaP 35V were implanted s.c. into 6-week-old castrated severe combined immunodeficient mice as previously described (4). Fifty castrated mice were used in this study. When the implanted tumor was observed to reach a volume of ~100 mm^3, animals were randomized into five groups (10 mice per group). Group 1 animals received human IgG treatment and were designated as controls. Group 2 animals received docetaxel treatment at a dose of 10 mg/kg. Group 3 animals received docetaxel treatment at a dose of 20 mg/kg. Group 4 animals received treatment of 10 mg/kg docetaxel and 40 mg/kg A12. Group 5 animals received treatment of 20 mg/kg docetaxel and 40 mg/kg A12. All treatments were given i.p. Docetaxel was given once a week. A12 was given thrice a week. All animals were treated for 4 weeks and monitored for additional 4 weeks before euthanization. Tumors were measured twice weekly. Tumor volume was estimated by the formula: volume = $L \times W^2/2$. Animals were weighed twice a week. Blood samples were collected from orbital sinus weekly. Serum was separated, and prostate-specific antigen (PSA) level was determined using the IMx Total PSA Assay (Abott Laboratories, Abott Park, IL). Bromodeoxyuridine (BrdUrd) was injected into the tumors 1 hour before the animals were euthanized for evaluation of *in vivo* tumor cell proliferation rate.

Following our University of Washington Institutional Animal Care and Use Committee–approved protocol, animals in the control group were euthanized at an earlier time point when tumors reached a volume of 1,000 mm^3. After euthanization, tumors were collected and halved. A portion of the tumors were fixed in 10% neutral buffer formalin and embedded in paraffin. The remaining portion of the tumors was separated into single cells mechanically by mincing and filtering through 70-μm nylon sieves.

Apoptosis and cell cycle assay. Apoptosis and cell cycle were measured by terminal deoxynucleotidyl transferase–mediated nick end labeling assay and propidium iodide staining using the ApoDirect kit (BD Biosciences, San Jose, CA) as previously described (4). Cells (1×10^6) from the single-cell suspension of tumors were fixed with 10% neutral buffer formalin followed by 70% ethanol at −20°C for 30 minutes. After several washes, cells were permeabilized with 0.1% Triton X-100 and incubated with FITC-conjugated dUTP and terminal deoxynucleotidyl transferase enzyme at 37°C for 1 hour, followed by an incubation with propidium iodide/RNase buffer (100 μg/mL of propidium iodide, 50 μg/mL RNase) at room temperature for 60 minutes. Samples were analyzed by flow cytometry using a BD FACScan. Data were analyzed with CellQuest^{PRO} software.

Evaluation of BrdUrd incorporation. Five-micrometer tumor sections were deparaffinized and rehydrated. Antigens were retrieved with 0.01 mol/L citric acid (pH 6) at 95°C for 10 minutes. After quenched endogenous peroxidase activity and blocked with 1.5% goat serum, sections were incubated with mouse anti-BrdUrd antibody (1 μg/mL) or control mouse IgG for 1 hour followed by sequential incubation at room temperature with biotinylated goat anti-mouse IgG for 30 minutes, peroxidase-labeled avidin for 15 minutes (Santa Cruz Biotechnology, Santa Cruz, CA), and diaminobenzidine/hydrogen peroxide chromogen substrate (Vector Laboratories, Burlingame, CA). Sections were counterstained with hematoxylin (Sigma, St. Louis, MO) and mounted with permount (Fisher Scientific, Fair Lawn, NJ). Slides were examined under a Zeiss Microscope, and digital images were obtained. Ten random views were evaluated from each section. Rate of BrdUrd uptake was calculated by the number of BrdUrd-positive nuclei divided by the total number of nuclei.

Androgen-dependent intraosseous study. Osseous LuCaP 23.1 human prostate tumor bits (20-30 mm^3) were mechanically digested as previously described (17). Viable LuCaP 23.1 cells ($2\text{-}5 \times 10^5$) were injected into the tibiae of 6- to 8-week-old severe combined immunodeficient mice. Twenty-one mice randomized into three groups were used for this study. After tumor injection, serum PSA was monitored weekly. Treatment started when serum PSA level reached 5 to 10 ng/mL, an indication of tumor growth. Group 1 received control vehicle saline buffer. Group 2 received 20 mg/kg of docetaxel i.p. once a week for 4 weeks. Group 3 received 20 mg/kg of docetaxel once a week and 40 μg/kg of A12 i.p. thrice a week for 4 weeks. To determine whether the response to treatment was osteoblastic or osteolytic, bone density was obtained by Dexa-scan and X-rays of the animals at the end point of all treatments.

Measurement of serum A12. Serum A12 was quantitated using a human IgG binding ELISA. Goat anti-human IgG (Sigma) was immobilized in 96-well plates and blocked with 1% skim milk/PBS. Mouse serum samples were tittered onto the plates, and bound human IgG was detected with horseradish peroxidase–conjugated goat anti-human IgG secondary antibody (Jackson ImmunoResearch, Bar Harbor, MN). Signal was visualized using TMB detection reagents (KPL, Guithersburg, MD), and absorbance was measured at 405 nm. A12 were quantitated using a standard curve.

Statistical analysis. Differences among treatment groups were assessed by a one-way ANOVA. Statistical significance between means of two paired groups was assayed using Student's t test with Bonferroni correction; 95% confidence interval ($P < 0.05$) was considered significant. Stepwise regression analysis for calculating tumor growth rate was done using Statview 5.0 (Calabasas, CA).

cDNA microarray analysis. Custom Prostate Expression Data Base cDNA microarrays were constructed as previously described using clones derived from the Prostate Expression Data Base, a sequence repository of human prostate expressed sequence tag data available to the public (http://www.pedb.org; refs. 4, 18, 19). The inserts of individual cDNA clones were amplified by PCR, purified, and spotted in duplicates onto glass microscope slides (Gold Seal, BD Biosciences) with GeneMachine OmniGrid 100. Methods of labeling with Cy3 and Cy5 fluorescent dyes, hybridization to the microarray slides, and array processing were as described (20).

Five tumors were pooled in each experimental group. RNA was prepared from the pooled tumors using Trizol (Invitrogen, San Diego, CA). cDNA was synthesized using the Ambion MessageAmp II Amplification kit. Hybridization probes were labeled, and quality control of the array experiments was done as described previously (20). Differences in gene expression associated with treatment groups were determined using the SAM procedure (http://www-stat.stanford.edu/_tibs/SAM/) with a false discovery rate of <0.05% considered significant (21).

Real-time reverse transcription-PCR. A standard PCR fragment of the target cDNA was purified. A series of dilutions of the standards from 10 ng/μL to 10^{-3} pg/μL were used for real-time reverse transcription-PCR to generate the standard curves. One microgram of total RNA from each group of pooled tumor was used for first-strand cDNA synthesis using Superscript First Strand Synthesis System (Invitrogen). Real-time reverse transcription-PCR was done in 20 μL of reaction mixture consisted of

1 μL of first strand of cDNA, specific primers sets, and Lightcycler FastStart DNA Master Plus SYBR Green using a Roche Lightcycler following the manufacturer's protocol (Roche, Nutley, NJ). Reverse transcription-PCR products were subjected to melting curve analysis on Lightcycler software v3.5. The amplicon sizes were confirmed by agarose gel electrophoresis. Each sample was assayed in duplicate.

Results

IGF-IR antibody A12 augments the inhibitory effect of docetaxel on tumor growth. Two doses of docetaxel were chosen for this study. The dose of 20 mg/kg had been shown in our preliminary studies to be a dose that had maximum suppression on tumor growth without significant toxicity to mice. A higher dose (30 mg/kg) did not show a greater rate of tumor suppression but did result in significant toxicities to animals, including weight loss and mortality (data not shown). We specifically chose 10 mg/kg as a suboptimal dose to show synergy with A12 in tumor suppression. The optimal dose of 40 μg/kg of A12 has been previously determined (3).

The LuCaP 35V xenograft tumors grew aggressively with an average increase in volume of 362.0 ± 72.0 mm^3/wk in animals that received control human IgG (Fig. 1A); all animals had to be sacrificed within 3 weeks after treatment initiation, due to tumor volumes exceeding 1,000 mm^3. When animals were treated with 40 μg/kg A12 alone, tumor growth rate was reduced to 192.7 ± 35.6 mm^3/wk during treatment. However, after stopping treatment, 50% of the animals have to be sacrificed at follow-up week 2, and all animals have to be sacrificed at follow-up week 4, due to recovery of tumor growth. When animals were treated with a suboptimal dose of docetaxel (10 mg/kg), tumor growth rate was reduced to an average of 29.6 ± 6.1 mm^3/wk. When treatment included 10 mg/kg of docetaxel in combination with A12, tumor growth rate was further reduced significantly to an average of 7.9 ± 1.0 mm^3/wk (Fig. 1B; $P < 0.01$). In addition, after termination of all therapy, the inhibitory effect of docetaxel combined with A12 persisted, whereas tumor growth recurred significantly in animals that had received docetaxel alone (Fig. 1B; $P < 0.01$).

When animals were treated with a high dose of docetaxel (20 mg/kg), tumor growth was significantly inhibited during the 4-week treatment period compared with 10 mg/kg of docetaxel (Fig. 1B; $P < 0.001$). The combination of 20 mg/kg of docetaxel with A12 did not significantly reduce tumor volume compared with 20 mg/kg docetaxel alone during the 4-week treatment period. However, following treatment cessation, tumor growth significantly recurred at an average rate of 32.0 ± 16.1 mm^3/wk in animals that had received 20 mg/kg docetaxel alone ($P < 0.01$), whereas there was no tumor growth in animals that had received 20 mg/kg of docetaxel combined with A12. The posttreatment suppression of tumor growth persisted for at least 4 weeks to the point when the study was terminated. Together, these results suggest that, for a given dose of docetaxel, combined treatment with A12 can enhance the inhibitory effect of docetaxel on tumor growth during treatment and after treatment follow-ups.

PSA is a commonly used clinical variable to assess prostate tumor growth (21, 22). We, thus, measured serum levels of PSA in animals during and after the treatments. As shown in Fig. 1C, except in animals treated with 10 mg/kg of docetaxel alone, no significant change in serum levels of PSA was seen during the 4-week treatment in the other groups of animals, reflecting the suppressed tumor growth. After treatment termination, serum PSA levels significantly increased in animals treated with docetaxel alone ($P < 0.05$) and remained unchanged or even decreased in animals treated with docetaxel in combination

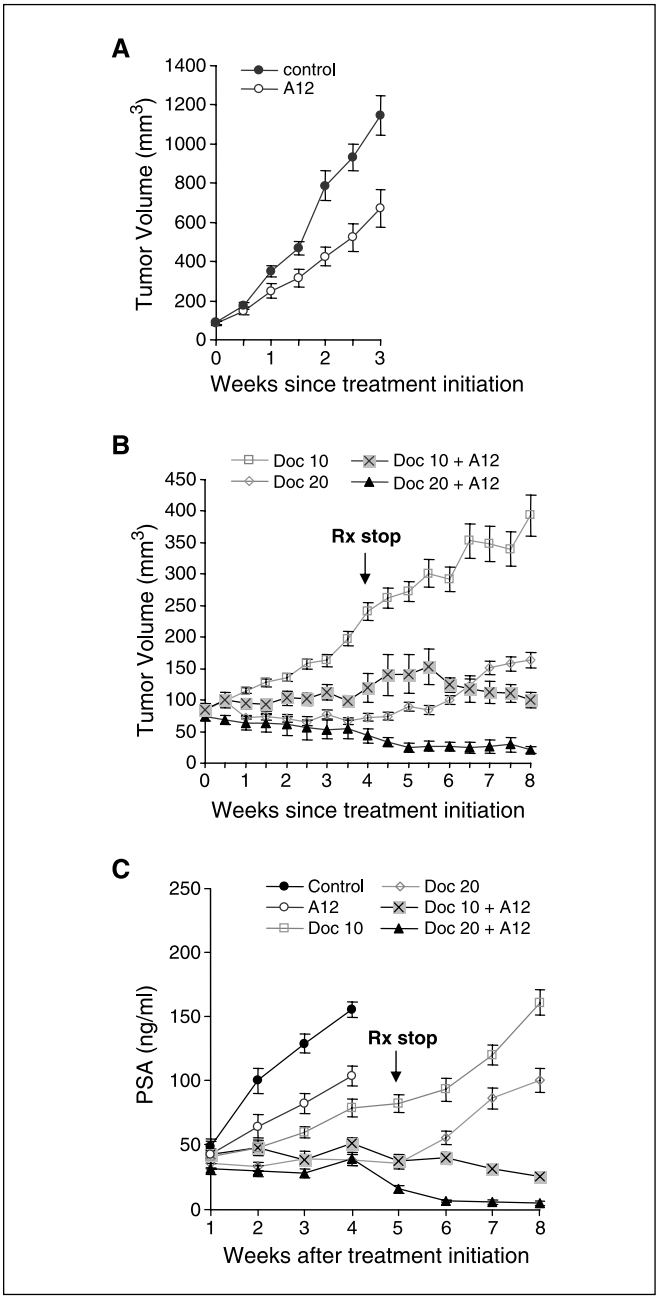

Fig. 1. Effects of A12, docetaxel, and docetaxel combined with A12 (40 mg/kg) on LuCaP 35V xenograft tumor growth during and posttreatment. Tumor bits of LuCaP 35V were implanted s.c. into castrated severe combined immunodeficient mice and allowed to grow to ~100 mm^3. Groups of animals were treated with control vehicle saline buffer, docetaxel (10 or 20 mg/kg body weight), or docetaxel and A12 (40 μg/kg) thrice a week. All treatment stopped at week 4, and animals were monitored for posttreatment response for four more weeks. Tumor size was measured twice a week, and tumor volume was estimated by the formula: volume = $L \times W^2/2$. *A,* tumor growth in animals treated with control human IgG or A12. *B,* tumor growth in animals during and after treatment (*Rx*) of 10 mg/kg of docetaxel (*Doc 10*), 20 mg/kg of docetaxel (*Doc 20*), Doc 10 + A12, and Doc 20 + A12. *C,* serum PSA levels reflect the differences in tumor growth. Serum was separated from blood by centrifugation, and levels of PSA were determined using the IMx Total PSA assay. Points, mean; bars, SE.

with A12 at experiment end points. These data are in agreement with the continued posttreatment inhibition of tumor growth in animals that had received docetaxel combined with A12.

Induction of apoptosis by docetaxel in combination with A12. We investigated the effect of docetaxel combined with A12 on cell cycle and cell survival after treatment cessation using terminal deoxynucleotidyl transferase–mediated nick end labeling assay and propidium iodide staining. In animals that had received A12 or docetaxel alone, no apoptosis was found in tumors at 4 weeks posttreatment (Fig. 2A). Instead, following treatment cessation, tumor growth recurred, and tumor cells proceeded to a normal control cell cycle index of G_1, S, and G_2-M phases, respectively, at 71.0 ± 1.4%, 6.2 ± 2.5%, and 21.0 ± 3.7% in the majority of animals (88-100%). On the contrary, in animals that had received docetaxel in combination with A12, tumor cells failed to proceed to normal cell cycle progression after therapy stopped; apoptosis or preapoptotic G_0-G_1 cell cycle arrest was found in tumors in a significant percentage of animals (77.8-100%). The average apoptotic events in these apoptosis-positive tumors occurred at an index of 15.0 ± 4.3% (data not shown).

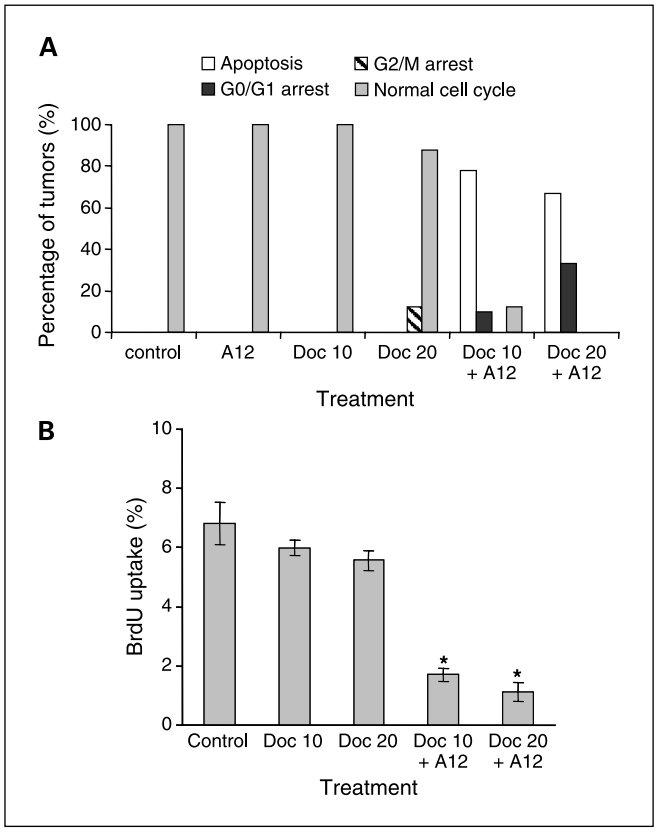

Fig. 2. *A,* cell cycle activity and apoptosis in percentage of tumors in each treatment group at the time of animal euthanization. Data showing posttreatment normal cycle progression with no apoptosis in tumors treated with docetaxel or A12 alone and apoptosis in tumors treated with docetaxel in combination with A12. Single-cell suspension of the tumor cells (1×10^6) were fixed and permeabilized for terminal deoxynucleotidyl transferase – mediated nick end labeling assay and propidium iodide staining as described in Materials and Methods. Apoptosis is shown by FITC-conjugated dUTP incorporation based on terminal deoxynucleotidyl transferase – mediated nick end labeling assay. Results were analyzed using a BD FACScan and CellQuest^{Pro} software. *B,* BrdUrd labeling showing significant posttreatment inhibition in cell proliferation in tumors treated with docetaxel in combination with A12 (*Doc + A12*). BrdUrd was injected into the tumors 1 hour before animals were euthanized. One-quarter portion of the tumor was fixed, embedded in paraffin, and sectioned for BrdUrd incorporation analysis by immunohistochemistry using the anti-BrdUrd antibody. Rate of BrdUrd uptake is calculated by the number of BrdUrd-positive nuclei divided by the total number of nuclei at ×200 magnification. Ten fields were observed per slide. Columns, mean; bars, SE.

Enhanced inhibition of cell proliferation by docetaxel in combination with A12. To further evaluate posttreatment tumor cell proliferation, paraffin sections of tumors were stained with anti-BrdUrd antibody. No significant difference in posttreatment BrdUrd uptake in tumors was found between docetaxel-treated animals and animals in the control group (Fig. 2B). A significant suppression in posttreatment BrdUrd uptake was shown in animals that had received combined treatment of docetaxel and A12 (Fig. 2B; $P < 0.01$). These data are consistent with the above observations of cell cycle and apoptosis, suggesting that A12 significantly enhanced the cytotoxic effects of docetaxel and, in turn, reduced tumor cell survival and proliferation.

Differential regulation of gene expression in tumors treated with docetaxel combined with A12 versus docetaxel alone. To determine potential mechanisms for the markedly enhanced effect of docetaxel by A12, we first examined IGF-IR expression in all harvested tumors by immunohistochemistry and flow cytometry analysis. There was no difference in surface IGF-IR expression among all the treatment groups or compared with the control group (data not shown). This suggests that the enhanced effect of docetaxel by A12 is unlikely, or in part, due to A12 induced down-regulation of IGF-IR expression, which is consistent with our previous observation in the LuCaP 35V xenografts (4). We next compared differences in posttreatment gene expression in tumors from animals that had received 20 mg/kg of docetaxel and 20 mg/kg of docetaxel combined with A12, using cDNA microarray analyses. Based on SAM analyses, 49 genes were identified as differentially expressed in tumors that received combined treatment of docetaxel and A12 compared with those received docetaxel alone, with >2-fold change and <10% false discovery rate (data not shown). Because the effects of docetaxel and docetaxel combined with A12 on tumors showed differences in apoptosis and cell proliferation, we have since identified 13 of the 49 genes that are potentially involved in regulation of apoptosis or cell cycle (Table 1). All 13 genes were at least 2-fold different between the two treatments and had a false discovery rate of <0.02%. Nine genes were down-regulated, and four genes were up-regulated in the docetaxel combined with A12-treated tumors compared with docetaxel alone–treated tumors. We validated these expression differences in selected genes by real-time reverse transcription-PCR and compared their expression to which in tumors with A12 treatment alone (Fig. 3).

Of the down-regulated genes, *TUBB* and *BIRC5* are of particular interest. Overexpression of *TUBB* has been shown to result in resistance to docetaxel (23); increased expression of *BIRC5* (*survivin*) has been shown to be associated with aggressive prostate cancer and resistance to antiandrogen therapy (24, 25). Here, we show that A12 treatment alone down-regulated TUBB and survivin expression, which may account for possible mechanisms of A12 augmenting the effect of docetaxel. Furthermore, *TUBB* is an IGF-IR–regulated gene that is involved with IGF-IR–mediated transformation (26). Of the four up-regulated genes, *IGFBP3* has been shown to inhibit IGF ligand signaling as well as to induce apoptosis in prostate tumor cells in a ligand-dependent manner (27–30).

Posttreatment serum levels of A12. We measured posttreatment serum levels of A12 in animals that had received

Table 1. Posttreatment differential gene expression in docetaxel + A12–treated tumors compared with docetaxel alone–treated tumors

HUGO	Name	GO function	Fold change	False discovery rate (%)
Down-regulated genes				
CDC2	Cell division cycle 2	Cytokinesis; mitosis	3.0	≤0.02
CDC6	CDC6 cell division cycle 6 homologue	Negative regulation of cell proliferation	2.2	≤0.02
CCNA2	Cyclin A2	Regulation of CDK activity	2.1	≤0.02
MYBL2	V-myb myeloblastosis viral oncogene homologue (avian)-like 2	Antiapoptosis; development; regulation of cell cycle	3.2	≤0.02
TUBB	Tubulin β polypeptide	Microtubule-based movement taxane resistance	2.3	≤0.02
K-Alpha-1	Tubulin α ubiquitous	Microtubule-based movement taxane resistance	2.5	≤0.02
BIRC5	Baculoviral IAP repeat-containing 5 (survivin)	Antiapoptosis	2.5	≤0.02
CDC25B	Cell division cycle 25B	Positive regulation of cell proliferation	2.0	≤0.02
MYC	V-*myc* myelocytomatosis viral oncogene homologue (avian)	Cell cycle arrest	2.5	≤0.02
Up-regulated genes				
TOB1	Transducer of ERBB21	Negative regulation of cell proliferation	2.2	≤0.02
CCNG2	Cyclin G2	Cell cycle checkpoint	2.1	≤0.02
IGFBP3	IGF binding protein 3	Regulation of cell growth, proapoptotic	2.0	≤0.02
BIRC3	Baculoviral IAP repeat-containing 3	Antiapoptosis; cell surface receptor–linked signal transduction	2.2	≤0.02

docetaxel combined with A12. Serum A12 levels declined 100-fold 2 weeks after treatment cessation (Fig. 4A). Serum A12 was detected only at a very low level in animals at posttreatment week 4 (Fig. 4A). These data suggest that posttreatment serum residual A12 may in part contribute to the prolonged inhibition of tumor growth.

Pharmacotoxicity evaluation. Although A12 has >95% cross-reactivity with murine IGF-IR,[6] no abnormal daily activity or behavior changes were apparent in animals treated with combined reagents or docetaxel alone compared with control tumor bearing. No significant effect on kidney cells was observed in any treatment group by both cell cycle and apoptosis assays (data not shown). No significant change in body weight was observed among treatment groups (Fig. 4B). These observations suggest that combined treatment of docetaxel and A12 did not display significant toxicity in animals.

A12 enhances the inhibitory effects of docetaxel on osseous human prostate cancer xenografts. We further investigated how the combined treatment of docetaxel and A12 would affect prostate tumor growth in a bone environment, using the established osseous prostate cancer xenograft model LuCaP23.1 (17). During treatment, docetaxel alone or docetaxel combined with A12 significantly inhibited LuCaP 23.1 tumor growth as reflected by suppression of serum PSA levels (Fig. 5A), with no significant difference between the two treatments. However, after treatment cessation, serum PSA began to increase significantly in animals that had been treated with docetaxel alone, indicating a regrowth of the tumor, whereas a continued suppression of serum PSA level was shown in animals that received combined treatment, indicating a prolonged period of posttreatment tumor quiescence. Serum PSA levels were shown to correlate with bone density and radiographed tumored bone sizes (Fig. 5B). As measured at week 5, the average bone density in the control, docetaxel 20, and docetaxel 20 combined with A12 treated animals was 0.112 ± 0.01, 0.09 ± 0.02, and 0.05 ± 0.009 (mean ± SE), respectively. There was an apparent trend towards a decrease in bone density with treatment.

Discussion

Recent studies have shown that treatment of androgen-independent prostate cancer with docetaxel results in a significant prolongation of life (11, 12, 18). Improving the efficacy of docetaxel by inhibiting prosurvival pathways or enhancing docetaxel effect on apoptosis has implications for treatment of prostate cancer and many other malignancies (13, 14). In this preclinical study, we showed that blocking signaling through

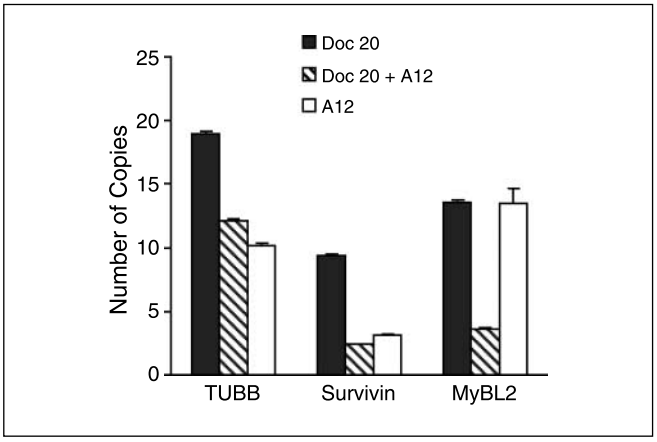

Fig. 3. Real-time reverse transcription-PCR showing the relative expression levels of TUBB, survivin, and MyBL2 in tumors received combined treatment of docetaxel and A12 compared with those that received docetaxel or A12 alone. Columns, mean; bars, SE.

[6] Ludwig, unpublished data.

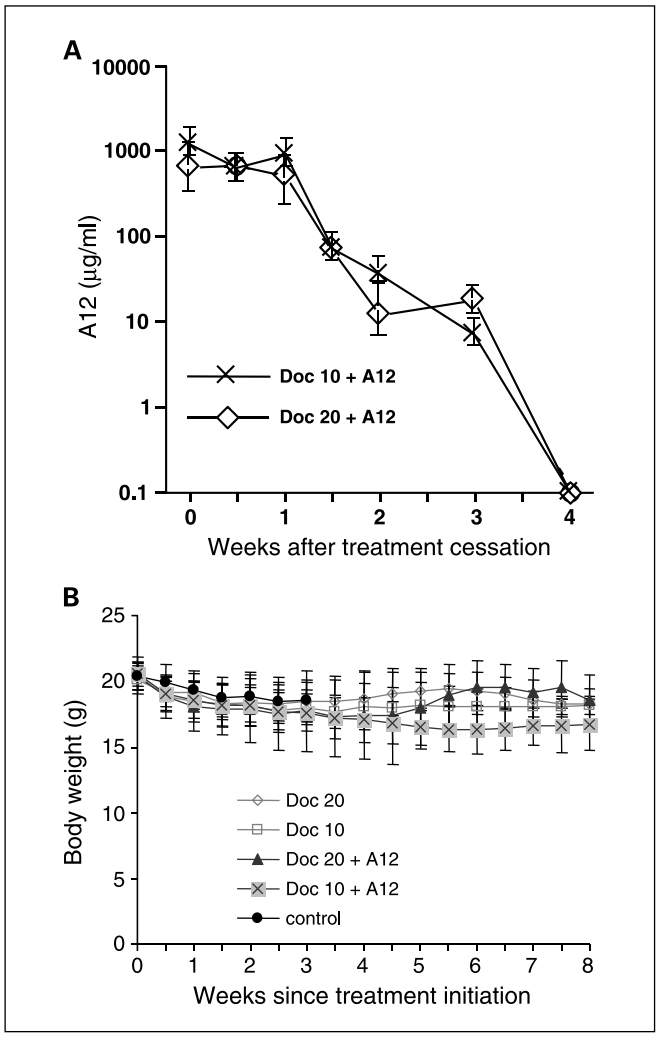

Fig. 4. *A,* posttreatment serum levels of A12, showing no significant amount of posttreatment residual A12 at the study end point. Serum A12 was quantitated using a human IgG binding ELISA and a standard A12 curve. *B,* pharmacotoxicity evaluation showing combined treatment of docetaxel (*Doc*) and A12 did not facilitate significant additional weight loss in animals compared with those treated with docetaxel or A12 alone. Points, mean; bars, SE.

the IGF-IR could enhance the therapeutic efficacy of docetaxel. The addition of A12 improved androgen-independent prostate tumor responses at two doses of docetaxel, the lower of which has shown less effective in inhibiting tumor growth in the current and other *in vivo* studies (31). In animals treated with docetaxel alone, androgen-independent tumor growth resumed almost immediately upon discontinuing therapy, and by 4 weeks, cell cycle kinetics and BrdUrd uptake were equivalent to the controls. In contrast, when A12 was given in conjunction with docetaxel, posttreatment suppression of androgen-independent tumor growth was significantly prolonged with ongoing apoptosis even up to 4 weeks after treatment was stopped. In the osseous human prostate cancer xenograft model LuCaP 23.1, the combination of A12 and docetaxel also produced a greater and more prolonged decrease in tumor growth than docetaxel alone.

We have previously reported that A12 given as a single agent inhibits tumor growth in the LuCaP35V by inducing cell cycle G_2-M arrest, rather than by induction of cell cycle G_1 arrest or apoptosis (4). In the present report, A12 enhanced the apoptotic effect induced by docetaxel. Multiple studies have shown that signaling through the IGF-IR with subsequent activation of antiapoptotic pathways is a mechanism for recovery of tumor cells from chemotherapeutic and radiation therapies, including taxanes (5). Although multiple antiapoptotic pathways are stimulated by activation of the IGF-IR, the phosphatidylinositol 3-kinase (PI3K)/Akt pathway is most prominent (32). We have previously shown that A12 inhibits the PI3K/Akt pathway in the LuCaP 35V xenograft (4). Therefore, the mechanism by which A12 prolongs or accentuates the effect of docetaxel seems to be, at least in part, by inhibition of antiapoptotic pathways that permit recovery from docetaxel treatment. It should also be noted that persistence of circulating A12 in serum due to the long half-life of antibody therapies may in part contribute to the prolonged inhibition of tumor growth. We measured posttreatment serum levels of A12 in animals that had received docetaxel combined with A12. Serum A12 was detectable in animals through posttreatment week 4 (Fig. 4A).

After treatment termination, apoptosis and cell cycle arrest continued in tumors from the combined treatment of A12 and docetaxel. Gene profiling analyses indicated that the posttreatment prolonged effects of combined reagents may largely be due to the continuation of A12 enhanced down-regulation of

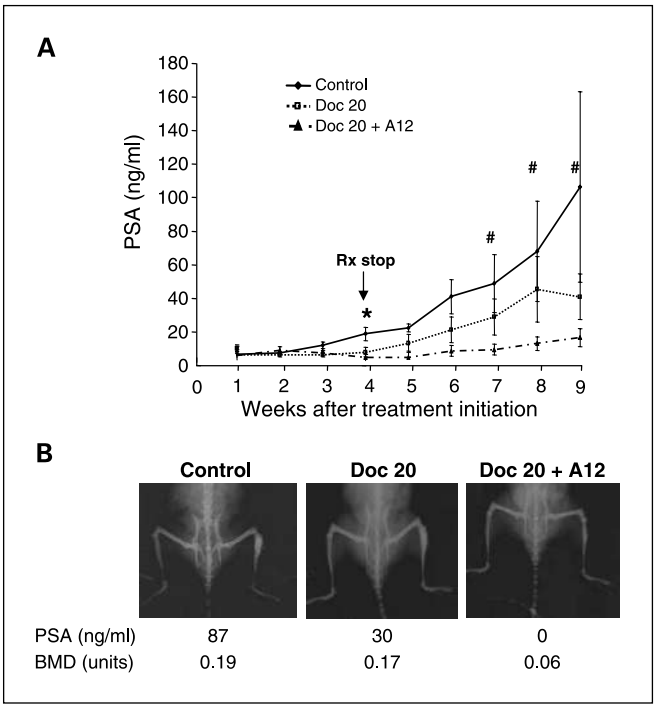

Fig. 5. *A,* serum PSA levels from severe combined immunodeficient mice in which LuCaP 23.1 human prostate xenografts were injected intratibially. Control animals were injected with vehicle saline buffer. Doc 20 animals received 20 mg/kg docetaxel once a week. Doc 20 + A12 animals received 20 mg/kg docetaxel once a week and 40 mg/kg A12 thrice a week. All treatment was stopped at 4 weeks. Note that the Doc 20 and Doc 20 + A12 animals had significantly lower levels of PSA at treatment week 4 (*, $P < 0.05$) compared with control animals. After treatment stopped, PSA levels in the Doc 20 animals began to arise within a week, whereas PSA levels in the Doc and A12 animals remained significantly lower than those in the control and Doc 20 animals throughout the remainder of the study (#, $P < 0.05$). *B,* representative radiographs, serum PSA, and Dexa bone density (*BMD*) of animals measured at week 5 from each group. Note the correlation between serum PSA and radiographed enlargement in the tumored leg (*right*).

cell cycle progression – or/and cell survival – associated genes and up-regulation of cell cycle – negative regulators or/and proapoptotic genes. Several gene products that positively regulate cell cycle progression (*CDC2*, *CDC6*, *CCNA2*, and *CDC25B*; refs. 33 – 35) or cell survival (*BIRC5* and *MYBL2*; refs. 24, 36) were significantly down-regulated in tumors pretreated with A12 and docetaxel compared with docetaxel alone, whereas other genes that negatively regulate cell cycle progression or survival were significantly up-regulated (e.g., *TOB1*, *CCNG2*, and *IGFBP3*; refs. 28, 30, 37, 38). These changes in posttreatment gene expression after the combined therapy are consistent with the failure of these tumor cells to reenter the cell cycle and eventually to undergo apoptosis. Interestingly, some of these down-regulated genes, such as *CDC6*, *CCNA2*, *BIRC5*, and *CDC25B*, were also found down-regulated in tumors treated with A12 alone (39), further suggesting that the posttreatment prolonged inhibition of tumor growth is due to the augmented effect of A12 in suppressing or mitigating the activity of cell cycle/survival – related genes during treatment. Two genes, *TUBB* and *K-Alpha-1* (23, 40), that are specifically related to docetaxel resistance are down-regulated following cessation of combined treatment, suggesting that blocking IGF-IR with A12 may potentially abrogate resistance mechanisms and allow a prolonged chemotherapeutic effect. Whether the down-regulation of these genes is simply an indication of the failure of tumors to reenter the cell cycle or represents specific therapy-related effects is the focus of ongoing studies.

Docetaxel induces cell death by multiple mechanisms, many of which might be augmented by suppression of IGF-IR signaling. Prerequisite for taxane cytotoxicity is initial perturbation of microtubule dynamics followed by induction of mitotic arrest and ultimately activation of the mitochondrial pathway of apoptosis. Resistance to taxanes may result from interference with each of the steps to induction of apoptosis. These include modulation of the isoforms of the taxane target β-tubulin (41), up-regulation of cell cycle regulatory protein $p21^{Cip1}$ (42), inhibition of proapoptotic BAD, and up-regulation of prosurvival pathways involving Bcl-2 and PI3K. IGF-IR signaling rescues cells from apoptotic stress by maintaining Bcl-2 levels, suppressing BAD and up-regulating PI3K activation (32, 43). Induction of the IGF-IR interacting protein RACK induces p21, p27, and G_0-G_1 arrest, all of which would be predicted to mediate resistance to taxanes (44). Previous work from our group shows that A12 treatment alone induces G_2-M arrest; the combination of A12 and docetaxel may induce mitotic catastrophe in tumor cells and fail to reenter cell cycle even after treatment cessation, which ultimately resulted in cell death. We have also shown previously that A12 treatment suppresses PI3K activity, suggesting that the cell cycle regulatory pathways and blockade of PI3K are among the most relevant to A12 enhancement of docetaxel cytotoxicity. The ability of A12 to both enhance initial chemotherapy responses and induce a persistent reduction in tumor growth with ongoing spontaneous apoptosis is unique among agents used to sensitize cells to taxanes. How this effect is mediated, either through prolonged down-regulation of IGF-IR expression, inhibition of drug efflux, or inhibition of tumor angiogenesis (45), will have important implications for its use in patients with advanced prostate cancer.

In summary, in this study, we have shown that addition of an IGF-IR antibody A12 to docetaxel results in a significant increase in antitumor activity in two human prostate cancer xenograft models. The effect seems to be due to A12-enhanced down-regulation of cell cycle progression/cell survival – associated genes and/or up-regulation of proapoptotic genes that results in an inhibition of recovery from apoptosis induced by docetaxel. No obvious toxicity was seen from the combination therapy that was not observed in our previous studies with A12 as a single agent (4). Furthermore, this study supports the potential for future clinical trials in androgen-independent and bone-metastasized prostate cancer with combinations of an approved chemotherapeutic agent and an inhibitor of IGF-IR signaling, such as the human monoclonal A12 antibody.

Acknowledgments

We thank Dr. Ruth Etzione and Sara Hawley at the Fred Hutchinson Cancer Research Center for their assistance in statistical analyses and Erik Corcoran and Lily Higgins for technical assistance. We also thank Nicole La Voie for assistance with animal studies and Dr. Eva Cory for bone densitometry measurements.

References

1. Maloney EK, McLaughlin JL, Dagdigian NE, et al. An anti-insulin-like growth factor I receptor antibody that is a potent inhibitor of cancer cell proliferation. Cancer Res 2003;63:5073 – 83.
2. Sachdev D, Li SL, Hartell JS, Fujita-Yamaguchi Y, Miller JS, Yee D. A chimeric humanized single-chain antibody against the type I insulin-like growth factor (IGF) receptor renders breast cancer cells refractory to the mitogenic effects of IGF-I. Cancer Res 2003; 63:627 – 35.
3. Burtrum D, Zhu Z, Lu D, et al. A fully human monoclonal antibody to the insulin-like growth factor I receptor blocks ligand-dependent signaling and inhibits human tumor growth *in vivo*. Cancer Res 2003;63: 8912 – 21.
4. Wu JD, Odman A, Higgins LM, et al. *In vivo* effects of the human type i insulin-like growth factor receptor antibody A12 on androgen-dependent and androgen-independent xenograft human prostate tumors. Clin Cancer Res 2005;11:3065 – 74.
5. Yu D, Watanabe H, Shibuya H, Miura M. Redundancy of radioresistant signaling pathways originating from insulin-like growth factor I receptor. J Biol Chem 2003;278:6702 – 9.
6. Montero A, Fossella F, Hortobagyi G, Valero V. Docetaxel for treatment of solid tumours: a systematic review of clinical data. Lancet Oncol 2005;6:229 – 39.
7. Bhalla KN. Microtubule-targeted anticancer agents and apoptosis. Oncogene 2003;22:9075 – 86.
8. Wang TH, Wang HS, Soong YK. Paclitaxel-induced cell death: where the cell cycle and apoptosis come together. Cancer 2000;88:2619 – 28.
9. Khan MA, Carducci MA, Partin AW. The evolving role of docetaxel in the management of androgen independent prostate cancer. J Urol 2003;170:1709 – 16.
10. Ganansia-Leymarie V, Bischoff P, Bergerat JP, Holl V. Signal transduction pathways of taxanes-induced apoptosis. Curr Med Chem Anti-Canc Agents 2003;3: 291 – 306.
11. Khan MA, Carducci MA, Partin AW. Docetaxel in androgen-independent prostate cancer: an update. BJU Int 2004;94:1209 – 10.
12. Strother JM, Beer TM, Dreicer R. Novel cytotoxic and biological agents for prostate cancer: where will the money be in 2005? Eur J Cancer 2005;41: 954 – 64.
13. Tannock IF, de Wit R, Berry WR, et al. Docetaxel plus prednisone or mitoxantrone plus prednisone for advanced prostate cancer. N Engl J Med 2004;351: 1502 – 12.
14. Petrylak DP, Tangen CM, Hussain MH, et al. Docetaxel and estramustine compared with mitoxantrone and prednisone for advanced refractory prostate cancer. N Engl J Med 2004;351:1513 – 20.
15. Petrylak DP. Docetaxel-based chemotherapy trials in androgen-independent prostate cancer: first demonstration of a survival benefit. Curr Oncol Rep 2005;7:205 – 6.
16. Corey E, Quinn JE, Buhler KR, et al. LuCaP 35: a new model of prostate cancer progression to androgen independence. Prostate 2003;55:239 – 46.
17. Corey E, Quinn J, Bladou F, et al. Establishment and characterization of osseous prostate cancer models: intra-tibial injection of human prostate cancer cells. Prostate 2002;52:20 – 33.
18. Hawkins V, Doll D, Bumgarner R, et al. PEDB: the Prostate Expression Database. Nucleic Acids Res 1999;27:204 – 8.
19. Nelson PS, Clegg N, Arnold H, et al. The program of androgen-responsive genes in neoplastic prostate epithelium. Proc Natl Acad Sci U S A 2002;99: 11890 – 5.

20. Bonham M, Arnold H, Montgomery B, Nelson PS. Molecular effects of the herbal compound PC-SPES: identification of activity pathways in prostate carcinoma. Cancer Res 2002;62:3920–4.

21. Tusher VG, Tibshirani R, Chu G. Significance analysis of microarrays applied to the ionizing radiation response. Proc Natl Acad Sci U S A 2001;9:5116–21.

22. Lee DK, Chang C. Molecular communication between androgen receptor and general transcription machinery. J Steroid Biochem Mol Biol 2003; 84:41–9.

23. Tanaka T, Tanimoto K, Otani K, et al. Concise prediction models of anticancer efficacy of 8 drugs using expression data from 12 selected genes. Int J Cancer 2004;111:617–26.

24. de Angelis PM, Fjell B, Kravik KL, et al. Molecular characterizations of derivatives of HCT116 colorectal cancer cells that are resistant to the chemotherapeutic agent 5-fluorouracil. Int J Oncol 2004;24:1279–88.

25. Zhang M, Latham DE, Delaney MA, Chakravarti A. Survivin mediates resistance to antiandrogen therapy in prostate cancer. Oncogene 2005;24: 2474–82.

26. Loughran G, Huigsloot M, Kiely P, et al. Gene expression profiles in cells transformed by overexpression of the IGF-I receptor. Oncogene 2005;24: 6185–93.

27. Grimberg A, Cohen P. Role of insulin-like growth factors and their binding proteins in growth control and carcinogenesis. J Cell Physiol 2000;183:1–9.

28. Devi GR, Sprenger CC, Plymate SR, Rosenfeld RG. Insulin-like growth factor binding protein-3 induces early apoptosis in malignant prostate cancer cells and inhibits tumor formation *in vivo*. Prostate 2002;51: 141–52.

29. Chan JM, Stampfer MJ, Ma J, et al. Insulin-like growth factor-I (IGF-I) and IGF binding protein-3 as predictors of advanced-stage prostate cancer. J Natl Cancer Inst 2002;9:1099–106.

30. Rajah R, Valentinis B, Cohen P. Insulin-like growth factor binding protein-3 induces apoptosis and mediates the effects of transforming-β1 on programmed cell death through a p53 and IGF-independent mechanism. J Biol Chem 1997;272:12181–8.

31. Egawa T, Kubota T, Suto A, et al. Antitumor activity of doxorubicin in combination with docetaxel against human breast cancer xenografts. *In vivo* 2003;17: 23–8.

32. Peruzzi F, Prisco M, Dews M, et al. Multiple signaling pathways of the insulin-like growth factor 1 receptor in protection from apoptosis. Mol Cell Biol 1999; 19:7203–15.

33. Hengstschlager M, Braun K, Soucek T, Miloloza A, Hengstschlager-Ottnad E. Cyclin-dependent kinases at the G_1-S transition of the mammalian cell cycle. Mutat Res 1999;436:1–9.

34. Okayama H, Nagata A, Igarashi M, Suto K, Jinno S. Mammalian G_2 regulatory genes and their possible involvement in genetic instability in cancer cells. Princess Takamatsu Symp 1991;22:231–8.

35. Nilsson I, Hoffmann I. Cell cycle regulation by the Cdc25 phosphatase family. Prog Cell Cycle Res 2000;4:107–14.

36. Bar-Shira A, Pinthus JH, Rozovsky U, et al. Multiple genes in human 20q13 chromosomal region are involved in an advanced prostate cancer xenograft. Cancer Res 2002;62:6803–7.

37. Kuo ML, Duncavage EJ, Mathew R, et al. Arf induces p53-dependent and -independent antiproliferative genes. Cancer Res 2003;63:1046–53.

38. Ito Y, Yoshida H, Uruno T, et al. Decreased expression of cyclin G_2 is significantly linked to the malignant transformation of papillary carcinoma of the thyroid. Anticancer Res 2003;23:2335–8.

39. Wu J, Haugk K, Woodke L, Nelson P, Coleman I, Plymate S. Interaction of IGF signaling and the androgen receptor in prostate cancer progression. J Cell Biochem 2006;99:392–401.

40. Dumontet C, Jaffrezou JP, Tsuchiya E, et al. Resistance to microtubule-targeted cytotoxins in a K562 leukemia cell variant associated with altered tubulin expression and polymerization. Bull Cancer 2004;91: E81–112.

41. Montgomery RB, Bonham M, Nelson PS, et al. Estrogen effects on tubulin expression and taxane mediated cytotoxicity in prostate cancer cells. Prostate 2005;65:141–50.

42. Yu D, Jing T, Liu B, et al. Overexpression of ErbB2 blocks Taxol-induced apoptosis by upregulation of p21Cip1, which inhibits p34Cdc2 kinase. Mol Cell 1998;2:581–91.

43. Singleton JR, Randolph AE, Feldman EL. Insulin-like growth factor I receptor prevents apoptosis and enhances neuroblastoma tumorigenesis. Cancer Res 1996;56:4522–9.

44. Hermanto U, Zong CS, Li W, Wang LH. RACK1, an insulin-like growth factor I (IGF-I) receptor-interacting protein, modulates IGF-I-dependent integrin signaling and promotes cell spreading and contact with extracellular matrix. Mol Cell Biol 2002;22:2345–65.

45. Reinmuth N, Liu W, Fan F, et al. Blockade of insulin-like growth factor I receptor function inhibits growth and angiogenesis of colon cancer. Clin Cancer Res 2002;8:3259–69.

Journal of Cellular Biochemistry 99:392–401 (2006)

Interaction of IGF Signaling and the Androgen Receptor in Prostate Cancer Progression

Jennifer D. Wu,[1] Kathy Haugk,[2] Libby Woodke,[2] Peter Nelson,[3] Ilsa Coleman,[3] and Stephen R. Plymate[1,2]*

[1]Department of Medicine, University of Washington, Seattle, Washington
[2]Geriatric Research, Education and Clinical Center, Veterans Affairs Puget Sound Health Care System, Seattle, Washington
[3]Fred Hutchinson Cancer Research Center, Seattle, Washington

Abstract The insulin-like growth factor type I receptor (IGF-IR) has been suggested to play an important role in prostate cancer progression and possibly in the progression to androgen-independent (AI) disease. The term AI may not be entirely correct, in that recent data suggest that expression of androgen receptor (AR) and androgen-regulated genes is the primary association with prostate cancer progression after hormone ablation. Therefore, signaling through other growth factors has been thought to play a role in AR-mediated prostate cancer progression to AI disease in the absence of androgen ligand. However, existing data on how IGF-IR signaling interacts with AR activation in prostate cancer are conflicting. In this Prospect article, we review some of the published data on the mechanisms of IGF-IR/AR interaction and present new evidence that IGF-IR signaling may modulate AR compartmentation and thus alter AR activity in prostate cancer cells. Inhibition of IGF-IR signaling can result in cytoplasmic AR retention and a significant change in androgen-regulated gene expression. Translocation of AR from the cytoplasm to the nucleus may be associated with IGF-induced dephosphorylation. Since fully humanized antibodies targeting the IGF-IR are now in clinical trials, the current review is intended to reveal the mechanisms of potential therapeutic effects of these antibodies on AI prostate cancers. J. Cell. Biochem. 99: 392–401, 2006.

Key words: insulin-like growth factor type I receptor (IGF-IR); androgen receptor (AR); androgen-independent (AI) prostate cancer; AR co-regulators

In the presence or possibly absence of androgen ligand, the androgen receptor (AR) translocates from the cytosol to the nucleus and functions as a transcriptional factor, which may be necessary or even crucial for the progression of prostate cancer [Scher and Sawyers, 2005]. Classically, in the absence of androgen ligand, AR remains in the cytosol and is not active. Thus, it is of particular interest that malignant prostate cancer progression occurs frequently in men who have been surgically or chemically castrated. The progression of prostate cancer after castration has been termed androgen-independent (AI) prostate cancer. More interestingly, animal studies showed that when the expression of AR was disrupted, prostate cancer ceased to progress [Taplin and Balk, 2004]. All these together posed a conundrum if the AR, rather than the androgen ligand, is a driving force in prostate cancer progression. If so, it would suggest that the AR is functioning in a non-classical manner in the absence of steroid ligand. Although non-genomic mechanisms for AR function have been proposed through an interaction with SRC–Raf–Ras–Map kinase in the cytosol rather than the nucleus, this "traditional" non-genomic mechanism also requires the presence of androgen ligand and would not explain progression of disease in a ligand-independent manner [Kousteni et al., 2001; Pandini et al., 2005].

The concept of AR functioning in AI progression was first proposed by Mohler and colleages

Grant sponsor: National Cancer Institute; Grant sponsor: Veterans Affairs Research Service; Grant sponsor: Department of Defense; Grant numbers: 1K01CA116002-01, PO1-CA85859, DOD-PC040364.

*Correspondence to: Stephen R. Plymate, MD, 325 9th Avenue, Box 359625, Seattle, WA 98104.
E-mail: splymate@u.washington.edu

Received 15 February 2006; Accepted 27 February 2006
DOI 10.1002/jcb.20929

[Gregory et al., 1998; Mohler et al., 2004]. In relevant studies, tumor biopsies were taken from prostate cancer patients who had been androgen ablated and presented with progression of the cancer [Gregory et al., 1998; Mohler et al., 2004] In these samples, the AR primarily resided in a nuclear location, contrary to what had been expected in a castrated environment. This may in part due to residual levels of androgen in the prostate tissue. When tissue levels of androgen, testosterone, and dihydrotestosterone (DHT), were measured, although lower than in non-castrated men, they were still detected in the nanomolar range in many of the castrated men [Titus et al., 2005a]. This subtle level of tissue androgen may account for the nuclear localization of the AR and signal to activate an AR transcriptional program. The failure of castration to completely abolish intraprostatic androgens has also been evidenced in the study where normal men were placed on a GnRH antagonist for 4 weeks and in whom serum levels of testosterone (T) and DHT were clearly in the castrate range (Page and Bremner, personal communication). The source of the androgens in these castrate men has yet to be determined; however, the most likely source would be conversion from adrenal androgens. The prostate has active 5α-reductase systems for both isoforms I and II ensuring that circulating T can be readily converted to DHT in the prostate [Titus et al., 2005b]. In addition, recent microarray data has shown that the prostate contains mRNAs for the enzymes necessary for the conversion of cholesterol precursor into DHT; however this conversion has not been demonstrated in the prostate. Anti-androgen drugs, such as biclutamide, have not been shown to alter the translocation of the AR to the nucleus in prostate specimens from men treated with combined androgen blockade [Mohler et al., 2004]. Therefore, it is not clear whether it is the low levels of androgens driving prostate cancer progression in castrated men. Until a total androgen ablation mechanism in men is developed, the importance of residual androgens in tumor progression cannot be determined.

Castration studies on prostate cancer xenograft and transgenic mouse models support the speculation that residual androgen production following castration is only the partial driving force for tumor progression. Since mice do not produce adrenal androgens to any significant degree, castration in a mouse results in "complete androgen ablation" [Van Weerden et al., 1992]. In these models, tumors progress from androgen-dependent (AD) to AI following castration in spite of the fact that prostate specific androgen levels decrease to nearly undetectable levels, suggesting that residual androgens are unlikely to play a part in post-castration tumor progression [Thalmann et al., 2000; Corey et al., 2003]. We and others have shown that, in these models, the majority of tumor nuclei still contain AR after castration although some of the AR moves from the nucleus to the cytoplasm (Fig. 1). Furthermore, androgen-regulated genes continue to be expressed in "AI" disease [Corey et al., 2003]. Together, these data suggest that other mechanisms beyond the traditional ligand-receptor interaction of AR signaling are responsible for AD to AI prostate cancer progression.

Alterations in co-regulators of the AR, which may enhance ligand-independent AR translocation to the nucleus and binding to DNA, have been suggested as one of the mechanisms for ligand-independent AR signaling [Gregory et al., 1998; Fujimoto et al., 1999; Kang et al., 1999; Sadar, 1999; Sadar and Gleave, 2000; Mohler et al., 2004]. It has been suggested that some peptide growth factors can act directly at the androgen-binding domain of the AR or indirectly through modifying the phosphoryla-

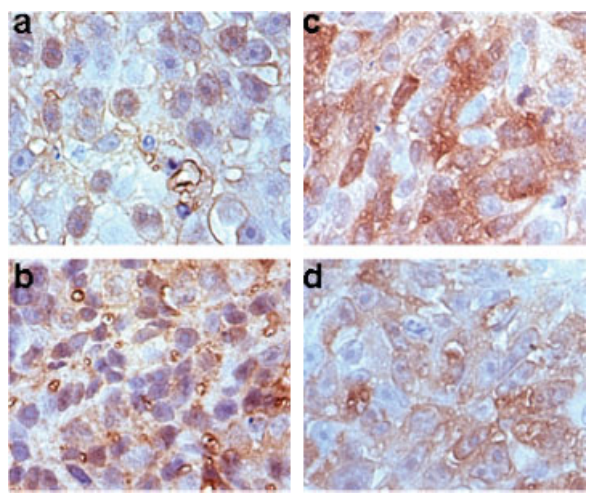

Fig. 1. IGF-IR signaling-induced translocation of AR into the nucleus in xenograft human prostate tumors. **a**: AR compartmentalization in the nucleus in intact animals. **b**: Blocking IGF-IR signaling with antibody A12 caused cytoplasmic retention of AR in intact animals. **c**: AR in the nucleus in castrated animals. **d**: A12 induced marked AR retention in the plasma in castrated animals.

tion status of the AR or its co-regulators to initiate AR signaling [Culig et al., 1994, 1995; Sadar, 1999; Sadar and Gleave, 2000; Lin et al., 2001]. In this "Prospectus" we examined the interactions between AR function and the activation of type 1 insulin-like growth factor receptor (IGF-IR). Among peptide growth factor-induced cell signaling, IGF activated IGF-IR signaling is a potential driving force for the growth of AI prostate cancer for several reasons as listed in Table I. In the following sections, we will examine the evidence for each of these components of potential interaction between the IGF-IR and AR.

IGF-IR IS NECESSARY FOR CELL TRANSFORMATION

Fibroblasts from IGF-IR knock out mice R^- do not transform spontaneously when compared to R^{wt} control cells. When the IGF-IR is re-expressed in these fibroblasts, transformation takes place. In SV40T immortalized prostate epithelial cells, inhibition of IGF-IR expression with an antisense construct significantly decreases colony formation in soft agar, a marker of transformation. In studies when growth hormone and IGF deficient LID mice were crossed with the transgenic prostate cancer (TRAMP) mouse, tumor development was significantly delayed Majeed et al., 2005). All these studies suggest an essential role of IGF-IR in cellular transformation. Hongo et al. [1998] have identified specific tyrosine residues on the β-subunit of the IGF-IR that are crucial for the transforming actions of the IGF-IR [O'connor et al., 1997; Liu et al., 1998].

TABLE I. Evidence for Interaction of the IGF-IR and AR in Prostate Cancer

1.	The IGF-IR is necessary for cell transformation
2.	Clinical data, although somewhat controversial suggests that higher levels of IGF-I in the serum of men predicts men at risk for developing clinical prostate cancer
3.	Androgens increase IGF-IR levels in prostate epithelial cells
4.	IGF-IR signaling alters AR phosphorylation
5.	IGF-IR signaling alters the AR transcriptional profile
6.	IGF-IR signaling effects translocation of the AR to the nucleus
7.	IGF-IR ligands increase in the progression of prostate cancer and are particularly abundant in bone where prostate cancer metastases are most abundant
8.	Xenograft models of prostate cancer respond differently to IGF-IR inhibition depending on the presence or absence of androgens
9.	IGF binding proteins (IGFBP) that enhance signaling of IGF ligands through the IGF-IR are increased in the period immediately after castration
10.	Inhibition of the IGF-IR in conjunction with castration
11.	Transcription factors that stimulate the IGF-IR promoter are also regulated by androgens

Since prostate cancer rarely develops in the absence of androgens, it is suspected that androgens are at least permissive in the transformation process of prostate epithelial cells. However, it should be noted that expression of the AR is necessary for normal luminal prostate epithelium to develop. It is suggested that maintaining certain levels of IGF-IR expression in the prostate may be necessary in normal prostate differentiation, increased levels of IGF-IR expression may be required for the prostate epithelia transformation process, and decreased IGF-IR expression may be required for prostate cancer malignant progression. This is consistent with the clinical findings that the levels of IGF-IR decrease following the initial transformation of the epithelium [Tennant et al., 1996]. This concept has been corroborated by the decrease in tumor metastases and increase in apoptosis associated with the re-expression IGF-IR in prostate cancer xenograft cell lines [Plymate et al., 1997a,b].

It should be pointed out that not all studies have shown an increase in IGF-IR expression during early prostate epithelia transformation or a decrease in IGF-IR expression in the progression to malignant prostate epithelia [Hellawell et al., 2002]. This may due to discrepancies in the choice of antibodies or technique in immunohistochemistry studies. The IGF-IR is a tyrosine kinase receptor that is only activated when located on the cell surface; although rapidly internalized upon activation, it is also rapidly processed through the golgi to be re-expressed on the cell surface.

CLINICAL DATA SUGGESTS THAT MEN IN THE HIGHER QUARTILES OF SERUM IGF-I LEVELS ARE AT A GREATER RISK FOR DEVELOPING PROSTATE CANCER

Large scale epidemiologic studies, such as the Physician's Health Study, have suggested that men with higher serum levels of IGF-1 as well as androgens may be at increased risk of developing prostate cancer in the following 6–9 years [Chan et al., 1998; Pollak, 2000; Pollak et al., 2004]. Also, in these studies serum levels of IGFBP-3 were inversely correlated with the risk of developing prostate cancer [Chan et al., 1998]. Of further note, the risk of cancer developing was more attributable to serum

IGF-I or IGFBP-3 than to serum testosterone. However, other studies have not shown an association of risk for prostate cancer with serum levels of IGF-I [Harman et al., 2000; Chen et al., 2005]. One should be aware that the risk of developing prostate cancer was not the primary end point of any of these studies nor did the results of the epidemiologic studies indicate a direct link between the IGF system and the risk of cancer.

ANDROGENS INCREASE IGF-IR EXPRESSION IN PROSTATE EPITHELIAL CELLS

We had initially detected an increase in IGF-IR expression at protein and mRNA levels in androgen-responsive prostate epithelial cell lines [Plymate et al., 2004]. This observation was subsequently confirmed by other investigators [Pandini et al., 2005]. The mechanism by which androgens increase the IGF-IR expression has been a topic of controversy. Pandini et al. [2005] have shown in their models that the increase in IGF-IR protein induced by androgens does not require nuclear translocation of the AR and is only partially blocked by bicluta-mide. On the other hand, this effect of AR on IGF-IR expression was completely inhibited by the ERK1/2 inhibitor PD980259 [Pandini et al., 2005]. These data suggested a "non-genomic" effect of androgen. This group further confirmed their findings using a mutated AR that will not translocate to the nucleus and demonstrated that the mutanted AR can activate the cytoplasmic Src–Raf–Ras–Map kinase pathway and enhance the transcriptional activity of IGF-IR promoter [Pandini et al., 2005]. Other investigators have not found that activation of this pathway is necessary for androgen-induced increases in IGF-IR expression [Plymate et al., 2004]. Other mechanisms including an increase in KFL6 (Kruppel factor like 6) in response to androgens have been suggested from the study in LnCaP lines (Levine-personal communication). We have shown that KFL6 increases IGF-IR expression by binding to the IGF-IR promoter [Rubinstein et al., 2004]. We have also shown in prostate cell lines that androgens can increase IGF-IR protein expression without an increase in its mRNA expression level, suggesting a post-transcriptional modification of IGF-IR expression, such as mRNA stability [Plymate et al., 2004]. Despite the existing controversials on the mechanisms, all the studies have consistently showed that androgens signaling through the AR result in increased IGF-IR protein expression in prostate epithelium, which is associated with increased phosphorylation of IGF-IR and increased cell proliferation in response to IGF ligands. However, it is not understood whether the induction of increased IGF-IR is part of the differentiation process of prostate epithelium or part of the mechanism for tumor progression. Since both IGF and androgens are necessary for epithelial differentiation, induction of increase in IGF-IR expression as part of the differentiating function of androgens may appear reasonable. On the other hand, increasing IGF-IR expression would be a mechanism by which androgens could enhance transformation and progression of prostate cancer.

IGF-IR ACTIVATION ALTERS AR PHOSPHORYLATION

One mechanism by which IGF-IR signaling could directly affect the function of the AR would be to alter AR phosphorylation. Studies by Lin et al. [2001] first suggested a role of IGF signaling in AR function. They observed that androgen induced apoptosis in AR transiently transfected DU-145 cells and treatment with IGF-1 decreased the transcriptional activity of the AR and inhibited apoptosis. We subsequently found that the effects on IGF-IR signaling on AR activity depended on whether the cells were from an orthotopic or a metastatic lesion [Plymate et al., 2004]. If the tumor was in the orthotopic site, IGF-IR activation inhibited AR transcription under a probasin promoter (AAR3) [Plymate et al., 2004]. In contrast, when the tumor was in the metastatic site, IGF-IR activation enhanced AR transcriptional activity on the AAR3 promoter. Interestingly, the effect of IGF-IR activation on the AR transcriptional activity in both primary and metastatic tumors appears to be mediated through the PI3K/AKT pathway [Plymate et al., 2004]. Lin et al. subsequently demonstrated that the effects of IGF on AR activity occurred in a biphasic manner in LnCaP cells: suppressing AR transcriptional activity at low passage numbers but enhancing AR transcriptional activity at high passage numbers [Lin et al., 2001]. Whether the effect is due to IGF-initiated phosphorylation of AR is rather controversial. Lin et al described that IGF-I phosphorylates AR at serines 210

and 790 [Lin et al., 2001], whereas Gioeli et al. [2002] failed to find any sites on the AR that were phosphorylated by IGF through a peptide terminal degeneration technique. We examined the effect of IGF-IR activation on AR phosphorylation in AR-transfected M12 (M12AR) cells. We showed that AR phosphorylation was decreased in the presence of IGF-I and that this effect was blocked by an inhibitory IGF-IR antibody A12 (Fig. 2a). Our newest study indicated that serine 16 on the AR is a potential site of dephosphorylation whereas serine 81 on the AR is a potential site of phosphorylation by IGF (Fig. 2b). The reasons for discrepancies between studies are not entirely clear. One possible reason for differences in phosphorylation would be differential expression of PP2A in different cell types.

IGF-IR SIGNALING EFFECTS TRANSLOCATION OF THE AR TO THE NUCLEUS

Phosphorylation of the AR may result in several changes that could alter the AR transcriptional functions. One of these effects could be translocation of the AR to the nucleus. Whereas AR phosphorylation was thought to be necessary for nuclear translocation, recent data has shown that phosphorylation of AR at serine 650, which takes place after the AR is in the nucleus and bound to DNA, results in the export of AR from the nucleus [Gioeli et al., 2006]. Thus, the process of dephosphorylation of specific serines on the AR may account for retention of AR in the nucleus and accentuated signaling. As we have shown in Figure 2, IGF decreases phosphorylation of the AR in our M12AR cells. We also have evidence that IGF can enhance AR nuclear translocation in the absence of androgens and that this effect can be inhibited by an IGF-IR inhibitory antibody (Fig. 3a). We have also demonstrated the changes in AR compartmentalization in nuclear and cytoplasmic fractions in response to IGF using Western blot analyses (Fig. 3b). Using the AAR3 probasin reporter assay, we show a significant transactivation of the AR in the absence of androgen and enhanced AR activation in the presence of androgen by IGF-I in M12AR cells. The AR transactivation response to IGF can be blocked by the IGF-IR antibody A12. These data indicate that even in the absence of androgen, IGF can induce transactivation of the AR. Whether this is attributed to changes in phosphorylation of the AR as we have discussed or to the recruitment of AR co-

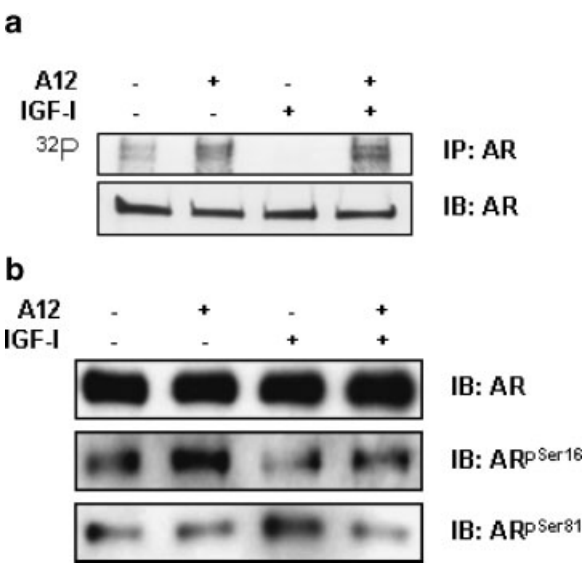

Fig. 2. IGF-I induces AR dephosphorylation. **a**: M12AR cells were labeled with ortho-^{32}P. Cell lysates were immunoprecipitated (IP) with AR-specific antibody. IB, western blotting. **b**: M12AR cells were IB with serine-specific anti-AR antibody.

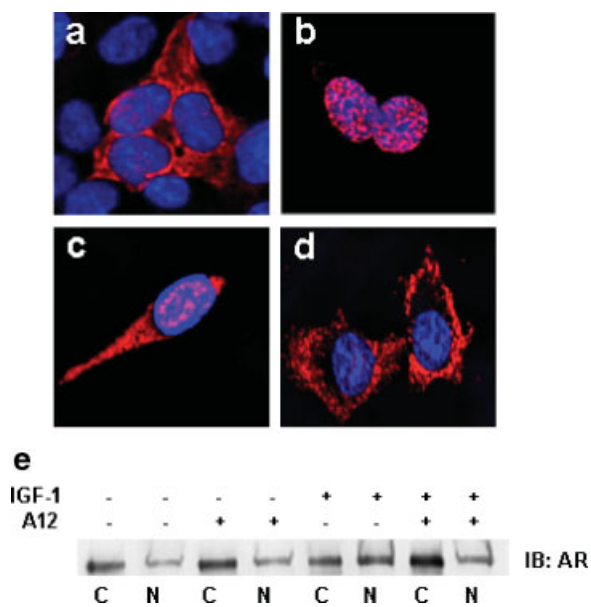

Fig. 3. Confocal image and cell fractionation showing IGF-I-induced AR translocation into the nucleus in M12AR cell lines. **a**: M12AR cells in IGF-I, DHT free medium. **b**: M12AR cells in medium containing 10^{-8}M of DHT. **c**: M12AR cells in medium containing 10 ng/ml of IGF-I. **d**: Medium containing 10 ng/ml of IGF-I and 10 μg/ml of anti-IGF-IR antibody A12. **e**: AR in cytosol and nuclear fractions of M12AR cells under various culture conditions. Red fluorescence. AR, androgen receptor. IGF-I, insulin-like growth factor I. DHT, dihydrotestosterone.

factors, or to both has yet to be determined. Regardless, these studies suggest that, in castrated patients, the increase in AR expression coupled with intact IGF-IR signaling can lead to AR-mediated AI prostate cancer progression. This marks the IGF-IR a potential therapeutic target in post-castrated prostate cancer.

XENOGRAFT MODELS OF PROSTATE CANCER RESPOND DIFFERENTLY TO IGF-IR INHIBITION DEPENDING ON THE PRESENCE OR ABSENCE OF ANDROGENS

We have reported in prostate cancer human xenograft models that inhibition of the IGF-IR with A12 results in a decreased rate of tumor growth in AD and AI tumors [Wu et al., 2005]. However, when we examined the mechanisms by which A12 caused decrease in growth rate, we noted marked differences depending on whether the tumors were AD or AI. In the AD tumors we found that A12 treatment resulted in a combination of apoptosis and G1 cell cycle arrest, whereas in the AI tumors we found that tumor cells arrested in G2 with no occurrence of apoptosis [Wu et al., 2005]. The question arose as to whether these differences in responses were due to a change in the character of the tumor or the absence of androgen. In order to address this issue, we implanted the AI tumor into intact animals. As predicted, tumor growth was inhibited in the A12 treated animals compared to vehicle treated controls. Interestingly, a majority of these tumors displayed an apoptotic response and G1 cell cycle arrest as opposed to the lack of apoptosis when implanted in the castrated animals. To determine potential mechanisms for this effect of androgen on the tumors, we performed cDNA microarray analyses of A12-treated AI tumors from castrated and intact animals and found marked differences in the gene expression profiles (Fig. 4). Some genes such as PP2A and TSC-22 were regulated in opposite direction with A12 treatment, depending on the presence or absence of androgens. It is of interest that TSC-22 has been shown to be androgen-regulated and its expression decreases from benign prostate luminal epithelium to cancer. Another interesting gene differentiated expressed is IGFBP-5, which has been demonstrated to increase post-castration and is associated with recovery from castration-induced apoptosis [Miyake et al., 2000a].

IGF BINDING PROTEINS (IGFBP) THAT ENHANCE SIGNALING OF IGF LIGANDS THROUGH THE IGF-IR ARE INCREASED IN THE PERIOD IMMEDIATELY AFTER CASTRATION

Following castration, IGFBP-2 and IGFBP-5 have been shown to increase significantly in both human prostate and mouse models of prostate cancer. Both of these IGFBPs can increase IGF-ligand signaling through the IGF-IR and enhance recovery from castration induced apoptosis and cell cycle arrest. These two IGFBPs accomplish this task by binding to extracelluar matrix and maintaining a higher concentration of IGF ligand in the proximity of the IGF-IR [Jones et al., 1995; Russo et al., 1997; Kiyama et al., 2003]. The functional importance of these changes has been demonstrated by the studies of Miyake et al. [2000b] in which overexpression of these IGFBPs in LnCaP cells markedly enhances cell growth following androgen withdraw. Using antisense oligonucleotides to IGFBP-2 or IGFBP-5, this group was able to demonstrate the stimulatory effects of the IGFBPs on tumor growth [Kiyama et al., 2003].

INHIBITION OF THE IGF-IR IN CONJUNCTION WITH CASTRATION THERAPY FOR PROSTATE CANCER

These studies suggest that blocking IGF-IR signaling at the time of castration would enhance the effects of androgen withdraw. Preliminary studies in our laboratory using mouse xenograft models have shown a marked enhancement of the castration effect on prostate tumor growth with the inhibitory IGF-IR antibody A12. Potential mechanisms of the augmented effect of A12 on androgen withdraw may include suppression of Survivin, a member of the Inhibitor of Apoptosis (IAP) family of proteins that has been shown to play a role in the recovery process of anti-androgen therapy [Zhang et al., 2005].

IGF-IR ACTIVATION CAN STIMULATE AR CO-FACTORS THAT ENHANCE AR SIGNALING

Insulin-like growth factor may also influence AR signaling by increasing the expression of AR

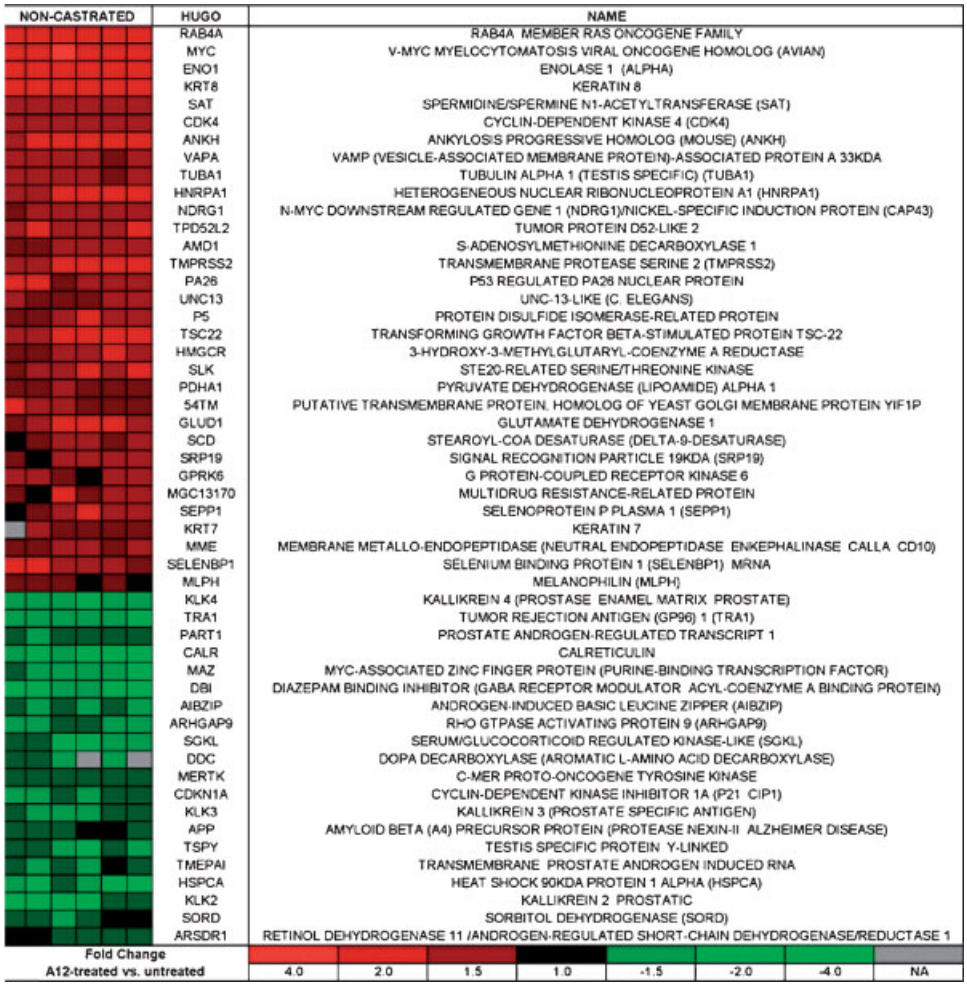

Fig. 4. cDNA microarray expression values of androgen-regulated genes differentially expressed in LuCaP 35V tumors from A12-treated relative to untreated non-castrated mice. There were 82 unique genes known to be androgen-regulated which had significantly consistent gene expression across all samples as compared to no change by a one-sample *t*-test in SAM (<1% FDR significance cut-off used). The scale represents fold-change in A12-treated relative to untreated tumors.

co-stimulatory factors. Given the known 100 or more AR co-regulatory factors, it is not surprising that IGF-IR activation would enhance the expression or activation of one or more co-regulators of the AR. Amongst them, TIF-2 (GRIP-1) and insulin degrading enzyme (IDE) are of particular interest. Studies in a series of human prostate specimens from men with prostate cancer, Mohler and Wilson have demonstrated an increased expression of TIF-2 in most of the recurrent AI prostate cancers that also have a high levels of AR in the nucleus [Gregory et al., 2001]. The same group has also shown the coincidence of increased TIF-2 expression with the recurrence of AI human prostate cancer in xenograft models. Mohler has also demonstrated that overexpression of TIF-2 in vitro can increase AR transcriptional activity in the presence of the physiological concentrations of adrenal androgen. Studies have shown that IDE is a potent co-stimulator of AR transcriptional activity and the ability of IDE to bind to the AR can be regulated by insulin and IGF ligands [Kupfer et al., 1994]. In addition, as the name implies, IDE can degrade insulin, IGF-I and IGF-II [Udrisar et al., 2005].

CONCLUSION

In this review, we have summarized our current understandings of the interactions between the IGF system and the AR (Fig. 5).

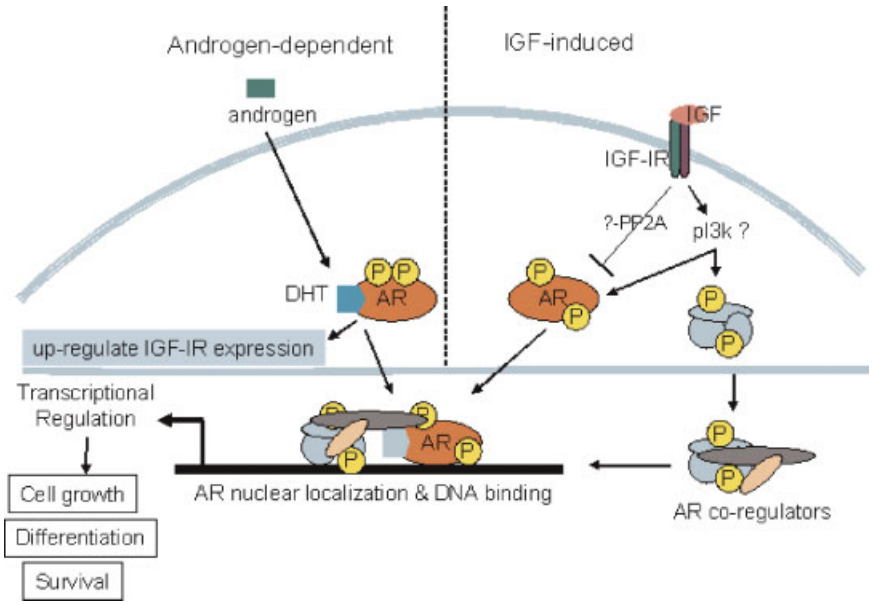

Fig. 5. Interactions of the IGF system with AR signaling. pI3k, phosphoinositide 3-kinase. PP2A, protein phosphotase 2A. [Color figure can be viewed in the online issue, which is available at www.interscience.wiley.com.]

The ability of IGF signaling to potentiate the transcriptional activity of the AR in the face of low to no androgen makes the IGF system, especially the IGF-IR, a strong candidate that leads progression of AI prostate cancer through AR signaling.

ACKNOWLEDGMENTS

Supported by NIH Temin Award 1K01CA116002-01 (J.D.W.), NIH grant PO1-CA85859, Veterans Affairs Research Service, and DOD Prostate Cancer Research grant PC040364 (S.R.P.). We thank our collaborators G.S. Yang and B.M. Paschal at the University of Virginia for donating Figure 2b.

REFERENCES

Chan JM, Stampfer MJ, Giovannucci E, Gann PH, Ma J, Wilkinson P, Hennekens CH, Pollak M. 1998. Plasma insulin-like growth factor-I and prostate cancer risk: A prospective study. Science 279:563–566.

Chen C, Lewis SK, Voigt L, Fitzpatrick A, Plymate SR, Weiss NS. 2005. Prostate carcinoma incidence in relation to prediagnostic circulating levels of insulin-like growth factor I, insulin-like growth factor binding protein 3, and insulin. Cancer 103:76–84.

Corey E, Quinn JE, Buhler KR, Nelson PS, Macoska JA, True LD, Vessella RL. 2003. LuCaP 35: A new model of prostate cancer progression to androgen independence. Prostate 55:239–246.

Culig Z, Hobisch A, Cronauer MV, Radmayr C, Trapman J, Hittmair A, Bartsch G, Klocker H. 1994. Androgen receptor activation in prostatic tumor cell lines by insulin-like growth factor-I, keratinocyte growth factor, and epidermal growth factor. Cancer Res 54:5474–5478.

Culig Z, Hobisch A, Cronauer MV, Hittmair A, Radmayr C, Bartsch G, Klocker H. 1995. Activation of the androgen receptor by polypeptide growth factors and cellular regulators. World J Urol 13:285–289.

Fujimoto N, Yeh S, Kang HY, Inui S, Chang HC, Mizokami A, Chang C. 1999. Cloning and characterization of androgen receptor coactivator, ARA55, in human prostate. J Biol Chem 274:8316–8321.

Gioeli D, Ficarro SB, Kwiek JJ, Aaronson D, Hancock M, Catling AD, White FM, Christian RE, Settlage RE, Shabanowitz J, Hunt DF, Weber MJ. 2002. Androgen receptor phosphorylation. Regulation and identification of the phosphorylation sites. J Biol Chem 277:29304–29314.

Gioeli D, Black BE, Gordon V, Spencer A, Kesler CT, Eblen ST, Paschal BM, Weber MJ. 2006. Stress kinase signaling regulates androgen receptor phosphorylation, transcription, and localization. Mol Endocrinol 20:503–515.

Gregory CW, Hamil KG, Kim D, Hall SH, Pretlow TG, Mohler JL, French FS. 1998. Androgen receptor expression in androgen-independent prostate cancer is associated with increased expression of androgen-regulated genes. Cancer Res 58:5718–5724.

Gregory CW, He B, Johnson RT, Ford OH, Mohler JL, French FS, Wilson EM. 2001. A mechanism for androgen receptor-mediated prostate cancer recurrence after androgen deprivation therapy. Cancer Res 61:4315–4319.

Harman SM, Metter EJ, Blackman MR, Landis PK, Carter HB. 2000. Serum levels of insulin-like growth factor I

(IGF-I), IGF-II, IGF-binding protein-3, and prostate-specific antigen as predictors of clinical prostate cancer. J Clin Endocrinol Metab 85:4258–4265.

Hellawell GO, Turner GD, Davies DR, Poulsom R, Brewster SF, Macaulay VM. 2002. Expression of the type 1 insulin-like growth factor receptor is up-regulated in primary prostate cancer and commonly persists in metastatic disease. Cancer Res 62:2942–2950.

Hongo A, Yumet G, Resnicoff M, Romano G, O'Connor R, Baserga R. 1998. Inhibition of tumorigenesis and induction of apoptosis in human tumor cells by the stable expression of a myristylated COOH terminus of the insulin-like growth factor I receptor. Cancer Res 58: 2477–2484.

Jones JI, Clemmons DR. 1995. Insulin-like growth factors and their binding proteins: Biological actions. Endocrinol Rev 16:3–34.

Kang HY, Yeh S, Fujimoto N, Chang C. 1999. Cloning and characterization of human prostate coactivator ARA54, a novel protein that associates with the androgen receptor. J Biol Chem 274:8570–8576.

Kiyama S, Morrison K, Zellweger T, Akbari M, Cox M, Yu D, Miyake H, Gleave ME. 2003. Castration-induced increases in insulin-like growth factor-binding protein 2 promotes proliferation of androgen-independent human prostate LNCaP tumors. Cancer Res 63:3575–3584.

Kousteni S, Bellido T, Plotkin LI, O'Brien CA, Bodenner DL, Han L, Han K, DiGregorio GB, Katzenellenbogen JA, Katzenellenbogen BS, Roberson PK, Weinstein RS, Jilka RL, Manolagas SC. 2001. Nongenotropic, sex-nonspecific signaling through the estrogen or androgen receptors: Dissociation from transcriptional activity. Cell 104:719–730.

Kupfer SR, Wilson EM, French FS. 1994. Androgen and glucocorticoid receptors interact with insulin degrading enzyme. J Biol Chem 269:20622–20628.

Lin HK, Yeh S, Kang HY, Chang C. 2001. Akt suppresses androgen-induced apoptosis by phosphorylating and inhibiting androgen receptor. Proc Natl Acad Sci USA 98:7200–7205.

Liu Y, Lehar S, Corvi C, Payne G, O'Connor R. 1998. Expression of the insulin-like growth factor I receptor C terminus as a myristylated protein leads to induction of apoptosis in tumor cells. Cancer Res 58:570–576.

Majeed N, Blouin MJ, Kaplan-Lefko PJ, Barry-Shaw J, Greenberg NM, Gaudreau P, Bismar TA, Pollak M. 2005. A germ line mutation that delays prostate cancer progression and prolongs survival in a murine prostate cancer model. Oncogene 24:4736–4740.

Miyake H, Nelson C, Rennie PS, Gleave ME. 2000a. Overexpression of insulin-like growth factor binding protein-5 helps accelerate progression to androgen-independence in the human prostate LNCaP tumor model through activation of phosphatidylinositol 3′-kinase pathway. Endocrinology 141:2257–2265.

Miyake H, Pollak M, Gleave ME. 2000b. Castration-induced up-regulation of insulin-like growth factor binding protein-5 potentiates insulin-like growth factor-I activity and accelerates progression to androgen independence in prostate cancer models. Cancer Res 60:3058–3064.

Mohler JL, Gregory CW, Ford OH III, Kim D, Weaver CM, Petrusz P, Wilson EM, French FS. 2004. The androgen axis in recurrent prostate cancer. Clin Cancer Res 10: 440–448.

O'Connor R, Kauffmann-Zeh A, Liu Y, Lehar S, Evan GI, Baserga R, Blattler WA. 1997. Identification of domains of the insulin-like growth factor I receptor that are required for protection from apoptosis. Mol Cell Biol 17: 427–435.

Pandini G, Mineo R, Frasca F, Roberts CT, Jr., Marcelli M, Vigneri R, Belfiore A. 2005. Androgens up-regulate the insulin-like growth factor-I receptor in prostate cancer cells. Cancer Res 65:1849–1857.

Plymate SR, Bae VL, Maddison L, Quinn LS, Ware JL. 1997a. Reexpression of the type 1 insulin-like growth factor receptor inhibits the malignant phenotype of simian virus 40 T antigen immortalized human prostate epithelial cells. Endocrinology 138:1728–1735.

Plymate SR, Bae VL, Maddison L, Quinn LS, Ware JL. 1997b. Type-1 insulin-like growth factor receptor reexpression in the malignant phenotype of SV40-T-immortalized human prostate epithelial cells enhances apoptosis. Endocrine 7:119–124.

Plymate SR, Tennant MK, Culp SH, Woodke L, Marcelli M, Colman I, Nelson PS, Carroll JM, Roberts CT, Jr., Ware JL. 2004. Androgen receptor (AR) expression in AR-negative prostate cancer cells results in differential effects of DHT and IGF-I on proliferation and AR activity between localized and metastatic tumors. Prostate 61: 276–290.

Pollak M. 2000. Insulin-like growth factor physiology and cancer risk. Eur J Cancer 36:1224–1228.

Pollak MN, Schernhammer ES, Hankinson SE. 2004. Insulin-like growth factors and neoplasia. Nat Rev Cancer 4:505–518.

Rubinstein M, Idelman G, Plymate SR, Narla G, Friedman SL, Werner H. 2004. Transcriptional activation of the insulin-like growth factor I receptor gene by the Kruppel-like factor 6 (KLF6) tumor suppressor protein: Potential interactions between KLF6 and p53. Endocrinology 145: 3769–3777.

Russo VC, Bach LA, Fosang AJ, Baker NL, Werther GA. 1997. Insulin-like growth factor binding protein-2 binds to cell surface proteoglycans in the rat brain olfactory bulb. Endocrinology 138:4858–4867.

Sadar MD. 1999. Androgen-independent induction of prostate-specific antigen gene expression via cross-talk between the androgen receptor and protein kinase A signal transduction pathways. J Biol Chem 274:7777–7783.

Sadar MD, Gleave ME. 2000. Ligand-independent activation of the androgen receptor by the differentiation agent butyrate in human prostate cancer cells. Cancer Res 60: 5825–5831.

Scher HI, Sawyers CL. 2005. Biology of progressive, castration-resistant prostate cancer: Directed therapies targeting the androgen-receptor signaling axis. J Clin Oncol 23:8253–8261.

Taplin ME, Balk SP. 2004. Androgen receptor: A key molecule in the progression of prostate cancer to hormone independence. J Cell Biochem 91:483–490.

Tennant MK, Thrasher JB, Twomey PA, Drivdahl RH, Birnbaum RS, Plymate SR. 1996. Protein and messenger ribonucleic acid (mRNA) for the type 1 insulin-like growth factor (IGF) receptor is decreased and IGF-II mRNA is increased in human prostate carcinoma

compared to benign prostate epithelium. J Clin Endocrinol Metab 81:3774–3782.

Thalmann GN, Sikes RA, Wu TT, Degeorges A, Chang SM, Ozen M, Pathak S, Chung LW. 2000. LNCaP progression model of human prostate cancer: Androgen-independence and osseous metastasis. Prostate 44 (2):91–103.

Titus MA, Gregory CW, Ford OH III, Schell MJ, Maygarden SJ, Mohler JL. 2005a. Steroid 5alpha-reductase isozymes I and II in recurrent prostate cancer. Clin Cancer Res 11:4365–4371.

Titus MA, Schell MJ, Lih FB, Tomer KB, Mohler JL. 2005b. Testosterone and dihydrotestosterone tissue levels in recurrent prostate cancer. Clin Cancer Res 11:4653–4657.

Udrisar DP, Wanderley MI, Porto RC, Cardoso CL, Barbosa MC, Camberos MC, Cresto JC. 2005. Androgen- and estrogen-dependent regulation of insulin-degrading enzyme in subcellular fractions of rat prostate and uterus. Exp Biol Med (Maywood) 230:479–486.

van Weerden WM, Bierings HG, van Steenbrugge GJ, de Jong FH, Schroder FH. 1992. Adrenal glands of mouse and rat do not synthesize androgens. Life Sci 50:857–861.

Wu JD, Odman A, Higgins LM, Haugk K, Vessella R, Ludwig DL, Plymate SR. 2005. In vivo effects of the human type I insulin-like growth factor receptor antibody A12 on androgen-dependent and androgen-independent xenograft human prostate tumors. Clin Cancer Res 11:3065–3074.

Zhang M, Latham DE, Delaney MA, Chakravarti A. 2005. Survivin mediates resistance to antiandrogen therapy in prostate cancer. Oncogene 24:2474–2482.

Journal of Cellular Biochemistry 99:392–401 (2006)

Interaction of IGF Signaling and the Androgen Receptor in Prostate Cancer Progression

Jennifer D. Wu,[1] Kathy Haugk,[2] Libby Woodke,[2] Peter Nelson,[3] Ilsa Coleman,[3] and Stephen R. Plymate[1,2]*

[1]Department of Medicine, University of Washington, Seattle, Washington
[2]Geriatric Research, Education and Clinical Center, Veterans Affairs Puget Sound Health Care System, Seattle, Washington
[3]Fred Hutchinson Cancer Research Center, Seattle, Washington

Abstract The insulin-like growth factor type I receptor (IGF-IR) has been suggested to play an important role in prostate cancer progression and possibly in the progression to androgen-independent (AI) disease. The term AI may not be entirely correct, in that recent data suggest that expression of androgen receptor (AR) and androgen-regulated genes is the primary association with prostate cancer progression after hormone ablation. Therefore, signaling through other growth factors has been thought to play a role in AR-mediated prostate cancer progression to AI disease in the absence of androgen ligand. However, existing data on how IGF-IR signaling interacts with AR activation in prostate cancer are conflicting. In this Prospect article, we review some of the published data on the mechanisms of IGF-IR/AR interaction and present new evidence that IGF-IR signaling may modulate AR compartmentation and thus alter AR activity in prostate cancer cells. Inhibition of IGF-IR signaling can result in cytoplasmic AR retention and a significant change in androgen-regulated gene expression. Translocation of AR from the cytoplasm to the nucleus may be associated with IGF-induced dephosphorylation. Since fully humanized antibodies targeting the IGF-IR are now in clinical trials, the current review is intended to reveal the mechanisms of potential therapeutic effects of these antibodies on AI prostate cancers. J. Cell. Biochem. 99: 392–401, 2006.

Key words: insulin-like growth factor type I receptor (IGF-IR); androgen receptor (AR); androgen-independent (AI) prostate cancer; AR co-regulators

In the presence or possibly absence of androgen ligand, the androgen receptor (AR) translocates from the cytosol to the nucleus and functions as a transcriptional factor, which may be necessary or even crucial for the progression of prostate cancer [Scher and Sawyers, 2005]. Classically, in the absence of androgen ligand, AR remains in the cytosol and is not active. Thus, it is of particular interest that malignant prostate cancer progression occurs frequently in men who have been surgically or chemically castrated. The progression of prostate cancer after castration has been termed androgen-independent (AI) prostate cancer. More interestingly, animal studies showed that when the expression of AR was disrupted, prostate cancer ceased to progress [Taplin and Balk, 2004]. All these together posed a conundrum if the AR, rather than the androgen ligand, is a driving force in prostate cancer progression. If so, it would suggest that the AR is functioning in a non-classical manner in the absence of steroid ligand. Although non-genomic mechanisms for AR function have been proposed through an interaction with SRC–Raf–Ras–Map kinase in the cytosol rather than the nucleus, this "traditional" non-genomic mechanism also requires the presence of androgen ligand and would not explain progression of disease in a ligand-independent manner [Kousteni et al., 2001; Pandini et al., 2005].

The concept of AR functioning in AI progression was first proposed by Mohler and colleages

Grant sponsor: National Cancer Institute; Grant sponsor: Veterans Affairs Research Service; Grant sponsor: Department of Defense; Grant numbers: 1K01CA116002-01, PO1-CA85859, DOD-PC040364.

*Correspondence to: Stephen R. Plymate, MD, 325 9th Avenue, Box 359625, Seattle, WA 98104.
E-mail: splymate@u.washington.edu

Received 15 February 2006; Accepted 27 February 2006
DOI 10.1002/jcb.20929

[Gregory et al., 1998; Mohler et al., 2004]. In relevant studies, tumor biopsies were taken from prostate cancer patients who had been androgen ablated and presented with progression of the cancer [Gregory et al., 1998; Mohler et al., 2004] In these samples, the AR primarily resided in a nuclear location, contrary to what had been expected in a castrated environment. This may in part due to residual levels of androgen in the prostate tissue. When tissue levels of androgen, testosterone, and dihydrotestosterone (DHT), were measured, although lower than in non-castrated men, they were still detected in the nanomolar range in many of the castrated men [Titus et al., 2005a]. This subtle level of tissue androgen may account for the nuclear localization of the AR and signal to activate an AR transcriptional program. The failure of castration to completely abolish intraprostatic androgens has also been evidenced in the study where normal men were placed on a GnRH antagonist for 4 weeks and in whom serum levels of testosterone (T) and DHT were clearly in the castrate range (Page and Bremner, personal communication). The source of the androgens in these castrate men has yet to be determined; however, the most likely source would be conversion from adrenal androgens. The prostate has active 5α-reductase systems for both isoforms I and II ensuring that circulating T can be readily converted to DHT in the prostate [Titus et al., 2005b]. In addition, recent microarray data has shown that the prostate contains mRNAs for the enzymes necessary for the conversion of cholesterol precursor into DHT; however this conversion has not been demonstrated in the prostate. Anti-androgen drugs, such as biclutamide, have not been shown to alter the translocation of the AR to the nucleus in prostate specimens from men treated with combined androgen blockade [Mohler et al., 2004]. Therefore, it is not clear whether it is the low levels of androgens driving prostate cancer progression in castrated men. Until a total androgen ablation mechanism in men is developed, the importance of residual androgens in tumor progression cannot be determined.

Castration studies on prostate cancer xenograft and transgenic mouse models support the speculation that residual androgen production following castration is only the partial driving force for tumor progression. Since mice do not produce adrenal androgens to any significant degree, castration in a mouse results in "complete androgen ablation" [Van Weerden et al., 1992]. In these models, tumors progress from androgen-dependent (AD) to AI following castration in spite of the fact that prostate specific androgen levels decrease to nearly undetectable levels, suggesting that residual androgens are unlikely to play a part in post-castration tumor progression [Thalmann et al., 2000; Corey et al., 2003]. We and others have shown that, in these models, the majority of tumor nuclei still contain AR after castration although some of the AR moves from the nucleus to the cytoplasm (Fig. 1). Furthermore, androgen-regulated genes continue to be expressed in "AI" disease [Corey et al., 2003]. Together, these data suggest that other mechanisms beyond the traditional ligand-receptor interaction of AR signaling are responsible for AD to AI prostate cancer progression.

Alterations in co-regulators of the AR, which may enhance ligand-independent AR translocation to the nucleus and binding to DNA, have been suggested as one of the mechanisms for ligand-independent AR signaling [Gregory et al., 1998; Fujimoto et al., 1999; Kang et al., 1999; Sadar, 1999; Sadar and Gleave, 2000; Mohler et al., 2004]. It has been suggested that some peptide growth factors can act directly at the androgen-binding domain of the AR or indirectly through modifying the phosphoryla-

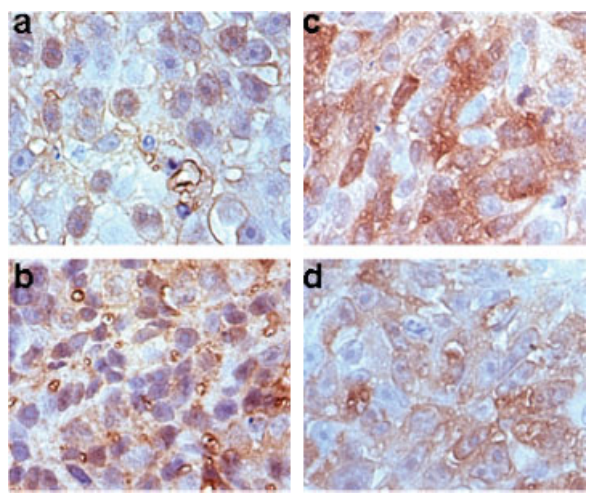

Fig. 1. IGF-IR signaling-induced translocation of AR into the nucleus in xenograft human prostate tumors. **a**: AR compartmentalization in the nucleus in intact animals. **b**: Blocking IGF-IR signaling with antibody A12 caused cytoplasmic retention of AR in intact animals. **c**: AR in the nucleus in castrated animals. **d**: A12 induced marked AR retention in the plasma in castrated animals.

tion status of the AR or its co-regulators to initiate AR signaling [Culig et al., 1994, 1995; Sadar, 1999; Sadar and Gleave, 2000; Lin et al., 2001]. In this "Prospectus" we examined the interactions between AR function and the activation of type 1 insulin-like growth factor receptor (IGF-IR). Among peptide growth factor-induced cell signaling, IGF activated IGF-IR signaling is a potential driving force for the growth of AI prostate cancer for several reasons as listed in Table I. In the following sections, we will examine the evidence for each of these components of potential interaction between the IGF-IR and AR.

IGF-IR IS NECESSARY FOR CELL TRANSFORMATION

Fibroblasts from IGF-IR knock out mice R^- do not transform spontaneously when compared to R^{wt} control cells. When the IGF-IR is re-expressed in these fibroblasts, transformation takes place. In SV40T immortalized prostate epithelial cells, inhibition of IGF-IR expression with an antisense construct significantly decreases colony formation in soft agar, a marker of transformation. In studies when growth hormone and IGF deficient LID mice were crossed with the transgenic prostate cancer (TRAMP) mouse, tumor development was significantly delayed Majeed et al., 2005). All these studies suggest an essential role of IGF-IR in cellular transformation. Hongo et al. [1998] have identified specific tyrosine residues on the β-subunit of the IGF-IR that are crucial for the transforming actions of the IGF-IR [O'connor et al., 1997; Liu et al., 1998].

TABLE I. Evidence for Interaction of the IGF-IR and AR in Prostate Cancer

1.	The IGF-IR is necessary for cell transformation
2.	Clinical data, although somewhat controversial suggests that higher levels of IGF-I in the serum of men predicts men at risk for developing clinical prostate cancer
3.	Androgens increase IGF-IR levels in prostate epithelial cells
4.	IGF-IR signaling alters AR phosphorylation
5.	IGF-IR signaling alters the AR transcriptional profile
6.	IGF-IR signaling effects translocation of the AR to the nucleus
7.	IGF-IR ligands increase in the progression of prostate cancer and are particularly abundant in bone where prostate cancer metastases are most abundant
8.	Xenograft models of prostate cancer respond differently to IGF-IR inhibition depending on the presence or absence of androgens
9.	IGF binding proteins (IGFBP) that enhance signaling of IGF ligands through the IGF-IR are increased in the period immediately after castration
10.	Inhibition of the IGF-IR in conjunction with castration
11.	Transcription factors that stimulate the IGF-IR promoter are also regulated by androgens

Since prostate cancer rarely develops in the absence of androgens, it is suspected that androgens are at least permissive in the transformation process of prostate epithelial cells. However, it should be noted that expression of the AR is necessary for normal luminal prostate epithelium to develop. It is suggested that maintaining certain levels of IGF-IR expression in the prostate may be necessary in normal prostate differentiation, increased levels of IGF-IR expression may be required for the prostate epithelia transformation process, and decreased IGF-IR expression may be required for prostate cancer malignant progression. This is consistent with the clinical findings that the levels of IGF-IR decrease following the initial transformation of the epithelium [Tennant et al., 1996]. This concept has been corroborated by the decrease in tumor metastases and increase in apoptosis associated with the re-expression IGF-IR in prostate cancer xenograft cell lines [Plymate et al., 1997a,b].

It should be pointed out that not all studies have shown an increase in IGF-IR expression during early prostate epithelia transformation or a decrease in IGF-IR expression in the progression to malignant prostate epithelia [Hellawell et al., 2002]. This may due to discrepancies in the choice of antibodies or technique in immunohistochemistry studies. The IGF-IR is a tyrosine kinase receptor that is only activated when located on the cell surface; although rapidly internalized upon activation, it is also rapidly processed through the golgi to be re-expressed on the cell surface.

CLINICAL DATA SUGGESTS THAT MEN IN THE HIGHER QUARTILES OF SERUM IGF-I LEVELS ARE AT A GREATER RISK FOR DEVELOPING PROSTATE CANCER

Large scale epidemiologic studies, such as the Physician's Health Study, have suggested that men with higher serum levels of IGF-1 as well as androgens may be at increased risk of developing prostate cancer in the following 6–9 years [Chan et al., 1998; Pollak, 2000; Pollak et al., 2004]. Also, in these studies serum levels of IGFBP-3 were inversely correlated with the risk of developing prostate cancer [Chan et al., 1998]. Of further note, the risk of cancer developing was more attributable to serum

IGF-I or IGFBP-3 than to serum testosterone. However, other studies have not shown an association of risk for prostate cancer with serum levels of IGF-I [Harman et al., 2000; Chen et al., 2005]. One should be aware that the risk of developing prostate cancer was not the primary end point of any of these studies nor did the results of the epidemiologic studies indicate a direct link between the IGF system and the risk of cancer.

ANDROGENS INCREASE IGF-IR EXPRESSION IN PROSTATE EPITHELIAL CELLS

We had initially detected an increase in IGF-IR expression at protein and mRNA levels in androgen-responsive prostate epithelial cell lines [Plymate et al., 2004]. This observation was subsequently confirmed by other investigators [Pandini et al., 2005]. The mechanism by which androgens increase the IGF-IR expression has been a topic of controversy. Pandini et al. [2005] have shown in their models that the increase in IGF-IR protein induced by androgens does not require nuclear translocation of the AR and is only partially blocked by bicluta-mide. On the other hand, this effect of AR on IGF-IR expression was completely inhibited by the ERK1/2 inhibitor PD980259 [Pandini et al., 2005]. These data suggested a "non-genomic" effect of androgen. This group further confirmed their findings using a mutated AR that will not translocate to the nucleus and demonstrated that the mutanted AR can activate the cytoplasmic Src–Raf–Ras–Map kinase pathway and enhance the transcriptional activity of IGF-IR promoter [Pandini et al., 2005]. Other investigators have not found that activation of this pathway is necessary for androgen-induced increases in IGF-IR expression [Plymate et al., 2004]. Other mechanisms including an increase in KFL6 (Kruppel factor like 6) in response to androgens have been suggested from the study in LnCaP lines (Levine-personal communication). We have shown that KFL6 increases IGF-IR expression by binding to the IGF-IR promoter [Rubinstein et al., 2004]. We have also shown in prostate cell lines that androgens can increase IGF-IR protein expression without an increase in its mRNA expression level, suggesting a post-transcriptional modification of IGF-IR expression, such as mRNA stability [Plymate et al., 2004]. Despite the existing controversials on the mechanisms, all the studies have consistently showed that androgens signaling through the AR result in increased IGF-IR protein expression in prostate epithelium, which is associated with increased phosphorylation of IGF-IR and increased cell proliferation in response to IGF ligands. However, it is not understood whether the induction of increased IGF-IR is part of the differentiation process of prostate epithelium or part of the mechanism for tumor progression. Since both IGF and androgens are necessary for epithelial differentiation, induction of increase in IGF-IR expression as part of the differentiating function of androgens may appear reasonable. On the other hand, increasing IGF-IR expression would be a mechanism by which androgens could enhance transformation and progression of prostate cancer.

IGF-IR ACTIVATION ALTERS AR PHOSPHORYLATION

One mechanism by which IGF-IR signaling could directly affect the function of the AR would be to alter AR phosphorylation. Studies by Lin et al. [2001] first suggested a role of IGF signaling in AR function. They observed that androgen induced apoptosis in AR transiently transfected DU-145 cells and treatment with IGF-1 decreased the transcriptional activity of the AR and inhibited apoptosis. We subsequently found that the effects on IGF-IR signaling on AR activity depended on whether the cells were from an orthotopic or a metastatic lesion [Plymate et al., 2004]. If the tumor was in the orthotopic site, IGF-IR activation inhibited AR transcription under a probasin promoter (AAR3) [Plymate et al., 2004]. In contrast, when the tumor was in the metastatic site, IGF-IR activation enhanced AR transcriptional activity on the AAR3 promoter. Interestingly, the effect of IGF-IR activation on the AR transcriptional activity in both primary and metastatic tumors appears to be mediated through the PI3K/AKT pathway [Plymate et al., 2004]. Lin et al. subsequently demonstrated that the effects of IGF on AR activity occurred in a biphasic manner in LnCaP cells: suppressing AR transcriptional activity at low passage numbers but enhancing AR transcriptional activity at high passage numbers [Lin et al., 2001]. Whether the effect is due to IGF-initiated phosphorylation of AR is rather controversial. Lin et al described that IGF-I phosphorylates AR at serines 210

and 790 [Lin et al., 2001], whereas Gioeli et al. [2002] failed to find any sites on the AR that were phosphorylated by IGF through a peptide terminal degeneration technique. We examined the effect of IGF-IR activation on AR phosphorylation in AR-transfected M12 (M12AR) cells. We showed that AR phosphorylation was decreased in the presence of IGF-I and that this effect was blocked by an inhibitory IGF-IR antibody A12 (Fig. 2a). Our newest study indicated that serine 16 on the AR is a potential site of dephosphorylation whereas serine 81 on the AR is a potential site of phosphorylation by IGF (Fig. 2b). The reasons for discrepancies between studies are not entirely clear. One possible reason for differences in phosphorylation would be differential expression of PP2A in different cell types.

IGF-IR SIGNALING EFFECTS TRANSLOCATION OF THE AR TO THE NUCLEUS

Phosphorylation of the AR may result in several changes that could alter the AR transcriptional functions. One of these effects could be translocation of the AR to the nucleus. Whereas AR phosphorylation was thought to be necessary for nuclear translocation, recent data has shown that phosphorylation of AR at serine 650, which takes place after the AR is in the nucleus and bound to DNA, results in the export of AR from the nucleus [Gioeli et al., 2006]. Thus, the process of dephosphorylation of specific serines on the AR may account for retention of AR in the nucleus and accentuated signaling. As we have shown in Figure 2, IGF decreases phosphorylation of the AR in our M12AR cells. We also have evidence that IGF can enhance AR nuclear translocation in the absence of androgens and that this effect can be inhibited by an IGF-IR inhibitory antibody (Fig. 3a). We have also demonstrated the changes in AR compartmentalization in nuclear and cytoplasmic fractions in response to IGF using Western blot analyses (Fig. 3b). Using the AAR3 probasin reporter assay, we show a significant transactivation of the AR in the absence of androgen and enhanced AR activation in the presence of androgen by IGF-I in M12AR cells. The AR transactivation response to IGF can be blocked by the IGF-IR antibody A12. These data indicate that even in the absence of androgen, IGF can induce transactivation of the AR. Whether this is attributed to changes in phosphorylation of the AR as we have discussed or to the recruitment of AR co-

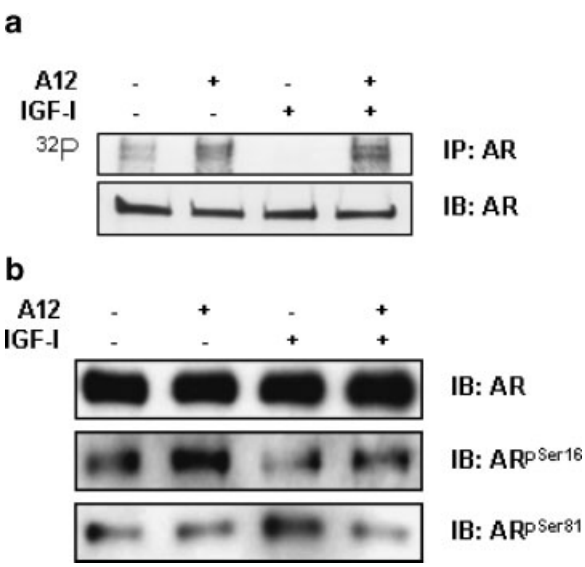

Fig. 2. IGF-I induces AR dephosphorylation. **a**: M12AR cells were labeled with ortho-^{32}P. Cell lysates were immunoprecipitated (IP) with AR-specific antibody. IB, western blotting. **b**: M12AR cells were IB with serine-specific anti-AR antibody.

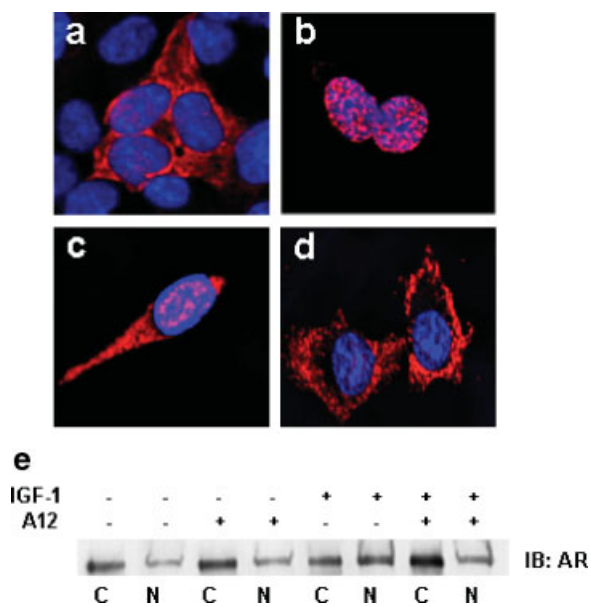

Fig. 3. Confocal image and cell fractionation showing IGF-I-induced AR translocation into the nucleus in M12AR cell lines. **a**: M12AR cells in IGF-I, DHT free medium. **b**: M12AR cells in medium containing 10^{-8}M of DHT. **c**: M12AR cells in medium containing 10 ng/ml of IGF-I. **d**: Medium containing 10 ng/ml of IGF-I and 10 μg/ml of anti-IGF-IR antibody A12. **e**: AR in cytosol and nuclear fractions of M12AR cells under various culture conditions. Red fluorescence. AR, androgen receptor. IGF-I, insulin-like growth factor I. DHT, dihydrotestosterone.

factors, or to both has yet to be determined. Regardless, these studies suggest that, in castrated patients, the increase in AR expression coupled with intact IGF-IR signaling can lead to AR-mediated AI prostate cancer progression. This marks the IGF-IR a potential therapeutic target in post-castrated prostate cancer.

XENOGRAFT MODELS OF PROSTATE CANCER RESPOND DIFFERENTLY TO IGF-IR INHIBITION DEPENDING ON THE PRESENCE OR ABSENCE OF ANDROGENS

We have reported in prostate cancer human xenograft models that inhibition of the IGF-IR with A12 results in a decreased rate of tumor growth in AD and AI tumors [Wu et al., 2005]. However, when we examined the mechanisms by which A12 caused decrease in growth rate, we noted marked differences depending on whether the tumors were AD or AI. In the AD tumors we found that A12 treatment resulted in a combination of apoptosis and G1 cell cycle arrest, whereas in the AI tumors we found that tumor cells arrested in G2 with no occurrence of apoptosis [Wu et al., 2005]. The question arose as to whether these differences in responses were due to a change in the character of the tumor or the absence of androgen. In order to address this issue, we implanted the AI tumor into intact animals. As predicted, tumor growth was inhibited in the A12 treated animals compared to vehicle treated controls. Interestingly, a majority of these tumors displayed an apoptotic response and G1 cell cycle arrest as opposed to the lack of apoptosis when implanted in the castrated animals. To determine potential mechanisms for this effect of androgen on the tumors, we performed cDNA microarray analyses of A12-treated AI tumors from castrated and intact animals and found marked differences in the gene expression profiles (Fig. 4). Some genes such as PP2A and TSC-22 were regulated in opposite direction with A12 treatment, depending on the presence or absence of androgens. It is of interest that TSC-22 has been shown to be androgen-regulated and its expression decreases from benign prostate luminal epithelium to cancer. Another interesting gene differentiated expressed is IGFBP-5, which has been demonstrated to increase post-castration and is associated with recovery from castration-induced apoptosis [Miyake et al., 2000a].

IGF BINDING PROTEINS (IGFBP) THAT ENHANCE SIGNALING OF IGF LIGANDS THROUGH THE IGF-IR ARE INCREASED IN THE PERIOD IMMEDIATELY AFTER CASTRATION

Following castration, IGFBP-2 and IGFBP-5 have been shown to increase significantly in both human prostate and mouse models of prostate cancer. Both of these IGFBPs can increase IGF-ligand signaling through the IGF-IR and enhance recovery from castration induced apoptosis and cell cycle arrest. These two IGFBPs accomplish this task by binding to extracelluar matrix and maintaining a higher concentration of IGF ligand in the proximity of the IGF-IR [Jones et al., 1995; Russo et al., 1997; Kiyama et al., 2003]. The functional importance of these changes has been demonstrated by the studies of Miyake et al. [2000b] in which overexpression of these IGFBPs in LnCaP cells markedly enhances cell growth following androgen withdraw. Using antisense oligonucleotides to IGFBP-2 or IGFBP-5, this group was able to demonstrate the stimulatory effects of the IGFBPs on tumor growth [Kiyama et al., 2003].

INHIBITION OF THE IGF-IR IN CONJUNCTION WITH CASTRATION THERAPY FOR PROSTATE CANCER

These studies suggest that blocking IGF-IR signaling at the time of castration would enhance the effects of androgen withdraw. Preliminary studies in our laboratory using mouse xenograft models have shown a marked enhancement of the castration effect on prostate tumor growth with the inhibitory IGF-IR antibody A12. Potential mechanisms of the augmented effect of A12 on androgen withdraw may include suppression of Survivin, a member of the Inhibitor of Apoptosis (IAP) family of proteins that has been shown to play a role in the recovery process of anti-androgen therapy [Zhang et al., 2005].

IGF-IR ACTIVATION CAN STIMULATE AR CO-FACTORS THAT ENHANCE AR SIGNALING

Insulin-like growth factor may also influence AR signaling by increasing the expression of AR

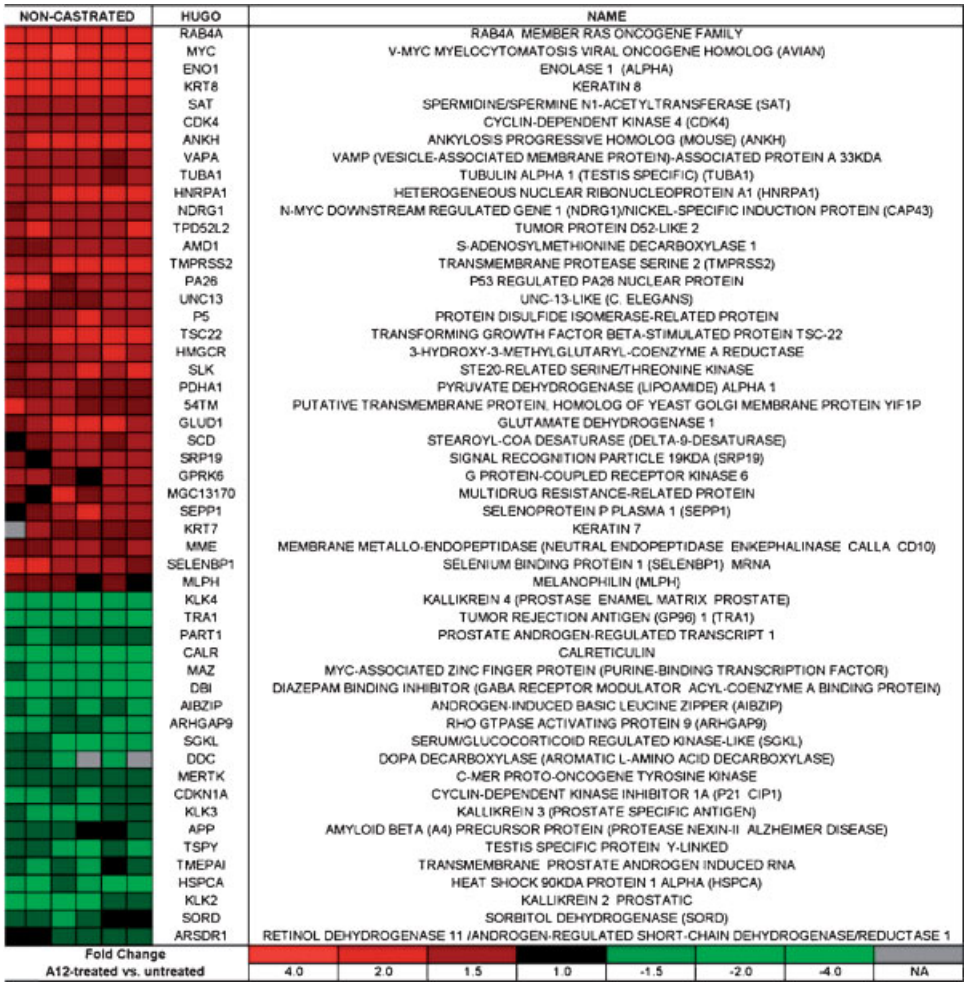

Fig. 4. cDNA microarray expression values of androgen-regulated genes differentially expressed in LuCaP 35V tumors from A12-treated relative to untreated non-castrated mice. There were 82 unique genes known to be androgen-regulated which had significantly consistent gene expression across all samples as compared to no change by a one-sample *t*-test in SAM (<1% FDR significance cut-off used). The scale represents fold-change in A12-treated relative to untreated tumors.

co-stimulatory factors. Given the known 100 or more AR co-regulatory factors, it is not surprising that IGF-IR activation would enhance the expression or activation of one or more co-regulators of the AR. Amongst them, TIF-2 (GRIP-1) and insulin degrading enzyme (IDE) are of particular interest. Studies in a series of human prostate specimens from men with prostate cancer, Mohler and Wilson have demonstrated an increased expression of TIF-2 in most of the recurrent AI prostate cancers that also have a high levels of AR in the nucleus [Gregory et al., 2001]. The same group has also shown the coincidence of increased TIF-2 expression with the recurrence of AI human prostate cancer in xenograft models. Mohler has also demonstrated that overexpression of TIF-2 in vitro can increase AR transcriptional activity in the presence of the physiological concentrations of adrenal androgen. Studies have shown that IDE is a potent co-stimulator of AR transcriptional activity and the ability of IDE to bind to the AR can be regulated by insulin and IGF ligands [Kupfer et al., 1994]. In addition, as the name implies, IDE can degrade insulin, IGF-I and IGF-II [Udrisar et al., 2005].

CONCLUSION

In this review, we have summarized our current understandings of the interactions between the IGF system and the AR (Fig. 5).

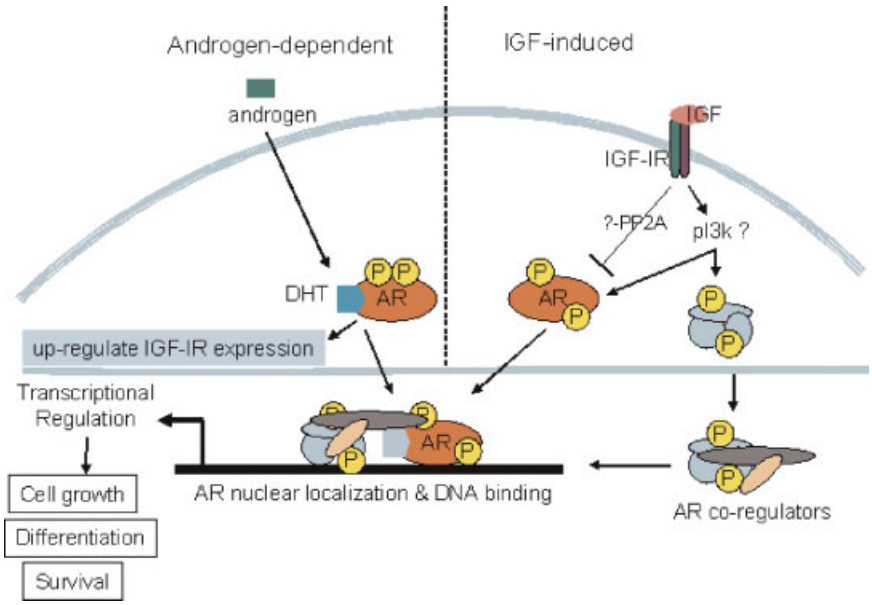

Fig. 5. Interactions of the IGF system with AR signaling. pI3k, phosphoinositide 3-kinase. PP2A, protein phosphotase 2A. [Color figure can be viewed in the online issue, which is available at www.interscience.wiley.com.]

The ability of IGF signaling to potentiate the transcriptional activity of the AR in the face of low to no androgen makes the IGF system, especially the IGF-IR, a strong candidate that leads progression of AI prostate cancer through AR signaling.

ACKNOWLEDGMENTS

Supported by NIH Temin Award 1K01CA116002-01 (J.D.W.), NIH grant PO1-CA85859, Veterans Affairs Research Service, and DOD Prostate Cancer Research grant PC040364 (S.R.P.). We thank our collaborators G.S. Yang and B.M. Paschal at the University of Virginia for donating Figure 2b.

REFERENCES

Chan JM, Stampfer MJ, Giovannucci E, Gann PH, Ma J, Wilkinson P, Hennekens CH, Pollak M. 1998. Plasma insulin-like growth factor-I and prostate cancer risk: A prospective study. Science 279:563–566.

Chen C, Lewis SK, Voigt L, Fitzpatrick A, Plymate SR, Weiss NS. 2005. Prostate carcinoma incidence in relation to prediagnostic circulating levels of insulin-like growth factor I, insulin-like growth factor binding protein 3, and insulin. Cancer 103:76–84.

Corey E, Quinn JE, Buhler KR, Nelson PS, Macoska JA, True LD, Vessella RL. 2003. LuCaP 35: A new model of prostate cancer progression to androgen independence. Prostate 55:239–246.

Culig Z, Hobisch A, Cronauer MV, Radmayr C, Trapman J, Hittmair A, Bartsch G, Klocker H. 1994. Androgen receptor activation in prostatic tumor cell lines by insulin-like growth factor-I, keratinocyte growth factor, and epidermal growth factor. Cancer Res 54:5474–5478.

Culig Z, Hobisch A, Cronauer MV, Hittmair A, Radmayr C, Bartsch G, Klocker H. 1995. Activation of the androgen receptor by polypeptide growth factors and cellular regulators. World J Urol 13:285–289.

Fujimoto N, Yeh S, Kang HY, Inui S, Chang HC, Mizokami A, Chang C. 1999. Cloning and characterization of androgen receptor coactivator, ARA55, in human prostate. J Biol Chem 274:8316–8321.

Gioeli D, Ficarro SB, Kwiek JJ, Aaronson D, Hancock M, Catling AD, White FM, Christian RE, Settlage RE, Shabanowitz J, Hunt DF, Weber MJ. 2002. Androgen receptor phosphorylation. Regulation and identification of the phosphorylation sites. J Biol Chem 277:29304–29314.

Gioeli D, Black BE, Gordon V, Spencer A, Kesler CT, Eblen ST, Paschal BM, Weber MJ. 2006. Stress kinase signaling regulates androgen receptor phosphorylation, transcription, and localization. Mol Endocrinol 20:503–515.

Gregory CW, Hamil KG, Kim D, Hall SH, Pretlow TG, Mohler JL, French FS. 1998. Androgen receptor expression in androgen-independent prostate cancer is associated with increased expression of androgen-regulated genes. Cancer Res 58:5718–5724.

Gregory CW, He B, Johnson RT, Ford OH, Mohler JL, French FS, Wilson EM. 2001. A mechanism for androgen receptor-mediated prostate cancer recurrence after androgen deprivation therapy. Cancer Res 61:4315–4319.

Harman SM, Metter EJ, Blackman MR, Landis PK, Carter HB. 2000. Serum levels of insulin-like growth factor I

(IGF-I), IGF-II, IGF-binding protein-3, and prostate-specific antigen as predictors of clinical prostate cancer. J Clin Endocrinol Metab 85:4258–4265.

Hellawell GO, Turner GD, Davies DR, Poulsom R, Brewster SF, Macaulay VM. 2002. Expression of the type 1 insulin-like growth factor receptor is up-regulated in primary prostate cancer and commonly persists in metastatic disease. Cancer Res 62:2942–2950.

Hongo A, Yumet G, Resnicoff M, Romano G, O'Connor R, Baserga R. 1998. Inhibition of tumorigenesis and induction of apoptosis in human tumor cells by the stable expression of a myristylated COOH terminus of the insulin-like growth factor I receptor. Cancer Res 58: 2477–2484.

Jones JI, Clemmons DR. 1995. Insulin-like growth factors and their binding proteins: Biological actions. Endocrinol Rev 16:3–34.

Kang HY, Yeh S, Fujimoto N, Chang C. 1999. Cloning and characterization of human prostate coactivator ARA54, a novel protein that associates with the androgen receptor. J Biol Chem 274:8570–8576.

Kiyama S, Morrison K, Zellweger T, Akbari M, Cox M, Yu D, Miyake H, Gleave ME. 2003. Castration-induced increases in insulin-like growth factor-binding protein 2 promotes proliferation of androgen-independent human prostate LNCaP tumors. Cancer Res 63:3575–3584.

Kousteni S, Bellido T, Plotkin LI, O'Brien CA, Bodenner DL, Han L, Han K, DiGregorio GB, Katzenellenbogen JA, Katzenellenbogen BS, Roberson PK, Weinstein RS, Jilka RL, Manolagas SC. 2001. Nongenotropic, sex-nonspecific signaling through the estrogen or androgen receptors: Dissociation from transcriptional activity. Cell 104:719–730.

Kupfer SR, Wilson EM, French FS. 1994. Androgen and glucocorticoid receptors interact with insulin degrading enzyme. J Biol Chem 269:20622–20628.

Lin HK, Yeh S, Kang HY, Chang C. 2001. Akt suppresses androgen-induced apoptosis by phosphorylating and inhibiting androgen receptor. Proc Natl Acad Sci USA 98:7200–7205.

Liu Y, Lehar S, Corvi C, Payne G, O'Connor R. 1998. Expression of the insulin-like growth factor I receptor C terminus as a myristylated protein leads to induction of apoptosis in tumor cells. Cancer Res 58:570–576.

Majeed N, Blouin MJ, Kaplan-Lefko PJ, Barry-Shaw J, Greenberg NM, Gaudreau P, Bismar TA, Pollak M. 2005. A germ line mutation that delays prostate cancer progression and prolongs survival in a murine prostate cancer model. Oncogene 24:4736–4740.

Miyake H, Nelson C, Rennie PS, Gleave ME. 2000a. Overexpression of insulin-like growth factor binding protein-5 helps accelerate progression to androgen-independence in the human prostate LNCaP tumor model through activation of phosphatidylinositol 3′-kinase pathway. Endocrinology 141:2257–2265.

Miyake H, Pollak M, Gleave ME. 2000b. Castration-induced up-regulation of insulin-like growth factor binding protein-5 potentiates insulin-like growth factor-I activity and accelerates progression to androgen independence in prostate cancer models. Cancer Res 60:3058–3064.

Mohler JL, Gregory CW, Ford OH III, Kim D, Weaver CM, Petrusz P, Wilson EM, French FS. 2004. The androgen axis in recurrent prostate cancer. Clin Cancer Res 10: 440–448.

O'Connor R, Kauffmann-Zeh A, Liu Y, Lehar S, Evan GI, Baserga R, Blattler WA. 1997. Identification of domains of the insulin-like growth factor I receptor that are required for protection from apoptosis. Mol Cell Biol 17: 427–435.

Pandini G, Mineo R, Frasca F, Roberts CT, Jr., Marcelli M, Vigneri R, Belfiore A. 2005. Androgens up-regulate the insulin-like growth factor-I receptor in prostate cancer cells. Cancer Res 65:1849–1857.

Plymate SR, Bae VL, Maddison L, Quinn LS, Ware JL. 1997a. Reexpression of the type 1 insulin-like growth factor receptor inhibits the malignant phenotype of simian virus 40 T antigen immortalized human prostate epithelial cells. Endocrinology 138:1728–1735.

Plymate SR, Bae VL, Maddison L, Quinn LS, Ware JL. 1997b. Type-1 insulin-like growth factor receptor reexpression in the malignant phenotype of SV40-T-immortalized human prostate epithelial cells enhances apoptosis. Endocrine 7:119–124.

Plymate SR, Tennant MK, Culp SH, Woodke L, Marcelli M, Colman I, Nelson PS, Carroll JM, Roberts CT, Jr., Ware JL. 2004. Androgen receptor (AR) expression in AR-negative prostate cancer cells results in differential effects of DHT and IGF-I on proliferation and AR activity between localized and metastatic tumors. Prostate 61: 276–290.

Pollak M. 2000. Insulin-like growth factor physiology and cancer risk. Eur J Cancer 36:1224–1228.

Pollak MN, Schernhammer ES, Hankinson SE. 2004. Insulin-like growth factors and neoplasia. Nat Rev Cancer 4:505–518.

Rubinstein M, Idelman G, Plymate SR, Narla G, Friedman SL, Werner H. 2004. Transcriptional activation of the insulin-like growth factor I receptor gene by the Kruppel-like factor 6 (KLF6) tumor suppressor protein: Potential interactions between KLF6 and p53. Endocrinology 145: 3769–3777.

Russo VC, Bach LA, Fosang AJ, Baker NL, Werther GA. 1997. Insulin-like growth factor binding protein-2 binds to cell surface proteoglycans in the rat brain olfactory bulb. Endocrinology 138:4858–4867.

Sadar MD. 1999. Androgen-independent induction of prostate-specific antigen gene expression via cross-talk between the androgen receptor and protein kinase A signal transduction pathways. J Biol Chem 274:7777–7783.

Sadar MD, Gleave ME. 2000. Ligand-independent activation of the androgen receptor by the differentiation agent butyrate in human prostate cancer cells. Cancer Res 60: 5825–5831.

Scher HI, Sawyers CL. 2005. Biology of progressive, castration-resistant prostate cancer: Directed therapies targeting the androgen-receptor signaling axis. J Clin Oncol 23:8253–8261.

Taplin ME, Balk SP. 2004. Androgen receptor: A key molecule in the progression of prostate cancer to hormone independence. J Cell Biochem 91:483–490.

Tennant MK, Thrasher JB, Twomey PA, Drivdahl RH, Birnbaum RS, Plymate SR. 1996. Protein and messenger ribonucleic acid (mRNA) for the type 1 insulin-like growth factor (IGF) receptor is decreased and IGF-II mRNA is increased in human prostate carcinoma

compared to benign prostate epithelium. J Clin Endocrinol Metab 81:3774–3782.

Thalmann GN, Sikes RA, Wu TT, Degeorges A, Chang SM, Ozen M, Pathak S, Chung LW. 2000. LNCaP progression model of human prostate cancer: Androgen-independence and osseous metastasis. Prostate 44 (2):91–103.

Titus MA, Gregory CW, Ford OH III, Schell MJ, Maygarden SJ, Mohler JL. 2005a. Steroid 5alpha-reductase isozymes I and II in recurrent prostate cancer. Clin Cancer Res 11:4365–4371.

Titus MA, Schell MJ, Lih FB, Tomer KB, Mohler JL. 2005b. Testosterone and dihydrotestosterone tissue levels in recurrent prostate cancer. Clin Cancer Res 11:4653–4657.

Udrisar DP, Wanderley MI, Porto RC, Cardoso CL, Barbosa MC, Camberos MC, Cresto JC. 2005. Androgen- and estrogen-dependent regulation of insulin-degrading enzyme in subcellular fractions of rat prostate and uterus. Exp Biol Med (Maywood) 230:479–486.

van Weerden WM, Bierings HG, van Steenbrugge GJ, de Jong FH, Schroder FH. 1992. Adrenal glands of mouse and rat do not synthesize androgens. Life Sci 50:857–861.

Wu JD, Odman A, Higgins LM, Haugk K, Vessella R, Ludwig DL, Plymate SR. 2005. In vivo effects of the human type I insulin-like growth factor receptor antibody A12 on androgen-dependent and androgen-independent xenograft human prostate tumors. Clin Cancer Res 11:3065–3074.

Zhang M, Latham DE, Delaney MA, Chakravarti A. 2005. Survivin mediates resistance to antiandrogen therapy in prostate cancer. Oncogene 24:2474–2482.

Regulation of Global Gene Expression in the Bone Marrow Microenvironment by Androgen: Androgen Ablation Increases Insulin-Like Growth Factor Binding Protein-5 Expression

Chang Xu,[1] Lynn F. Graf,[2] Ladan Fazli,[3] Ilsa M. Coleman,[4] Denise E. Mauldin,[4] Danbin Li,[3] Peter S. Nelson,[4] Martin Gleave,[3] Stephen R. Plymate,[5] Michael E. Cox,[3] Beverly J. Torok-Storb,[2] and Beatrice S. Knudsen[1]*

[1]*Division of Public Health Sciences, Fred Hutchinson Cancer Research Center, Seattle, Washington*
[2]*Division of Clinical Research, Fred Hutchinson Cancer Research Center, Seattle, Washington*
[3]*Clinical Research, The Prostate Centre, Vancouver General Hospital, Vancouver, British Columbia, Canada*
[4]*Division of Human Biology, Fred Hutchinson Cancer Research Center, Seattle, Washington*
[5]*Department of Medicine, Division of Gerontology and Geriatric Medicine, University of Washington and GRECC VAPSHCS, Seattle, Washington*

BACKGROUND. Prostate cancer frequently metastasizes to bone. Androgen suppression treatment is initially highly effective, but eventually results in resistant cancer cells. This study evaluates the effects of androgen suppression on the bone and bone marrow (BM). In particular we questioned whether the androgen therapy could adversely facilitate prostate cancer progression through an increase growth factor secretion by the bone microenvironment.

METHODS. Global gene expression is analyzed on mPEDB DNA microarrays. Insulin-like growth factor binding protein-5 (IGFBP5) is detected by immunohistochemistry in mouse tissues and its regulation measured by qPCR and Western blotting in human BM stromal cells. Effects of extracellular matrix-associated IGFBP5 on human prostate epithelial cells are tested in an MTS cell-growth assay.

RESULTS. Castration increases expression of 159 genes (including 4 secreted cytokines) and suppresses expression of 84 genes. IGFBP5 is most consistently increased and the increase in expression is reversed by testosterone administration. IGFBP5 protein is detected in vivo in osteoblasts, BM stromal cells, and endothelial cells. Primary human stromal cell cultures secrete IGFBP5. In vitro, treatment of immortalized human marrow stromal cells with charcoal-stripped serum increases IGFBP5 mRNA expression, which is reversed by androgen supplementation. IGFBP5 is incorporated into the extracellular matrix. Further, IGFBP5 immobilized on extracellular matrices of stromal cells enhances the growth of immortalized prostate epithelial cells.

CONCLUSIONS. Androgen suppressive therapy increases IGFBP5 in the BM microenvironment and thereby may facilitate the progression of prostate cancer. *Prostate 67: 1621–1629, 2007.*

KEY WORDS: **bone marrow microenvironment; androgen suppression; IGFBP5; prostate cancer**

This article contains supplementary material, which may be viewed at the The Prostate website at http://www.interscience.wiley.com/jpages/0270-4137/suppmat/index.html.

Grant sponsor: Department of Defense; Grant numbers: DAMD17-02-1-0159, W81XWH-06-1-0171; Grant sponsor: PNW Prostate Cancer SPORE; Grant number: CA97186; Grant sponsor: NIH; Grant numbers: CA85859, DK65204, DK56465, HL62923; Grant sponsor: Fred Hutchinson Cancer Research Center; Grant number: P30CA015704.

*Correspondence to: Beatrice S. Knudsen, MD, PhD, PHS, M5-A864, Fred Hutchinson Cancer Research Center, 1100 Fairview Ave. N., Seattle, WA 98109. E-mail: bknudsen@fhcrc.org

Received 7 June 2007; Accepted 23 July 2007
DOI 10.1002/pros.20655
Published online 6 September 2007 in Wiley InterScience (www.interscience.wiley.com).

INTRODUCTION

Androgen suppressive therapy has proven a significant benefit when administered in an adjuvant setting together with radiation therapy for the treatment of prostate cancer [1]. Systemic androgen deprivation kills disseminated prostate cancer cells; however, some cells survive the treatment. Survival under androgen deficient conditions may be an inherent property of certain cancer cells but may also be stimulated by factors in the microenvironment. Since prostate cancer commonly metastasizes to the skeleton [2], the environment consists primarily of bone marrow (BM) stroma and hematopoietic BM. Disseminated prostate cancer cells extraversate from the circulation through BM sinusoids [3]. Prostate specific antigen (PSA)-expressing cells are detectable in BM specimens of 54% of patients at the time of prostatectomy, indicating that cancer cells disseminate early [4]. However, disease progression is often delayed by years, suggesting that disseminated cancer cells can remain in a state of dormancy before renewing their growth. Here we investigate whether a decrease in androgen level affects the BM and whether it generates a permissive microenvironment for the growth of prostate cancer cells.

In the BM microenvironment, the androgen receptor is expressed by BM stromal cells, osteoblasts, endothelial cells, osteocytes, and chondrocytes [5,6]. Androgens increase the thickness of bone, augment the hematocrit and regulate the expansion of B-cells [7,8]. The effects of androgen on hematopoiesis are, to a large extent, mediated indirectly through the androgen receptor activity in BM stromal cells [9]. However, androgen-sensitive factors that regulate hematopoiesis are unknown.

Insulin-like growth factors (IGF) and their binding proteins (IGFBP 1–6) are involved in normal and malignant growth of prostate epithelial cells [10]. While there were conflicting results about the expression of the IGF1 receptor (IGFR) in localized and metastatic prostate cancer in formalin-fixed tissues [11–14], a recent study using frozen tissues clearly demonstrates high IGFR expression in localized and metastatic cancer as well as in stromal cells surrounding the tumor [15]. In addition, pre-clinical studies with an inhibitory IGFR antibody (A12) reduces the growth of prostate cancer xenografts [16]. IGFs are abundant growth factors in bone and activation of the IGF pathway may lead to ligand-independent activation of the AR [17–19]. The bioavailability of IGF is regulated by a group of IGF binding proteins (IGFBP 1–6). Androgen regulates the expression of IGFBP 2, 3, 4, and 5 in the prostate [20–22]. In the bone, IGFBP 4 and 5 are the two major binding proteins that modulate the IGF activity [23] and IGFBP5 is sequestered by the bone matrix. IGFBP5 may also act independently of IGF as a growth stimulator for osteoblasts, through binding to a separate receptor on the cell surface [24,25]. In human bone and BM, IGFBP5 is expressed in chondrocytes, osteoblasts and osteocytes. These cell types express androgen receptors [26–29], however only androgen regulation of IGFBP 2, 3, 4 and not of IGFBP5 has been examined in-vitro [30].

In this study we sought to measure the effects of androgen suppressive therapy on the BM environment by transcriptional profiling of castrated and sham operated mice. We observed a predominant increase in gene expression after androgen suppression and in particular of IGFBP5. Subsequent in vitro experimentation confirmed IGFBP5 regulation by androgen in human BM stromal cells and demonstrated the functional relevance of elevated IGFBP5 in the BM microenvironment.

MATERIALS AND METHODS

Mice

Castrated or sham-castrated C57BL/6 mice were purchased from the Jackson Laboratory (Bar Harbor, ME) after surgery at 7 weeks of age. Testosterone or placebo pellets (12.5 mg 60-day slow release, Innovative Research of America, Sarasota, FL) were implanted for 4 weeks. Femoral, tibial and humeral bones were collected from 17-week old (young mice, 10 weeks after castration) and 59-week old (old mice, 52 weeks after castration) mice. The experiment was performed in accordance with an approved Animal Care and Use Committee (IACUC) protocol.

Cells

Primary bone stromal cells HB5, HB6, and HB15 were derived from three individuals with IRB approval and maintained in MEM-alpha medium with 10% FBS (Hyclone, Logan, UT). Human immortalized bone stromal cells, HS27a [42] and prostate epithelial cells, P69 [43] were propagated in RPMI1640 with 10% FBS. Human sarcoma MG63 cells were maintained in DMEM with 10% FBS. Human primary prostate stromal and epithelial cells were cultured as previously described [44].

RNA Isolation and Microarrays

Total RNA was isolated from pulverized bone or cultured cells using TRIZOL® (Invitrogen, Carlsbad, CA) and the RNeasy® kit (Qiagen, Valencia, CA). Microarray hybridization and processing of raw data is described in Ref. [45]. Differentially expressed genes

were analyzed by hierarchical clustering using Cluster 3.0 [46]. The microarray data have been submitted to the Gene Expression Omnibus (GEO) public database at NCBI. The accession numbers are GSE5775 for castration versus sham-operation and GSE5776 for testosterone replacement versus placebo.

Reverse Transcription and Quantitative Real-Time PCR (qPCR)

cDNA was synthesized using SuperScript™ II Reverse Transcriptase (Invitrogen). Primers for qPCR spanned across intron–exon junctions and the sequences are listed in Supplementary Table I. qPCR conditions with Platinum® SYBR® Green in an ABI Prism 7700 Sequence Detector (Applied Biosystems, Foster City, CA) were: 10 min at 95°C, 40 cycles at 95°C for 15 sec, 30 sec at 60°C, 30 sec at 72°C.

Immunohistochemical Staining

Mouse femurs were fixed in 10% buffered formalin at 4°C overnight and decalcified in EDTA (Decal Corp., Tallman, NY). Antigens were retrieved with EDTA, pH8 at 95°C for 8 min. The anti-IGFBP5 antibody (sc-6006, Santa Cruz Biotechnology Inc., Santa Cruz, CA) was diluted 1:100 for incubation in the Vantana autostainer model Discover XT™ (Vantana Medical System, Tuscan, AZ).

Serum Testosterone Measurement

Mouse blood samples were collected by cardiac puncture and sent for measurement of serum testosterone to the Center for Reproductive Biology, Washington State University, Pullman, WA. The sensitivity of the measurement was 0.10 ng/ml.

Preparation of Cell Lysate, Conditioned Medium (CM), and Extracellular Matrix (ECM)

Cells were lyzed in RIPA buffer [47] containing protease and phosphatase inhibitors (Roche Applied Science, Mannheim, Germany). Serum-free medium was conditioned for 48 hr and concentrated with an Amicon Ultra-15, 5 kDa Centrifugal Filter (Millipore, Billerica, MA). ECM was prepared as described by Knudsen et al. [48]. ECM on plates was used immediately for growth assays or solubilized in RIPA buffer.

Immunoprecipitation and Immunoblotting

Proteins (500 μg) were precipitated with 10 μl anti-IGFBP5 (Catalog # 06-110, Chemicon International, Inc., Temecula, CA) overnight and proteinG agarose beads (Sigma, Saint Louis, MO) for 2 hr. Total proteins (40 μg) were analyzed on 12% NuPAGE or 4–12% Bis-Tris Gels (Invitrogen) and transferred to Immobilon-P (Millipore). Membranes were blocked with 5% milk and probed with 1:1,000 anti-IGFBP5. Blots were developed with the Pico Chemiluminescent (Pierce Biotechnology, Inc., Rockford, IL).

Regulation of IGFBP5 Expression in HS27a

HS27a cells were cultured in Phenol red-free medium with 10% charcoal-stripped FBS (100 ml of FBS stirred with 15 g of dextran-treated charcoal at 4°C overnight and sterilized). Methyltrienolone (R1881, PerkinElmer Life And Analytical Sciences, Inc., Wellesley, MA) was added as a synthetic androgen.

P69 Proliferation in Response to IGFBP5

HS27a ECM in 24-well plates was incubated with rIGFBP5 without or with human rIGF1 (Sigma) or mono-biotinyl IGF2 (GroPep Limited, Adelaide, SA, Australia) for 4 hr. After the plates were washed, 40,000 P69 cells were seeded per well in serum free medium containing 10 ng/ml IGF1 or IGF2. MTS assays were performed after 48 hr using the CellTiter 96® AQ_{ueous} cell proliferation assay kit (Promega, Madison WI). The experiment was repeated four times. Statistical analysis was conducted using ANOVA.

RESULTS

Gene Expression Changes in Mouse Bone and Bone Marrow After Androgen Deprivation

The regulation of gene expression by androgen suppression in the BM has not been reported. Therefore we undertook a global approach to analyze gene expression changes in mouse BM and bone that occur upon castration. We separated bone and BM from young (17 weeks) castrated and sham-operated C57BL/6 mice for comparison in array experiments. Purified RNA from bone or BM cells was labeled and hybridized to mPEDB arrays. Results obtained with bone samples were similar to those obtained with BM samples; therefore we tested combined bone and BM preparations in subsequent experiments. In these experiments, we compared the effects of castration in old (59 weeks) and young (17 weeks) mice. In addition, we analyzed castrated mice with and without testosterone supplementation.

Analysis of array data revealed that 243 genes exhibited significant and consistent differential expression in bone and BM of young castrated compared to sham-operated mice. Of these, 159 were up-regulated and 84 were down-regulated in. The effectiveness of the castration procedure was documented by a reduction in serum androgen levels and seminal vesicle size

TABLE I. Serum Testosterone and Seminal Vesicle Size*

	Testosterone (ng/ml)	Seminal vesicle (g)
Sham-operation	0.69 ± 0.52	0.1337 ± 0.0234
Castration	<0.1	0.0021 ± 0.0005
T-replacement	13.17 ± 1.94	0.1527 ± 0.0213

*Measurements are the average ± standard deviation of tissue samples from three mice.

(Table I). Next, gene expression changes in BM and bone from young and old mice were compared (Fig. 1A). Of the up-regulated genes, 25/159 were differentially expressed across all arrays. These experiments clearly demonstrate that androgen suppression affects gene expression in the BM, that most of the responsive genes are increased in expression upon androgen suppression and that the expression changes are similar in young versus old mice. Quantitative real-time PCR (qPCR) was used to confirm the expression changes from array data for 22 genes. The fold changes were highly correlated between the two methods ($r = 0.97$; Fig. 1B).

To further confirm the regulation of gene expression by androgen, we treated castrated mice with testosterone. The treatment increased serum testosterone levels above those in control mice (13 vs. 0.7 ng/ml, see Table I) and the seminal vesicles grew to the size found in sham-operated controls (Table I). Elevated serum testosterone levels reversed the castration effects for a subgroup of genes. Of the 159 genes that were up regulated in castrated mice, 69 were reversed by testosterone treatment (Fig. 1A).

The array data were examined to identify genes that encode for secreted proteins, capable of interacting with metastatic prostate cancer cells. We identified 4 genes for growth factors/cytokines, and 18 genes that encode proteins that are associated with the extracellular matrix (ECM; Fig. 1C). In the group of growth factors/cytokines, IGFBP5 was consistently overexpressed in castrated mice across all arrays and suppressed after treatment with testosterone. Thus we further explored the regulation of expression, localization, and growth stimulatory activity for prostate cancer cells of IGFBP5.

Expression and Regulation of IGFBP5 Expression in Bone and Bone Marrow

IGFBP5 is highly expressed in bone [31]. IGFBP4 is also expressed by cells in bone and BM stroma and antagonizes the activity of IGFBP5. However in contrast to IGFBP5, IGFBP4 mRNA expression did not change after castration. The fold expression change for IGBP5 mRNA as determined by qPCR in three pairs of mice was 2.7 ± 0.88 in young mice and 2.0 ± 0.17 in old mice. In the same samples the fold expression change for IGFBP4 was 0.86 ± 0.50 in young mice and 1.14 ± 0.41 in old mice. To identify cell types expressing IGFBP5 we used immunohistochemistry. IGFBP5 expression in sections of mouse bone and BM was observed primarily in osteoblastic cells lining the bone and in endothelial cells (Fig. 2). While we observed weak diffuse staining in the BM stroma, individual BM cells were difficult to discern by morphologic criteria. Thus, the expression of IGFBP5 in BM stromal cells was demonstrated subsequently in cultures of primary BM stromal cells.

To determine whether IGFBP5 is expressed in human bone and BM stroma, we measured IGFBP5 mRNA expression in cultures of primary human BM stromal cells (Fig. 3A). IGFBP5 RNA expression was detected in cells from three separate individuals and in immortalized HS27a BM stromal cells. While IGFBP5 was expressed in primary cultures of prostate stromal cells, it was not expressed in prostate epithelial cultures under standard growth conditions. IGFBP5 protein was secreted from primary marrow stromal cells (Fig. 3B) and HS27a cells (Fig. 3C) and accumulated in the conditioned medium. In addition, IGFBP5 became incorporated into the HS27a ECM (Fig. 3C). To exclude the possibility that the IGFBP5 antibody cross-reacts with other IGFBPs or that IGFBP5 is derived from fetal calf serum, we used MG63 osteosarcoma cells transfected with an IGFBP5 containing plasmid (MG63-BP5). A band of the size expected for IGFBP5 was only detected in the MG63-BP5 cells, but not in the parent control cells (Fig. 3B).

To determine whether IGFBP5 expression is regulated by androgen in human BM stromal cells, we first confirmed expression of the AR in HS27a cells. Both AR mRNA and protein (Fig. 4A) were detectable in cultures of HS27a cells, although to a lesser amount than in fresh prostate tissue. When HS27 cells were cultured in serum that was depleted of steroid hormones by incubation with surface-activated charcoal, IGFBP5 mRNA increased 25-fold after 3 days and IGFBP5 protein increased in parallel (Fig. 4B,C). The increase of IGFBP5 mRNA was reversed by addition of physiological concentrations of androgen (Fig. 4D). These results demonstrate that the level of AR expression in Hs27a cells is sufficient to regulate IGFBP5 expression.

IGFBP5 Stimulates the Growth of Immortalized Prostate Epithelial Cells

In contrast to IGFBP5 in conditioned medium, which is growth inhibitory, IGFBP5 in ECM was shown to

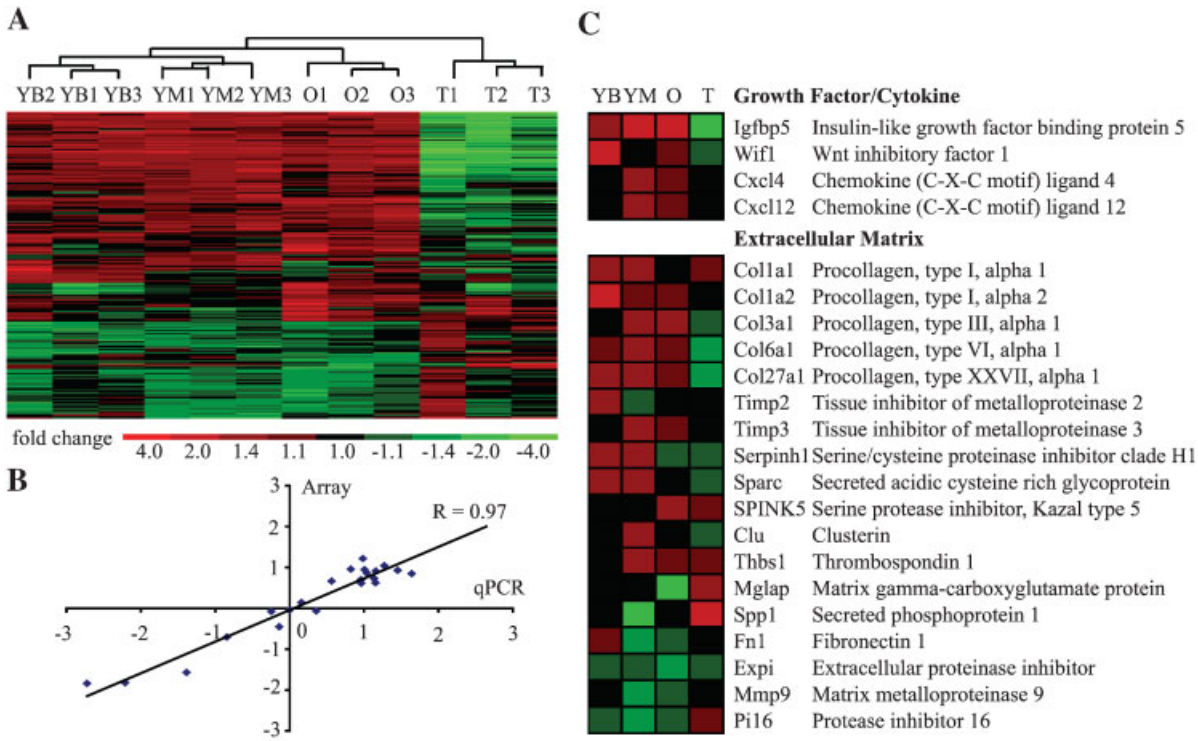

Fig. 1. Differentially expressed genes in bone and bone marrow after androgen deprivation. **A**: Hierarchical clustering of genes that are differentially expressed in paired castrated versus sham-operated mouse tissues: young bone (YBI-3, I0 weeks after castration), young BM I0 weeks after castration (YMI-3), old bone and BM 52 weeks after castration (OI-3), and bone and BM after castration and testosterone replacement (TI-3). The displayed genes possess an expression difference of at least 1.5-fold and a false discovery rate <0.05 as determined by SAM. **B**: Confirmation of Expression changes by qPCR. Fold changes in selected gene expression are determined using three pairs of castrated and sham-operated mice after normalization to mouse GAPDH. Average fold changes in gene expression from qPCR or microarray measurements are plotted on the *x*-axis and *y*-axis, respectively. The Pearson's correlation coefficient (r) is calculated. **C**: Genes for secreted and ECM proteins.

promote the growth of fibroblasts [32]. We therefore tested whether IGFBP5 bound to ECM could also stimulate the growth of epithelial cells and used P69 immortalized prostate epithelial cells to evaluate the growth-promoting activity of matrix-bound IGFBP5. P69 cells are immortalized human prostate epithelial cells, deficient in Rb and p53 protein function and are highly responsive to IGF1. ECM from HS27a cells was incubated with recombinant IGFBP5 and IGF1 or IGF2. The unbound proteins were removed and P69 cells were plated on the ECM in serum-free medium (Fig. 5A). Two days later, P69 cell numbers were determined using an MTS assay. Compared to untreated matrix, larger numbers of P69 cells were observed on matrices incubated with IGFBP5 alone. Addition of IGF1 or IGF2 to IGFBP5 further increased cell growth. The effects of IGFBP5, IGF1 and IGF2 on growth induction of P69 cells reached a plateau, suggesting a saturable mechanism (Fig. 5B). While growth increased in a linear fashion up to incubation with 25 ng/ml IGFBP5, there was no further increase with 50 or 100 ng/ml IGFBP5. IGF1 or IGF2 in the absence of exogenous IGFBP5 also stimulated cell growth.

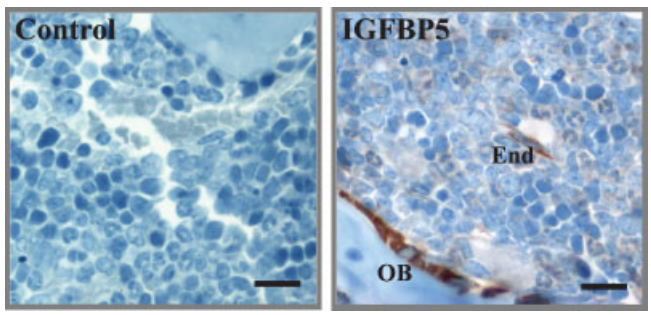

Fig. 2. Expression of IGFBP5 in mouse bone and bone marrow. Decalcified sections of femoral BM are stained with anti-IGFBP5 antibodies and the expression of IGFBP5 is visualized by DAB (brown color). OB: osteoblasts; End: endothelial cells. The scale bar measures 30 μM. Control: no primary antibody.

DISCUSSION

We identified gene expression changes in bone and BM after castration of C57BL/6 mice. The expression of 159 genes increased and the greatest and most

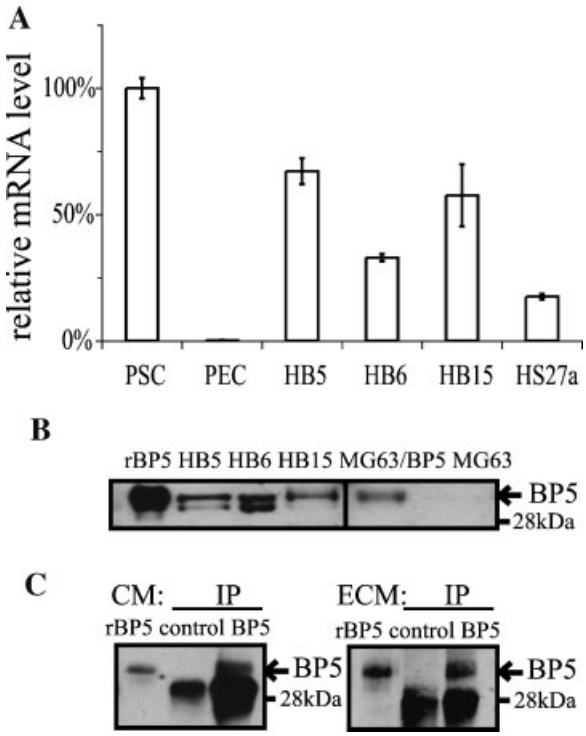

Fig. 3. RNA and protein expression of IGFBP5 in human bone stromal cells. **A**: Steady state IGFBP5 mRNA is measured by qPCR in human primary bone stromal cells HB5, HB6, and HBI5, human immortalized HS27a bone stromal cells, human primary prostate epithelial cells (PEC) and stromal cells (PSC). Expression is normalized to β-actin and is plotted relative to expression in PSC. Results are the average of three measurement replicates. Error bar indicates the standard deviation. **B**: Detection of IGFBP5 protein from conditioned medium of human primary bone stromal cells. A representative Western blot is shown. **lane 1**: Recombinant IGFBP5 (rBP5, 25 ng); **lanes 2 – 4**: primary bone stromal cell culture; **lane 5**: human sarcoma cell line MG63 expressing IGFBP5 (MG63/BP5); and **lane 6**: MG63 control cells. **C**: IGFBP5 protein is immunoprecipitated from conditioned medium (CM, **left panel**) or extracellular matrix (ECM, **right panel**) of HS27a cells. Lane 1: Recombinant IGFBP5 (rBP5, 25 ng); lane 2: Protein G bead control; and lane 3: IGFBP5 immunoprecipitation. Arrow: IGFBP5.

consistent increase was observed for IGFBP5. Immunohistochemical staining indicated that BM stromal cells, osteoblasts and endothelial cells express IGFBP5. In the human immortalized bone stromal cell line HS27a, IGFBP5 gene and protein expression were increased by treatment with charcoal-stripped serum and were inhibited by addition of androgen. In-vitro, IGFBP5 was secreted into the medium and deposited into ECM by primary human BM stromal cells and HS27a cells. When bound to ECM, IGFBP5 increased the growth of P69 immortalized prostate epithelial cells. We conclude from these results that IGFBP5 expression increases after androgen ablation, which may promote the growth of prostate cancer cells in the BM environment.

A limitation in the interpretation of castration induced gene expression changes is that castration alters the levels of several hormones, and not only decreases circulating T levels. Thus, changes in other hormones could be responsible for the regulation of gene expression in the BM. Bone is specifically responsive to estrogens, which are decreased in castrated mice and increased with testosterone supplementation. Castration also increases FSH/LH. The distinction between the effects of androgen and estrogen in-vivo would require blockade with an aromatase inhibitor. While the effects of decreased androgen and estrogen cannot be distinguished in-vivo, in-vitro, IGFBP5 induction by charcoal-stripped medium is suppressed by R1881, which cannot be aromatized. These data suggest that the regulation of IGFBP5 expression is mediated by androgen; however it does not exclude a contribution of estrogen in-vivo.

Androgens are known to augment the thickness of bone and accordingly, the AR is expressed in osteoblasts, osteocytes and at sites of endochondrial ossification in proliferating, mature and hypertrophic chondrocytes [5]. In several reports, AR copy numbers range between 150 and 5,000 per cell in cultured human BM stromal cells, which include osteoblastic cells [33,34]. Consistent with these results, we detected expression of AR mRNA and protein in HS27a cells. In vivo androgens regulate cell types that lack detectable AR expression presumably through the BM stroma. Anecdotally, androgens were used to treat anemia and the higher hematocrit in men compared to women is attributed to differences in circulating androgen levels [35]. Androgen, but not estrogen or IGF1, regulates the maturation and expansion of the B-cell compartment [8,36,37]. In castrated animals, stromal cells expressing the AR were able to promote the expansion of B-cells from mice afflicted by testicular feminization (Tfm), which possess non-functional AR. In the reverse situation, stromal cells from Tfm mice did not cause changes in B-cell numbers after castration [9]. Interestingly, the activity from the stroma is specific for B-cells and does not affect the T-cell compartment in the BM [38].

Several other studies analyzed the response of IGFBP5 expression to androgen stimulation or androgen suppression and the results are inconsistent. The reason for the discrepancies lies in the difference in cell type and source (cell cultures, xenografts, patient tissue samples), and in the reagents and methods that were used for the analysis. In the prostate and bone, the expression of IGFBP5 RNA is observed in the mesenchymal cells, for example, prostate stromal cells, BM stromal cells and osteoblasts (Ref. [14] and Fig. 3).

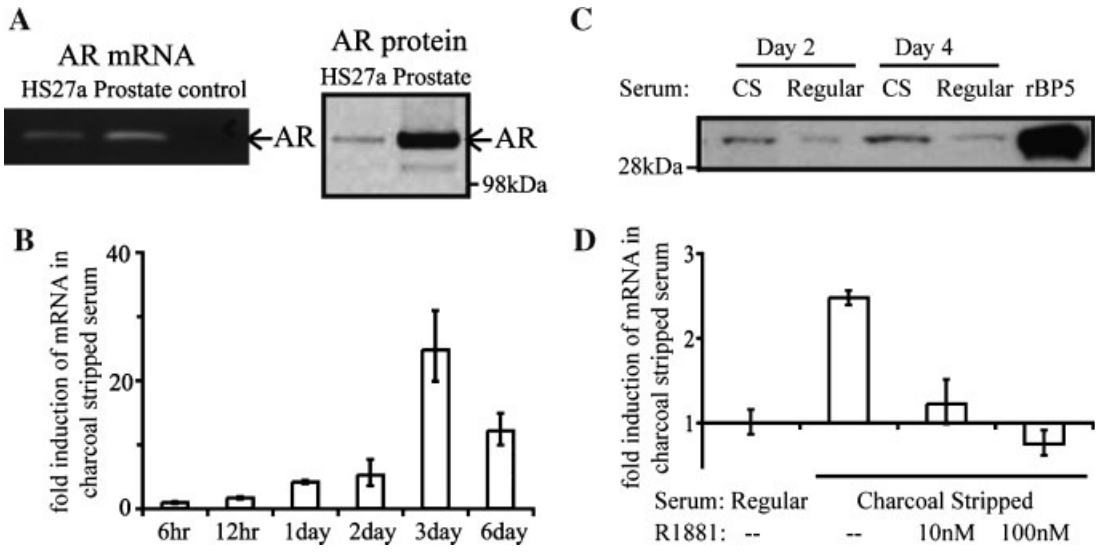

Fig. 4. Regulation of IGFBP5 expression in HS27a cells by androgen. **A**: AR RNA expression (**left panel**) and protein expression (**right panel**) in HS27a. **Lane 1**: HS27a; **lane 2**: prostate tissue, **lane 3**: negative control. AR protein is detected by Western blot in whole cell lysates of HS27a cells or prostate tissue. **B**: Induction of IGFBP5 expression by charcoal stripped serum. HS27a cells are cultured in charcoal-stripped serum for indicated time periods. The mRNA expression of IGFBP5 is measured by qPCR and compared to cells grown in regular serum. Expression is normalized to β-actin. **C**: HS27a cells are cultured in charcoal stripped serum (CS) or regular serum for 2 and 4 days. IGFBP5 expression in equal amounts of whole cell lysate is measured by Western blotting. **D**: Suppression of IGFBP5 expression by androgen. HS27a cells are cultured in regular serum or charcoal-stripped serum with R1881 testosterone for 24 hr. The experiment was repeated twice with similar results. The fold difference of IGFBP5 RNA expression is calculated as described in B.

Our primary prostate epithelial cultures, which are of the basal/intermediate cell types, did not express IGFBP5 RNA. An immunohistochemical study found about 4% of prostate epithelial cells were stained positive for IGFBP5 protein after 18–43 days of androgen suppressive therapy, an increase compared to the 0.2% as in the placebo group [39]. The regulation of IGFBP5 expression by androgen was also analyzed in xenografts. While IGFBP5 expression increased after castration in the Shinogii xenograft [40], it increased with androgen stimulation in the CWR22 xenograft [41]. This study is the first to examine the regulation of IGFBP5 expression by androgen in bone and BM stromal cells. The results of this study are consistent between in-vivo and in-vitro systems and between mouse and human. Androgen withdrawal clearly increased IGFBP5 expression and the increase in bone and BM in-vivo is sustained for at least 1 year (Fig. 1).

Both, the IGF1 receptor and IGFBP5 are targeted by novel drugs that are undergoing clinical trials for treatment of metastatic prostate cancer [16,40]. This study suggests that the drug target, IGFBP5, is expressed in the microenvironment of metastatic cancer cells. This may increase the opportunity of

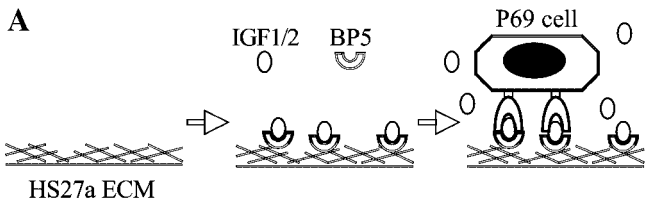

B

BP5 concentration (ng/ml)	Matrix Treatment		
	BP5	BP5+IGF1	BP5+IGF2
0	100 ± 0	147 ± 10	154 ± 20
6.25	170 ± 28	190 ± 53	170 ± 16
12.5	236 ± 50	256 ± 53	231 ± 29
25	233 ± 56	303 ± 88	276 ± 81
50	223 ± 47	330 ± 69	319 ± 76
100	228 ± 54	328 ± 73	312 ± 85

Fig. 5. Growth stimulation of P69 cells by IGFBP5. **A**: Cartoon of the experimental design. Extracellular matrix (ECM) is prepared from HS27a cells and treated with increasing amounts of recombinant IGFBP5 (BP-5) and 10 ng/ml IGF1 or IGF2. After washing, P69 cells are added together with IGF1 or IGF2 and cell numbers are measured 2 days later. **B**: Growth P69 cells on HS27a matrix. The increase in P69 cell numbers on treated matrices is calculated relative to growth on untreated matrix. Values represent the average increase in cell numbers from four experiments ± standard deviation. The ANOVA test indicates that addition of IGFBP5 significantly increases P69 cell growth ($P < 0.001$) and that IGF1 or IGF2 further increase cell growth ($P < 0.001$). The experiment was repeated twice with different passage numbers of HS27a cells.

IGFBP5 targeted therapies of treating bone metastatic disease. Because IGF1 and IGFBP5 stimulate the progression of cancer cells to androgen independence, early administration of drugs that inhibit their activities may augment the clinical response to androgen ablative treatment. In addition to its therapeutic interest, IGF1 and IGFBP5 levels in the bone and BM could affect the progression of micrometastatic disease. Studies are under way to determine whether progression of micrometastatic disease at the time of radical prostatectomy is increased in men with low serum testosterone levels due to an elevated IGFBP5 concentration. In summary, IGFBP5 functions as a key androgen-sensitive modulator of the BM microenvironment.

ACKNOWLEDGMENTS

We thank all members of the Knudsen and Nelson laboratories for helpful discussions. This study was supported in part by DOD grants DAMD17-02-1-0159 and W81XWH-06-1-0171, the PNW Prostate Cancer SPORE CA97186, NIH grants CA85859, DK65204, DK56465, HL62923, and Fred Hutchinson Cancer Research Center grant P30CA015704.

REFERENCES

1. Ryan CJ, Small EJ. Early versus delayed androgen deprivation for prostate cancer: New fuel for an old debate. J Clin Oncol 2005;23(32):8225–8231.
2. Pinski J, Dorff TB. Prostate cancer metastases to bone: Pathophysiology, pain management, and the promise of targeted therapy. Eur J Cancer 2005;41(6):932–940.
3. Simpson MA, Reiland J, Burger SR, Furcht LT, Spicer AP, Oegema TR Jr, McCarthy JB. Hyaluronan synthase elevation in metastatic prostate carcinoma cells correlates with hyaluronan surface retention, a prerequisite for rapid adhesion to bone marrow endothelial cells. J Biol Chem 2001;276(21):17949–17957.
4. Ellis WJ, Pfitzenmaier J, Colli J, Arfman E, Lange PH, Vessella RL. Detection and isolation of prostate cancer cells from peripheral blood and bone marrow. Urology 2003;61(2):277–281.
5. Abu EO, Horner A, Kusec V, Triffitt JT, Compston JE. The localization of androgen receptors in human bone. J Clin Endocrinol Metab 1997;82(10):3493–3497.
6. Mantalaris A, Panoskaltsis N, Sakai Y, Bourne P, Chang C, Messing EM, Wu JH. Localization of androgen receptor expression in human bone marrow. J Pathol 2001;193(3):361–366.
7. Seeman E. Estrogen, androgen, and the pathogenesis of bone fragility in women and men. Curr Osteoporos Rep 2004;2(3):90–96.
8. Hero M, Wickman S, Hanhijarvi R, Siimes MA, Dunkel L. Pubertal upregulation of erythropoiesis in boys is determined primarily by androgen. J Pediatr 2005;146(2):245–252.
9. Olsen NJ, Gu X, Kovacs WJ. Bone marrow stromal cells mediate androgenic suppression of B lymphocyte development. J Clin Invest 2001;108(11):1697–1704.
10. Gennigens C, Menetrier-Caux C, Droz JP. Insulin-like growth factor (IGF) family and prostate cancer. Crit Rev Oncol Hematol 2006;58(2):124–145.
11. Krueckl SL, Sikes RA, Edlund NM, Bell RH, Hurtado-Coll A, Fazli L, Gleave ME, Cox ME. Increased insulin-like growth factor I receptor expression and signaling are components of androgen-independent progression in a lineage-derived prostate cancer progression model. Cancer Res 2004;64(23):8620–8629.
12. Hellawell GO, Turner GD, Davies DR, Poulsom R, Brewster SF, Macaulay VM. Expression of the type 1 insulin-like growth factor receptor is up-regulated in primary prostate cancer and commonly persists in metastatic disease. Cancer Res 2002;62(10):2942–2950.
13. Chott A, Sun Z, Morganstern D, Pan J, Li T, Susani M, Mosberger I, Upton MP, Bubley GJ, Balk SP. Tyrosine kinases expressed in vivo by human prostate cancer bone marrow metastases and loss of the type 1 insulin-like growth factor receptor. Am J Pathol 1999;155(4):1271–1279.
14. Tennant MK, Thrasher JB, Twomey PA, Birnbaum RS, Plymate SR. Insulin-like growth factor-binding proteins (IGFBP)-4,-5, and -6 in the benign and malignant human prostate: IGFBP-5 messenger ribonucleic acid localization differs from IGFBP-5 protein localization. J Clin Endocrinol Metab 1996;81(10):3783–3792.
15. Ryan CJ, Haqq CM, Simko J, Nonaka DF, Chan JM, Weinberg V, Small EJ, Goldfine ID. Expression of insulin-like growth factor-1 receptor in local and metastatic prostate cancer. Urol Oncol 2007;25(2):134–140.
16. Wu JD, Haugk K, Coleman I, Woodke L, Vessella R, Nelson P, Montgomery RB, Ludwig DL, Plymate SR. Combined in vivo effect of A12,a type 1 insulin-like growth factor receptor antibody, and docetaxel against prostate cancer tumors. Clin Cancer Res 2006;12(20 Pt 1):6153–6160.
17. Canalis E, McCarthy T, Centrella M. Isolation of growth factors from adult bovine bone. Calcif Tissue Int 1988;43(6):346–351.
18. Bautista CM, Baylink DJ, Mohan S. Isolation of a novel insulin-like growth factor (IGF) binding protein from human bone: A potential candidate for fixing IGF-II in human bone. Biochem Biophys Res Commun 1991;176(2):756–763.
19. Wu JD, Haugk K, Woodke L, Nelson P, Coleman I, Plymate SR. Interaction of IGF signaling and the androgen receptor in prostate cancer progression. J Cell Biochem 2006.
20. Nickerson T, Pollak M, Huynh H. Castration-induced apoptosis in the rat ventral prostate is associated with increased expression of genes encoding insulin-like growth factor binding proteins 2,3,4 and 5. Endocrinology 1998;139(2):807–810.
21. Nickerson T, Pollak M. Bicalutamide (Casodex)-induced prostate regression involves increased expression of genes encoding insulin-like growth factor binding proteins. Urology 1999;54(6):1120–1125.
22. Le H, Arnold JT, McFann KK, Blackman MR. DHT and testosterone, but not DHEA or E2, differentially modulate IGF-I, IGFBP-2, and IGFBP-3 in human prostatic stromal cells. Am J Physiol Endocrinol Metab 2006;290(5):E952–E960.
23. Mohan S, Nakao Y, Honda Y, Landale E, Leser U, Dony C, Lang K, Baylink DJ. Studies on the mechanisms by which insulin-like growth factor (IGF) binding protein-4 (IGFBP-4) and IGFBP-5 modulate IGF actions in bone cells. J Biol Chem 1995;270(35):20424–20431.
24. Miyakoshi N, Richman C, Kasukawa Y, Linkhart TA, Baylink DJ, Mohan S. Evidence that IGF-binding protein-5 functions as a growth factor. J Clin Invest 2001;107(1):73–81.

25. Xu Q, Li S, Zhao Y, Maures TJ, Yin P, Duan C. Evidence that IGF binding protein-5 functions as a ligand-independent transcriptional regulator in vascular smooth muscle cells. Circ Res 2004; 94(5):E46–E54.
26. Kveiborg M, Flyvbjerg A, Eriksen EF, Kassem M. 1,25-Dihydroxyvitamin D3 stimulates the production of insulin-like growth factor-binding proteins-2, -3 and -4 in human bone marrow stromal cells. Eur J Endocrinol 2001;144(5):549–557.
27. Kiepe D, Ciarmatori S, Hoeflich A, Wolf E, Tonshoff B. Insulin-like growth factor (IGF)-I stimulates cell proliferation and induces IGF binding protein (IGFBP)-3 and IGFBP-5 gene expression in cultured growth plate chondrocytes via distinct signaling pathways. Endocrinology 2005;146(7):3096–3104.
28. Boonyaratanakornkit V, Strong DD, Mohan S, Baylink DJ, Beck CA, Linkhart TA. Progesterone stimulation of human insulin-like growth factor-binding protein-5 gene transcription in human osteoblasts is mediated by a CACCC sequence in the proximal promoter. J Biol Chem 1999;274(37):26431–26438.
29. Zhou Y, Mohan S, Linkhart TA, Baylink DJ, Strong DD. Retinoic acid regulates insulin-like growth factor-binding protein expression in human osteoblast cells. Endocrinology 1996;137(3):975–983.
30. Gori F, Hofbauer LC, Conover CA, Khosla S. Effects of androgens on the insulin-like growth factor system in an androgen-responsive human osteoblastic cell line. Endocrinology 1999;140(12):5579–5586.
31. Richman C, Baylink DJ, Lang K, Dony C, Mohan S. Recombinant human insulin-like growth factor-binding protein-5 stimulates bone formation parameters in vitro and in vivo. Endocrinology 1999;140(10):4699–4705.
32. Jones JI, Gockerman A, Busby WH Jr, Camacho-Hubner C, Clemmons DR. Extracellular matrix contains insulin-like growth factor binding protein-5: Potentiation of the effects of IGF-I. J Cell Biol 1993;121(3):679–687.
33. Hofbauer LC, Khosla S. Androgen effects on bone metabolism: Recent progress and controversies. Eur J Endocrinol 1999; 140(4):271–286.
34. Vanderschueren D, Vandenput L, Boonen S, Lindberg MK, Bouillon R, Ohlsson C. Androgens and bone. Endocr Rev 2004; 25(3):389–425.
35. Navarro JF, Mora C. Androgen therapy for anemia in elderly uremic patients. Int Urol Nephrol 2001;32(4):549–557.
36. Medina KL, Kincade PW. Pregnancy-related steroids are potential negative regulators of B lymphopoiesis. Proc Natl Acad Sci USA 1994;91(12):5382–5386.
37. Medina KL, Smithson G, Kincade PW. Suppression of B lymphopoiesis during normal pregnancy. J Exp Med 1993; 178(5):1507–1515.
38. Ellis TM, Moser MT, Le PT, Flanigan RC, Kwon ED. Alterations in peripheral B cells and B cell progenitors following androgen ablation in mice. Int Immunol 2001;13(4):553–558.
39. Thomas LN, Wright AS, Lazier CB, Cohen P, Rittmaster RS. Prostatic involution in men taking finasteride is associated with elevated levels of insulin-like growth factor-binding proteins (IGFBPs)-2,-4, and -5. Prostate 2000;42(3):203–210.
40. Miyake H, Pollak M, Gleave ME. Castration-induced up-regulation of insulin-like growth factor binding protein-5 potentiates insulin-like growth factor-I activity and accelerates progression to androgen independence in prostate cancer models. Cancer Res 2000;60(11):3058–3064.
41. Gregory CW, Kim D, Ye P, D'Ercole AJ, Pretlow TG, Mohler JL, French FS. Androgen receptor up-regulates insulin-like growth factor binding protein-5 (IGFBP-5) expression in a human prostate cancer xenograft. Endocrinology 1999;140(5):2372–2381.
42. Li L, Milner LA, Deng Y, Iwata M, Banta A, Graf L, Marcovina S, Friedman C, Trask BJ, Hood L, Torok-Storb B. The human homolog of rat Jagged1 expressed by marrow stroma inhibits differentiation of 32D cells through interaction with Notch1. Immunity 1998;8(1):43–55.
43. Plymate SR, Tennant M, Birnbaum RS, Thrasher JB, Chatta G, Ware JL. The effect on the insulin-like growth factor system in human prostate epithelial cells of immortalization and transformation by simian virus-40 T antigen. J Clin Endocrinol Metab 1996;81(10):3709–3716.
44. Gmyrek GA, Walburg M, Webb CP, Yu H-M, You X, Vaughan ED, Vande Woude GF, Knudsen BS. Normal and malignant prostate epithelial cells differ in their response to hepatocyte growth factor/scatter factor. Am J Pathol 2001;159(2):579–590.
45. Wang S, Gao J, Lei Q, Rozengurt N, Pritchard C, Jiao J, Thomas GV, Li G, Roy-Burman P, Nelson PS, Liu X, Wu H. Prostate-specific deletion of the murine Pten tumor suppressor gene leads to metastatic prostate cancer. Cancer Cell 2003;4(3):209–221.
46. de Hoon MJ, Imoto S, Nolan J, Miyano S. Open source clustering software. Bioinformatics 2004;20(9):1453–1454.
47. Gustafson MP, Xu C, Grim JE, Clurman BE, Knudsen BS. Regulation of cell proliferation in a stratified culture system of epithelial cells from prostate tissue. Cell Tissue Res 2006.
48. Knudsen BS, Harpel PC, Nachman RL. Plasminogen activator inhibitor is associated with the extracellular matrix of cultured bovine smooth muscle cells. J Clin Invest 1987;80(4):1082–1089.

An Antibody Targeting the Type I Insulin-like Growth Factor Receptor Enhances the Castration-Induced Response in Androgen-Dependent Prostate Cancer

Stephen R. Plymate,[1,3] Kathy Haugk,[3] Ilsa Coleman,[4] Lillie Woodke,[1] Robert Vessella,[2,3] Peter Nelson,[4] R. Bruce Montgomery,[1] Dale L. Ludwig,[5] and Jennifer D. Wu[1]

Abstract

Purpose: To determine the effect of inhibition of insulin-like growth factor-IR (IGF-IR) signaling with an antibody to the IGF-IR, A12, in conjunction with androgen withdrawal on prostate cancer progression in a human prostate xenograft model, LuCaP 35.

Experimental Design: LuCaP 35 was implanted s.c. in severe combined immunodeficient mice. At the time of castration, mice were randomized to one of three groups. Group 1 was castrate only; group 2 received A12 40 mg/kg i.p. for 2 weeks beginning 1 week after castration; and group 3 received A12 40 mg/kg i.p. for 2 weeks beginning 2 weeks after castration.

Results: In group 1, tumor volume decreased to 60% of the starting volume 4 weeks post-castration. In groups 2 and 3, tumor volumes nadired 6 weeks after castration at <10% of the volume at time of castration ($P < 0.01$). Tumor regrowth was not seen in groups 2 or 3 until 15 weeks after castration. Androgen receptor (AR) localization in tumors showed a decrease in nuclear staining in groups 2 and 3 compared with group 1 ($P < 0.001$). Tumor volume correlated with nuclear AR intensity. AR-regulated genes increased early in group 1, but did not increase in groups 2 and 3. Thus, tumor-specific survival was prolonged by the addition of A12 to castration.

Conclusions: This study shows that the inhibition of IGF-IR enhances the effects of castration in prostate cancer. These effects are associated with a decrease in AR signaling and nuclear AR localization, and recurrence is associated with an increase in AR-regulated gene expression.

Castration is one of the most effective therapies available for metastatic prostate cancer, with >80% response as measured by a decline in prostate-specific antigen (1, 2). However, recurrence following castration is inevitable. Recently, studies from several groups have shown that following castration, significant amounts of androgens are still detected in the prostate (3). Moreover, androgen receptor (AR) is still detected in the nucleus, and increased AR expression is correlated with prostate cancer progression following androgen withdrawal (3–6). These data suggest that further targeting of the AR and mechanisms of cell survival that occur following castration could significantly enhance castration effects and potentially prolong survival.

Following castration, signaling through the mitogenic and antiapoptotic insulin-like growth factor (IGF) system is increased by several mechanisms (7–10). Within 24 to 48 h post-castration, enhancement of ligand-induced signaling through the type I IGF tyrosine kinase receptor (IGF-IR) occurs by an increase in IGF binding proteins 2 and 5 (7–14). Although IGF-IR expression is decreased immediately after castration, clinical studies show that the receptor increases as time after castration increases (15). These data suggest that signaling through the IGF-IR may be a pathway contributing to prostate cancer cell survival and the emergence of androgen-insensitive disease (16). Zhang et al. (17) have shown that an increase in survivin, an inhibitor of apoptosis, via signaling through the IGF-IR/AKT pathway is a mechanism for the development of resistance to anti-androgen therapy. Other laboratories have also shown that growth factor stimulation of AKT enhances AR signaling, such that the AR is sensitized to transactivation by low levels of androgen (18–22). Taken together, these data suggest that in prostate cancer, signaling through the IGF-IR leads to the development of resistance to androgen deprivation. We have previously reported that A12 as a single agent in LuCaP 35 androgen-dependent (AD) and LuCaP 35v androgen-independent (AI; ref. 16) human prostate cancer xenografts results in a significant decline in the rate of tumor growth, but does not halt or reverse tumor growth (23). We have reported that the inhibition of IGF-IR signaling in AD and AI human prostate xenograft models results in decreased nuclear distribution of the AR (24).

Authors' Affiliations: Departments of [1]Medicine and [2]Urology and Immunology, University of Washington, [3]Veterans Affairs Puget Sound Health Care System, and [4]Fred Hutchinson Cancer Research Center, Seattle, Washington; and [5]ImClone Systems, New York, New York

Received 3/19/07; revised 7/19/07; accepted 7/26/07.

Grant support: NIH Grants PO1-CA85859, Veterans Affairs Research Program, and U.S. Department of Defense (DOD) Prostate Cancer Research Program to S.R. Plymate, DAMD17-03-2-033, and the Pacific Northwest Prostate Cancer Specialized Programs of Research Excellence to P.S. Nelson, and DOD New Investigator's Award W81XWH-04-1-0577 and NIH Temin Award 1KO1CA116002 to J. Wu.

The costs of publication of this article were defrayed in part by the payment of page charges. This article must therefore be hereby marked *advertisement* in accordance with 18 U.S.C. Section 1734 solely to indicate this fact.

Requests for reprints: Stephen R. Plymate, Box 359625, Department of Medicine, University of Washington, Seattle, WA 98104. Phone: 206-341-4275; Fax: 206-341-5302; E-mail: splymate@u.washington.edu.

doi:10.1158/1078-0432.CCR-07-0648

Based on the data from our published studies (23, 25) as well as data from other groups, we hypothesize that treatment of AD prostate tumors with A12 at the time of castration would generate a synergy to enhance the effects of castration and prolong the time for AD tumors to progress to the AI phenotype. In this study, we show that targeting the IGF-IR with the fully human monoclonal antibody A12 following castration significantly enhances the effect of castration and time to occurrence of AI disease in the LuCaP 35 human xenograft model of AD prostate cancer.

Materials and Methods

Xenograft cell line. The LuCaP 35 human prostate cancer xenograft model is an androgen-dependent human xenograft maintained in severe combined immunodeficient (SCID) mice (23, 26). The xenograft regresses following androgen withdrawal, and tumor regrowth recurs ~5 weeks after castration. The LuCaP 35 human prostate xenograft was selected for these studies because it has a wild-type AR, secretes PSA, and is representative of the prostate cancer xenografts that develop resistance to androgen deprivation by increasing AR expression (5). LuCaP 35 is pTEN negative (27).

A12 antibody. A12 is a fully human antibody antagonist to the human IGF-IR, generated by screening a naïve bacteriophage Fab library (28). A12 does not cross-react with the insulin receptor (28).

In vivo *study.* To study the *in vivo* effect of A12 on castration, tumor bits (20-30 mm^3) of the LuCaP 35 AD human prostate cancer xenograft were implanted s.c. into 6- to 8-week-old intact SCID mice as previously described (23, 26). Tumors were allowed to grow to ~400 mm^3, at which time, the animal is surgically castrated (23, 26). At the time of castration, animals were randomized into one of three groups of 20 animals each: group 1 (castration), castration plus vehicle i.p. thrice a week beginning 1 week after castration; group 2 (early A12), castration plus A12 antibody i.p. at a dose of 40 mg/kg body weight thrice a week for 2 weeks beginning 1 week after castration; and group 3 (late A12), castration plus A12 antibody 40 mg/kg body weight i.p. thrice a week for 2 weeks beginning 2 weeks after castration (Fig. 1). After the single 2-week administration of A12, no further A12 treatments were given. We have shown detectable levels of antibody with the A12 dosing schedule used in this study for up to 4 weeks following cessation of therapy (25). Group 1 was considered the castration control group. The timing of A12 administration for 2 weeks beginning either 1 or 2 weeks after castration was based on published data with the LuCaP 35 cell

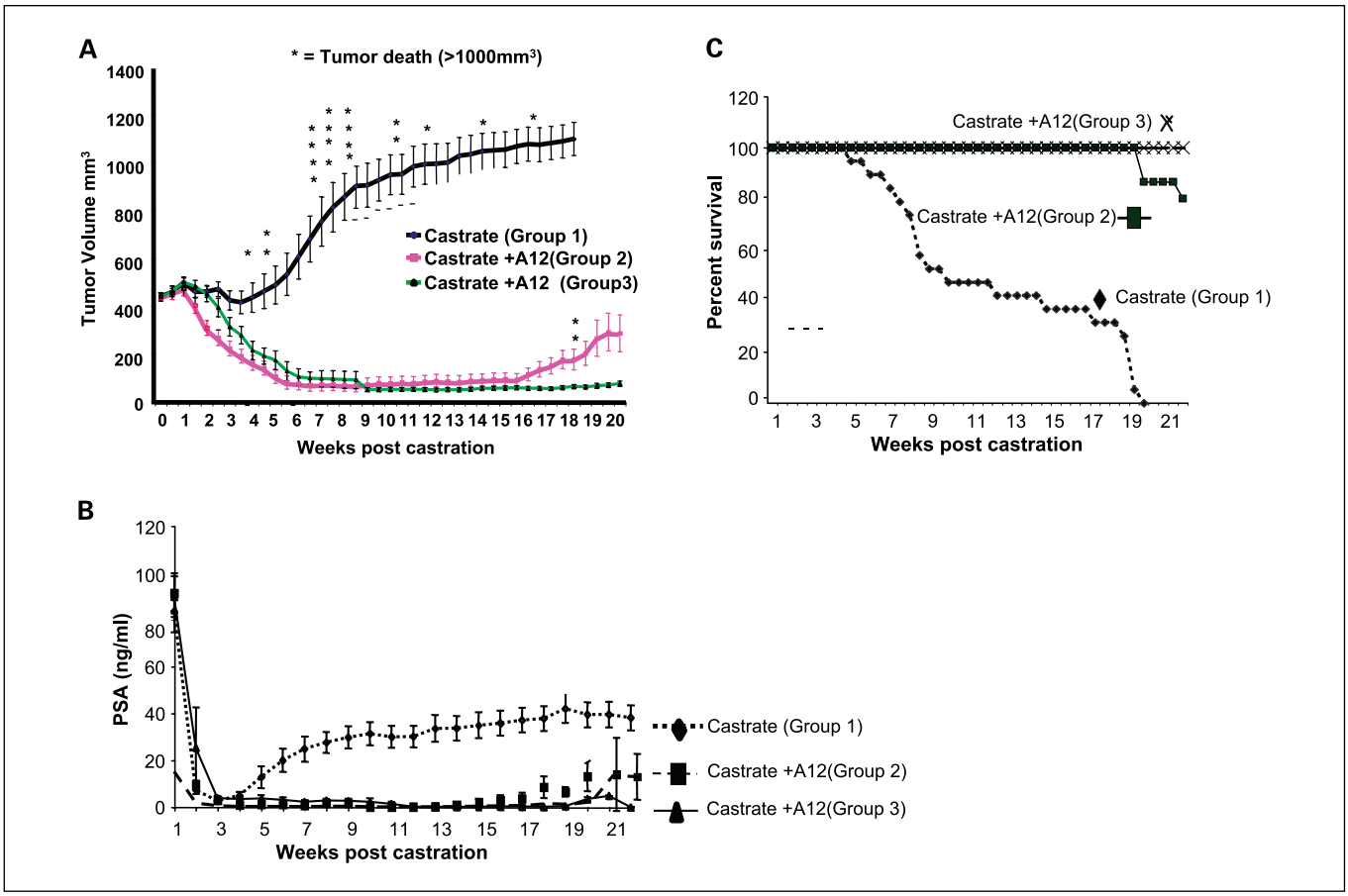

Fig. 1. *A,* tumor volume versus time. The differences between the castrate group (group 1), the group with A12 started 1 wk after castration (group 2), and the group with A12 started 2 wk after castration (group 3) became significant at $P < 0.01$ after week 4 and remained significant throughout the remainder of the study. *, $P < 0.05$, significant differences between groups 2 and 3 began at week 17 and remained different until the end of the study. Tumor volume in group 1 was >1,000 mm^3. *B,* serum PSA levels from animals in the three groups. PSA drops similarly in all three groups after castration, but has reached its nadir in the castrate group by week 3, following which PSA begins to increase, indicating an increase in tumor growth that is detectable by week 5. In contrast, the PSA level remains at its nadir in the two castrate + A12 groups until tumor recurrence begins at week 18. *C,* survival curves demonstrating the percent of animals in each group that have survived a tumor-induced death. Tumor death occurs when the tumor volume is >1,000 mm^3. Data show the markedly enhanced survival of the animals receiving A12 and castration (groups 2 and 3) compared with castration alone (group 1).

line, indicating that maximum castration-induced apoptosis occurs within 4 days of castration (26). Because the inhibition of IGF-IR signaling could cause cell cycle arrest and prevent cells from undergoing apoptosis, we decided to start A12 when apoptosis was complete following castration (26, 29). In preliminary studies using docetaxel and the M12 human prostate cancer cell line, we noted that the administration of A12 before taxanes decreased taxane-induced apoptosis by arresting the cells in the G_1 phase of the cell cycle (25). A12 was administered for 2 weeks and then stopped to determine the efficacy with castration and a prolonged effect of A12 as a single agent following castration. Animals were weighed twice weekly. Blood samples were collected from orbital sinus weekly. The serum was separated, and PSA levels were determined using the IMx Total PSA Assay (Abbott Laboratories). Tumors were measured twice weekly, and tumor volume was estimated by the formula: volume = length $\times$ width^2/2. Following our University of Washington–approved animal protocol, animals were euthanized when the tumor reached a volume of 1,000 mm^3 or when animal weight loss exceeded 20% of the initial body weight.

After euthanization, tumors were collected and treated as previously described (23, 25). A portion of the tumors were fixed in 10% neutral buffer formalin (NFB) and embedded in paraffin. Sections of 5 μm were prepared for immunohistochemistry (IHC) staining. One quarter of the tumor was separated into single cells mechanically. Total RNA and cell lysates for protein analysis were prepared at previously described (23, 25).

During the study, we sacrificed three animals from each group to represent two arbitrary time periods post-castration (period 1 was 17-70 days post-castration, and period 2 was 70-140 days post-castration). Due to the size of the tumors, adequate RNA was collected from group 1 to construct three arrays for each of the two intervals; however, due to the small size of the tumors in groups 2 and 3, two arrays could be constructed at each interval for group 2 and one array for group 3. Because the response and time to recurrence was very similar, we combined the results from the arrays in groups 2 and 3 for analysis. All animal studies and procedures were approved by the University of Washington Institutional Animal Care and Use Committee (IACUC).

Flow cytometry. To measure tumor IGF-IR expression, 5×10^5 cells were incubated with anti–IGF-IRα antibody SC-461 (Santa Cruz Biotechnology) and phycoerythrin-conjugated goat anti-mouse antibody and analyzed using a BD FACscan. Data were analyzed using CellQuest^{PRO} software (BD BioScience; ref. 23).

Apoptosis. Apoptosis was determined by terminal nucleotidyl transferase–mediated nick end labeling (TUNEL) assay and propidium iodide staining using the Apop-Direct kit (BD BioScience) as previously described (23). Apoptosis was also determined using the TUNEL assay on formalin-fixed tissue using the Apop-Tag kit (Millipore Co.) following the manufacturer's recommendations. Apoptotic cells were determined per 300 cells per tissue slide.

Immunohistochemistry. Tumor samples were fixed in 10% NBF, embedded in paraffin, and sectioned at 5 μm onto slides. After blocking with 1.5% normal goat serum in PBS containing 0.05% Tween 20 (PBST) for 1 h, slides were incubated with mouse anti-bromodeoxyuridine (BrdUrd) antibody (1 μg/mL) for 1 h, followed by sequential incubation with biotinylated goat anti-mouse immunoglobulin G (IgG) for 30 min, peroxidase-labeled avidin for 30 min (Santa Cruz Biotechnology), and 3,3′-diaminobenzidine (DAB)/hydrogen peroxide chromogen substrate (Vector Laboratories). All incubation steps were done at room temperature. For negative control, mouse IgG (Vector Laboratories) was used instead of the primary anti-BrdUrd antibody. Numbers of BrdUrd-labeled nucleus and total nucleus were collected from 10 random views of each section. Proliferation index was calculated by the number of BrdUrd-positive nuclei divided by the total number of nuclei. Ten fields were counted per slide. AR used an AR human monoclonal antibody (F36.4.1, Biogenex), and IGF-IR used a monoclonal antibody from Santa Cruz Biotechnology against the α-subunit of the IGF-IR (23).

Cytosol and nuclear fractionation. LnCap cells were grown in T-Medium with 5% fetal bovine serum (FBS) until 40% confluent. Media was replaced with RPMI T&S with 2% charcoal stripped serum (CSS) for 24 h. Nuclear extracts were collected using the Nuclear/Cytosol Fractionation Kit (BioVision K266-100) according to the manufacturer's protocol. Purity of fractionation was validated by Western blot using a specific antibody to Golgi, sc20587 or histone 2B, sc-8650 (Santa Cruz Biotechnology).

Deconvolution microscopy. LnCaP cells were plated in T-Medium supplemented with 5% FBS until 40% confluent. Media was replaced with RPMI T&S with 2% CSS for 24 h and/or treated with A12 antibody overnight. Another sample received A12 antibody for 1° treatment before adding 10^{-8} mol/L of dihydrotestosterone, and 20 ng/mL of IGF-I in RPMI T&S with 2% CSS. After treatment, cells were fixed in cold acetone/methanol (1:1) for 10 min and stained with an AR-specific antibody sc-7305 (Santa Cruz Biotechnology) followed by a biotin-SP–conjugated goat anti-mouse IgG F(ab′)$_2$ (Santa Cruz Biotechnology) and a Streptavidin-Alexa^{594} (Molecular Probes). About 5 μg/mL of 4′-6-diamidino-2-phenylindole (DAPI) was used to stain the nucleus. Cells were mounted with Prolong Anti-Fade reagent (Molecular Probes) and examined with Deltavision SA3.1 Wide-field Deconvolution Microscope. Three-dimensional results of ROI Z-stacks were analyzed using the Image J Analysis software (NIH).

Western blotting. Western blotting was done as previously described and probed with survivin ab (FL-142). sc-10811 is from Santa Cruz Biotechnology using a 1:200 dilution (23).

Prostate and serum testosterone and dihydrotestosterone. Measurements of serum testosterone and dihydrotestosterone measurements were done as previously described (6). Prostate tissue testosterone and dihydrotestosterone measurements were done in the laboratory of Dr. David Hess (Oregon Primate Center) and have also been previously described (8). Briefly, the tissue was flash frozen at the time of collection and kept at -70°C until assayed. At the time of assay, the tissue was thawed to 4°C, homogenized, and extracted with diethyl ether. Extracts were dried under NO_2 and then stored in ethanol until the time of assay. Separation of steroids was done on Sephadex LH-20 columns as described, and appropriate fractions were assayed by RIA.

cDNA microarray analysis. Custom cDNA microarrays were constructed using clones derived from the Prostate Expression Database (PEDB), a sequence repository of human prostate expressed sequence tag (EST) data available to the public[6] (30). Methods of labeling with Cy3 and Cy5 fluorescent dyes, hybridization to the microarray slides, and array processing were as described (31).

Three tumors were pooled in each experimental group. To provide a reference standard RNA for use on cDNA microarrays, we isolated and pooled equal amounts of total RNA from LNCaP, DU145, PC3, and CWR22rV1 cell lines (American Type Culture Collection), growing at log phase in dye-free RPMI 1640 supplemented with 10% FBS (Life Technologies). mRNA was amplified one round using the Ambion MessageAmp II Amplification Kit (Ambion Inc.). Hybridization probes were labeled, and quality control of the array experiments was done as described previously (31). Differences in gene expression associated with treatment groups were determined using the SAM procedure,[7] with a false discovery rate (FDR) of <10% considered significant (32). Similarities between samples were assessed by unsupervised, hierarchical clustering of genes and samples using Cluster 3.0 software[8] and viewed by TreeView.[9]

Real-time reverse transcription-PCR. Survivin and β-tubulin III were assayed by PCR using primers and methods previously described (25). A standard PCR fragment of the target cDNA was purified. About 1 μg of total RNA from each group of pooled tumor was used for first-strand

[6] www.pedb.org
[7] http://www-stat.stanford.edu/.tibs/SAM/
[8] http://bonsai.ims.u-tokyo.ac.jp/-mdehoon/software/cluster/software.htm
[9] http://rana.lbl.gov/EisenSoftware.htm

cDNA synthesis using Superscript First Strand Synthesis System (Invitrogen). Real-time reverse transcription-PCR (RT-PCR) was done in 20 μL of reaction mixture consisting of 1 μL of first strand of cDNA, specific primers sets, and Lightcycler FastStart DNA Master Plus SYBR Green using a Roche Lightcycler following the manufacturer's protocol (Roche). RT-PCR products were subjected to melting curve analysis on Lightcycler software v3.5. The amplicon sizes were confirmed by agarose gel electrophoresis. Each sample was assayed in duplicate.

Results

Inhibition of IGF-IR with A12 significantly enhances tumor regression induced by castration and delays time to tumor recurrence. Figure 1A shows a decrease in LuCaP 35 tumor volume following castration ($P \leq 0.05$) at 5 weeks when compared with maximum tumor volume at the time of castration. The nadir in PSA occurred at week 3 and subsequently increased throughout the remainder of the study (Fig. 1B). The addition of A12 at either the early or late time points resulted in a rapid decrease in tumor volume that was significantly different from group 1 (Fig. 1A). The slopes of the decrease in tumor volumes were similar between both A12 groups. The apparent difference between groups 2 and 3 during the first 9 weeks of the study is accounted for by the 1-week difference in time between the initiation of A12 treatment. The initial decrease in PSA was similar in each group, and the subsequent increase in PSA began with the regrowth of the tumors. Group 1 tumor volume decreased to 60% of the starting volume 4 weeks after castration ($P < 0.01$). By 17 weeks, all animals in group 1 had to be sacrificed because tumor volumes had reached 1,000 mm^3. In contrast, in the A12 plus castration groups, only two animals had to be sacrificed because of tumor volume by the end of the study, and these events occurred at 14 weeks after the castration.

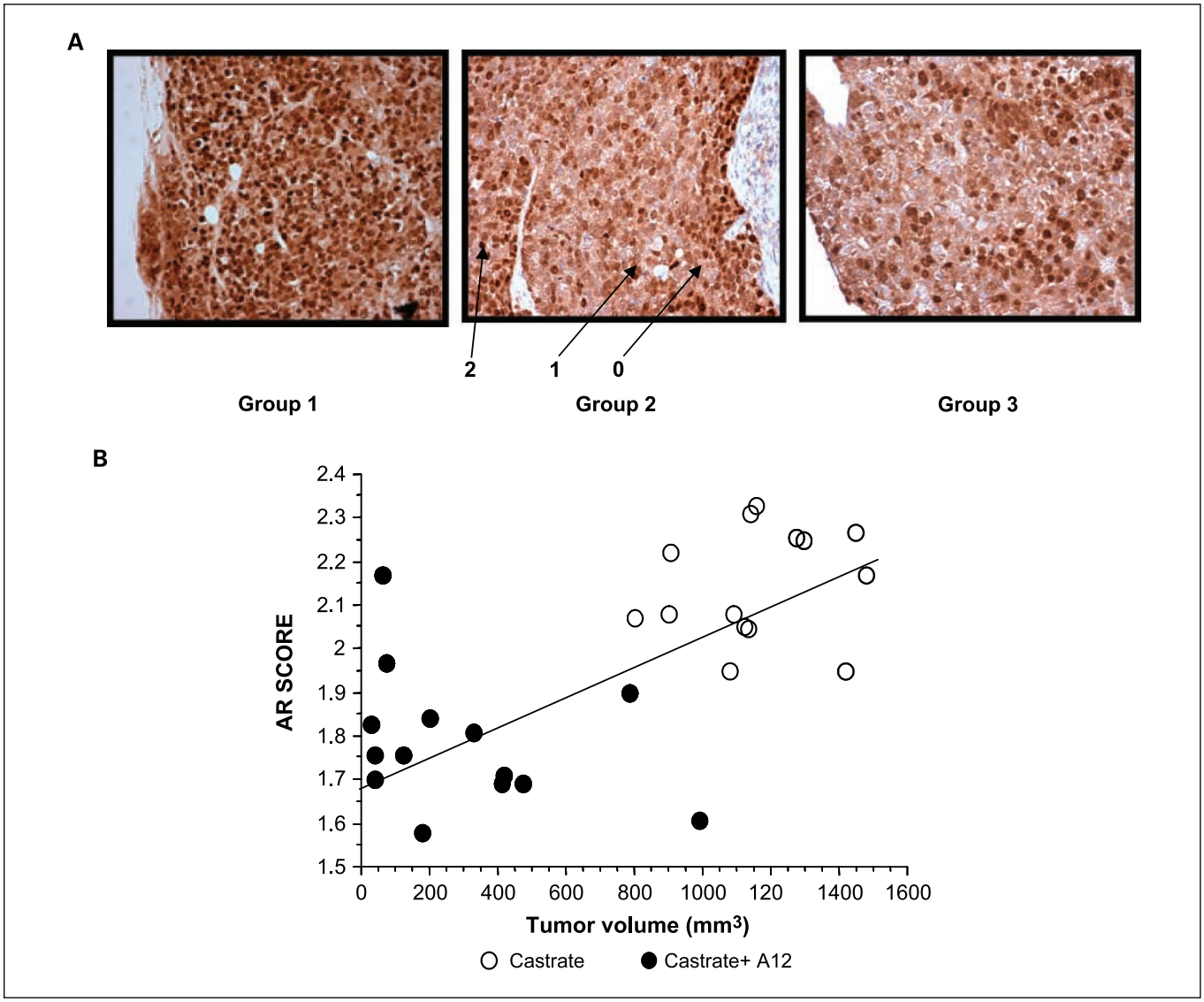

Fig. 2. *A,* a representative tumor sections from groups 1, 2, and 3 with IHC for the AR. Arrows and numbers, relative values given to nuclear AR staining. Magnification, 40×; no counterstain. Note the marked number of tumor cells with nuclear AR in castrate only group 1 in spite of the fact that the tumor was removed >10 wk after castration. *B,* correlation between nuclear AR intensity and tumor volume. $r = 0.66$; $P < 0.01$. ○, group 1 values; ●, castrate + A12 early and late values, groups 2 and 3. Values are the mean value for 100 nuclei graded per tumor.

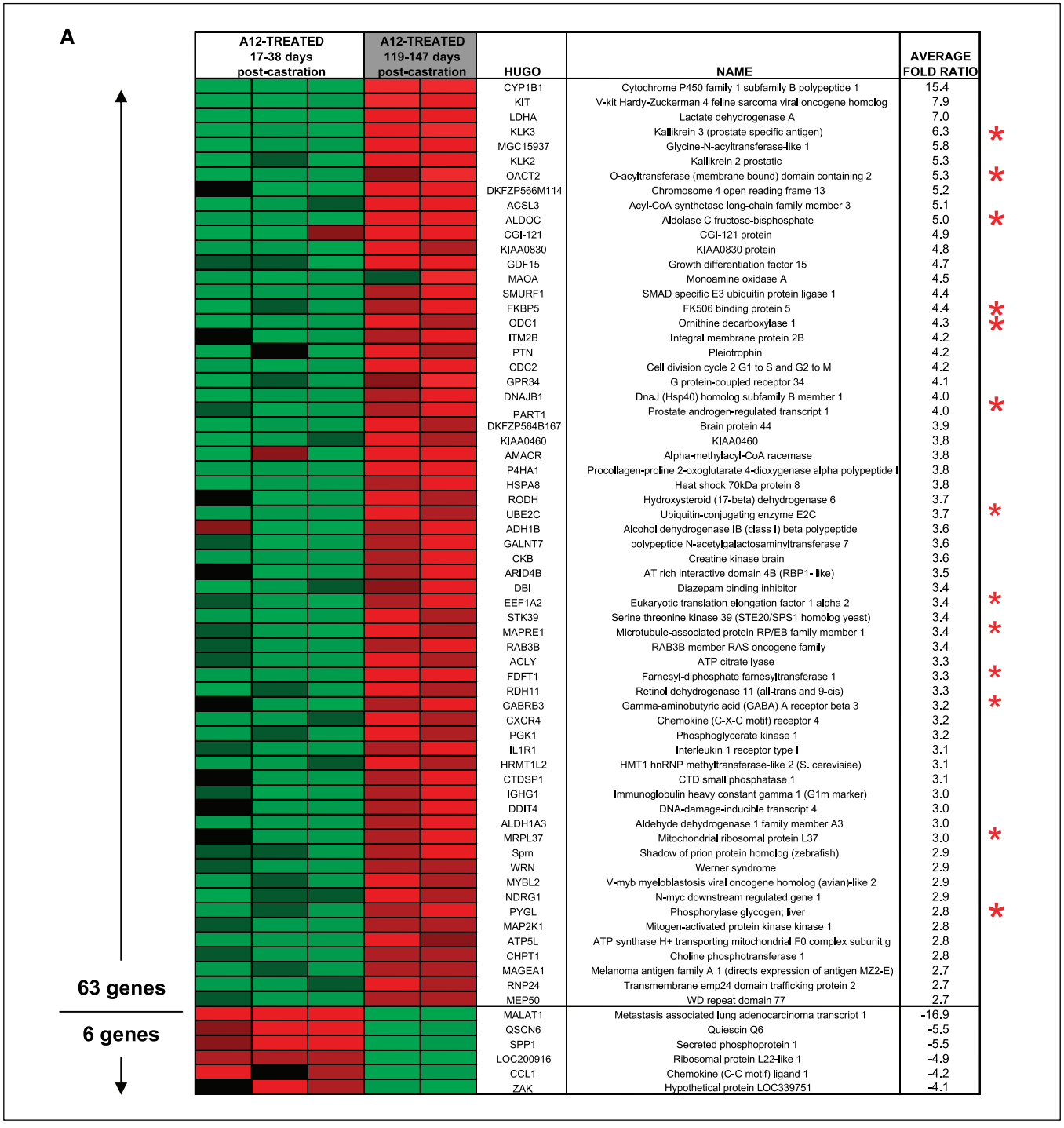

HUGO	NAME	AVERAGE FOLD RATIO	
CYP1B1	Cytochrome P450 family 1 subfamily B polypeptide 1	15.4	
KIT	V-kit Hardy-Zuckerman 4 feline sarcoma viral oncogene homolog	7.9	
LDHA	Lactate dehydrogenase A	7.0	
KLK3	Kallikrein 3 (prostate specific antigen)	6.3	*
MGC15937	Glycine-N-acyltransferase-like 1	5.8	
KLK2	Kallikrein 2 prostatic	5.3	
OACT2	O-acyltransferase (membrane bound) domain containing 2	5.3	*
DKFZP566M114	Chromosome 4 open reading frame 13	5.2	
ACSL3	Acyl-CoA synthetase long-chain family member 3	5.1	
ALDOC	Aldolase C fructose-bisphosphate	5.0	*
CGI-121	CGI-121 protein	4.9	
KIAA0830	KIAA0830 protein	4.8	
GDF15	Growth differentiation factor 15	4.7	
MAOA	Monoamine oxidase A	4.5	
SMURF1	SMAD specific E3 ubiquitin protein ligase 1	4.4	
FKBP5	FK506 binding protein 5	4.4	*
ODC1	Ornithine decarboxylase 1	4.3	*
ITM2B	Integral membrane protein 2B	4.2	
PTN	Pleiotrophin	4.2	
CDC2	Cell division cycle 2 G1 to S and G2 to M	4.2	
GPR34	G protein-coupled receptor 34	4.1	
DNAJB1	DnaJ (Hsp40) homolog subfamily B member 1	4.0	
PART1	Prostate androgen-regulated transcript 1	4.0	*
DKFZP564B167	Brain protein 44	3.9	
KIAA0460	KIAA0460	3.8	
AMACR	Alpha-methylacyl-CoA racemase	3.8	
P4HA1	Procollagen-proline 2-oxoglutarate 4-dioxygenase alpha polypeptide I	3.8	
HSPA8	Heat shock 70kDa protein 8	3.8	
RODH	Hydroxysteroid (17-beta) dehydrogenase 6	3.7	
UBE2C	Ubiquitin-conjugating enzyme E2C	3.7	*
ADH1B	Alcohol dehydrogenase IB (class I) beta polypeptide	3.6	
GALNT7	polypeptide N-acetylgalactosaminyltransferase 7	3.6	
CKB	Creatine kinase brain	3.6	
ARID4B	AT rich interactive domain 4B (RBP1- like)	3.5	
DBI	Diazepam binding inhibitor	3.4	
EEF1A2	Eukaryotic translation elongation factor 1 alpha 2	3.4	*
STK39	Serine threonine kinase 39 (STE20/SPS1 homolog yeast)	3.4	*
MAPRE1	Microtubule-associated protein RP/EB family member 1	3.4	
RAB3B	RAB3B member RAS oncogene family	3.4	
ACLY	ATP citrate lyase	3.3	*
FDFT1	Farnesyl-diphosphate farnesyltransferase 1	3.3	
RDH11	Retinol dehydrogenase 11 (all-trans and 9-cis)	3.3	*
GABRB3	Gamma-aminobutyric acid (GABA) A receptor beta 3	3.2	
CXCR4	Chemokine (C-X-C motif) receptor 4	3.2	
PGK1	Phosphoglycerate kinase 1	3.2	
IL1R1	Interleukin 1 receptor type I	3.1	
HRMT1L2	HMT1 hnRNP methyltransferase-like 2 (S. cerevisiae)	3.1	
CTDSP1	CTD small phosphatase 1	3.1	
IGHG1	Immunoglobulin heavy constant gamma 1 (G1m marker)	3.0	
DDIT4	DNA-damage-inducible transcript 4	3.0	
ALDH1A3	Aldehyde dehydrogenase 1 family member A3	3.0	
MRPL37	Mitochondrial ribosomal protein L37	3.0	*
Sprn	Shadow of prion protein homolog (zebrafish)	2.9	
WRN	Werner syndrome	2.9	
MYBL2	V-myb myeloblastosis viral oncogene homolog (avian)-like 2	2.9	
NDRG1	N-myc downstream regulated gene 1	2.9	
PYGL	Phosphorylase glycogen; liver	2.8	*
MAP2K1	Mitogen-activated protein kinase kinase 1	2.8	
ATP5L	ATP synthase H+ transporting mitochondrial F0 complex subunit g	2.8	
CHPT1	Choline phosphotransferase 1	2.8	
MAGEA1	Melanoma antigen family A 1 (directs expression of antigen MZ2-E)	2.7	
RNP24	Transmembrane emp24 domain trafficking protein 2	2.7	
MEP50	WD repeat domain 77	2.7	
MALAT1	Metastasis associated lung adenocarcinoma transcript 1	-16.9	
QSCN6	Quiescin Q6	-5.5	
SPP1	Secreted phosphoprotein 1	-5.5	
LOC200916	Ribosomal protein L22-like 1	-4.9	
CCL1	Chemokine (C-C motif) ligand 1	-4.2	
ZAK	Hypothetical protein LOC339751	-4.1	

Fig. 3. Significant gene expression changes between the two time periods of A12-treated tumors. *A,* out of 3,170 unique genes on the array with sufficient data to test, there were 21 up-regulated [including many androgen-regulated (*)] and 41 down-regulated with ≤10% *q* value in the late time period when tumors began to recur compared with the early time period.

In groups 2 and 3, tumor volumes reached their nadir 6 weeks after castration at <10% of the volume at castration ($P < 0.01$). Figure 1C presents survival data on the three groups using tumor death as an end point. Tumor death is based on the tumor volume reaching 1,000 mm^3 because this is the tumor volume at which the animal must be euthanized according to the University of Washington IACUC protocol. The study was terminated when all of the group 1 animals met the criteria for tumor volume.

To investigate whether the change in AR nuclear translocation with A12 treatment was a potential mechanism for the interaction of A12 and castration in this study, we did AR IHC on tumors from each of the three groups. We assigned a nuclear AR staining score to 100 nuclei from each tumor (Fig. 2A).

Nuclei were scored blindly by two individuals, and the mean of the two scores was counted as the score for the respective tissue. There was a significant positive correlation between tumor volume and nuclear AR intensity ($r = 0.66$; $P \leq 0.01$; Fig. 2B).

Enhanced effect of castration plus A12 treatment is associated with a decrease in AR-regulated gene expression. cDNA microarrays were done on RNA samples from tumors in each group at the time frames indicated in Materials and Methods. The arrays done before day 73 were included into the "early" time period, and those after that point were termed the "late" time period. No genes were found to be significantly altered between the time periods for group 1 (castration alone) when tested by two-sample *t* test in SAM (q value $\geq$100%) In addition, unsupervised, hierarchical clustering of known androgen-regulated genes did not segregate the two time periods. This may not be surprising because the animals in group 1 had PSA and growth recurrence and increased nuclear AR scores in the tumors removed for array analysis at early and late time points. In contrast, there were significant changes in gene expression between the two time periods of A12-treated tumors in groups 2 and 3. Out of 3,170 unique genes on the array, 21 were up-regulated (including many androgen regulated), and 41 were down-regulated with $\leq$10% q value in the late time period when tumors began to recur compared with the early time period (Fig. 3A). Unsupervised, hierarchical clustering of known androgen-regulated genes clearly differentiated the A12-treated, two time periods into two separate clusters (Fig. 3B). Changes in the expression of representative AR-regulated genes, such as KLK3, FKBP5, and PART1 were further validated by qRT-PCR (Fig. 3C). These data indicate that with progression to AI disease

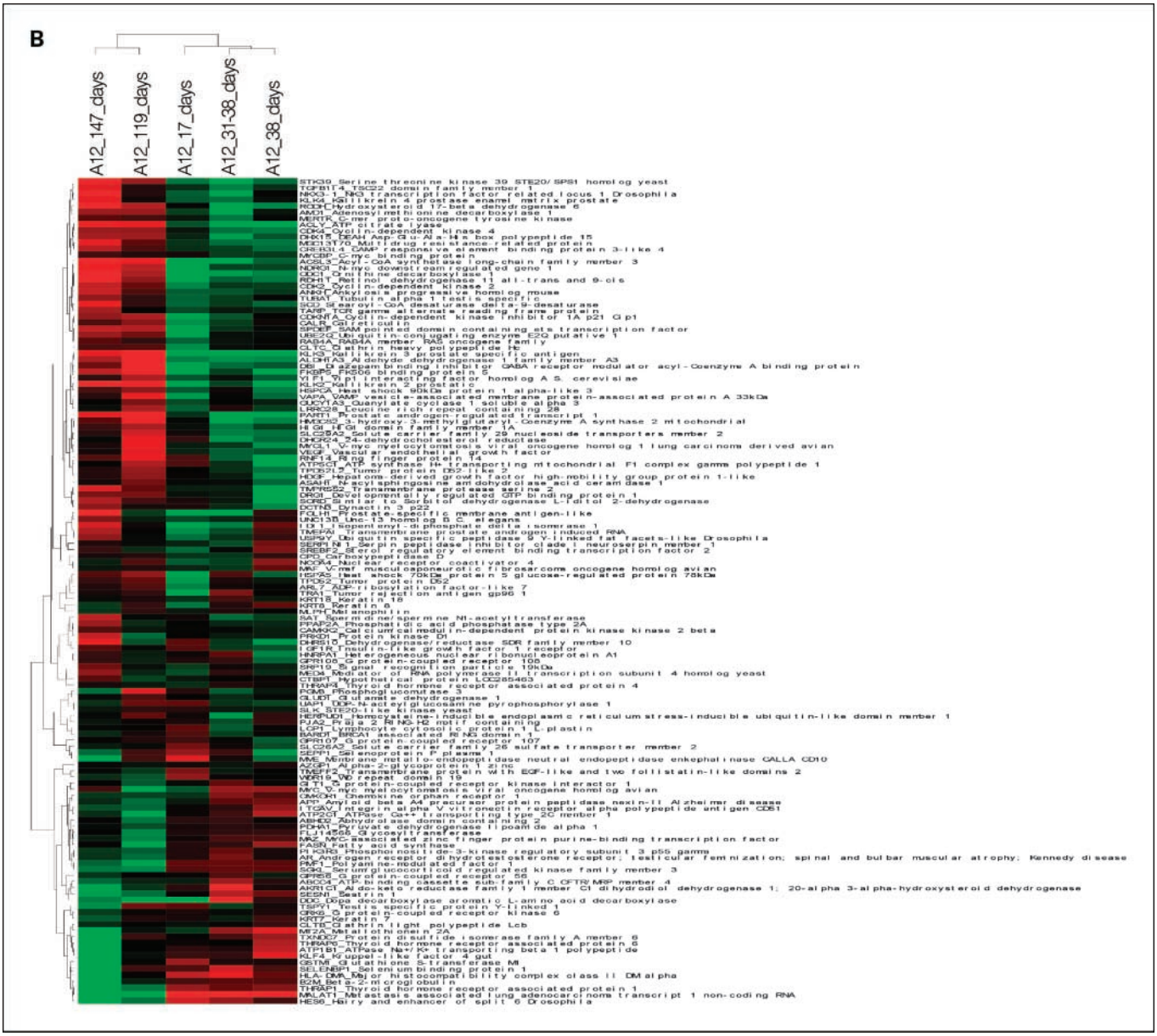

Fig. 3 *Continued. B,* furthermore, unsupervised, hierarchical clustering of known androgen-regulated genes clearly differentiated the A12-treated, two time periods into two separate clusters. Gene annotations are in the Supplementary Data for (*B*).

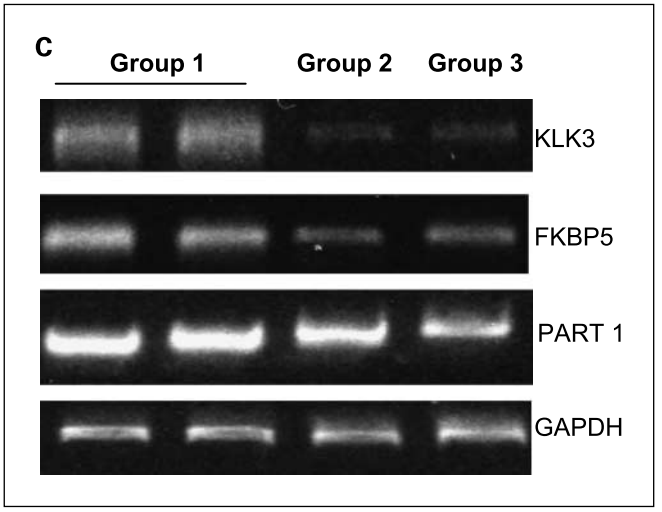

Fig. 3 *Continued. C,* RT-PCR of three androgen-regulated genes that had decreased expression in the A12 + castration treatment versus castration alone. Note that the changes on the gel are consistent with changes noted on the array. Gene identification compares to HUGO definition in Fig. 4A.

after A12 treatment plus castration, greater localization of AR to the nucleus is associated with AR transcriptional activity as a probable mechanism of progression.

Survivin and β-tubulin (TUBB) expression are significantly decreased by A12. Survivin was selected for evaluation because it is an antiapoptotic protein regulated by IGFs and associated with the resistance to castration and progression in prostate cancer (17, 33, 34). As shown in Fig. 4A, qRT-PCR shows a significant positive correlation between survivin copy number and tumor volume ($r = 0.66$; $P \leq 0.01$). A second gene that correlates with IGF-IR–induced tumor formation is β-tubulin, TUBB (35). In Fig. 4B, TUBB expression was decreased significantly in groups 2 and 3 compared with group 1. The copy numbers of TUBB correlate positively with tumor volume ($r = 0.59$; $P \leq 0.01$). A third gene that was not differentially expressed over on the microarrays in group 1 but was decreased in the two early time periods in the groups 2 and 3 was PSA. The change in PSA expression was confirmed by a similar pattern in the serum PSA levels (Fig. 1B).

BrdUrd and TUNEL staining show A12 plus castration results in decreased proliferation. As shown in Table 1A, proliferation was significantly greater in the group 1 tumors compared with groups 2 and 3 ($P \leq 0.01$). In contrast, apoptosis as determined by TUNEL staining was higher in group 1 compared with groups 2 and 3 (Table 1A).

Changes in tumor cell surface IGF-IR expression. In group 1, IGF-IR increased with time following castration ($r = 0.32$; $P \leq 0.02$). No changes in IGF-IR expression over time were seen in either group 2 or 3 and seemed to remain low throughout the course of the study (Fig. 5).

Tumor androgens are not modulated by A12 treatment. We assayed tumor tissue androgens to explore whether A12 might mediate its effect by further suppressing tissue androgen levels. Testosterone and dihydrotestosterone levels were readily detectable in the xenografts when tumors were removed at the time of sacrifice at least 5 weeks after castration (Table 1B; ref. 5). There was no significant difference in tissue androgens in the tumors treated with castration alone versus those treated with castration plus A12 at the time of sacrifice in all three groups. Reduced serum testosterone levels as well as the decrease in PSA confirmed that the animals were castrated, and that modulation of tissue androgen levels is not a mechanism by which A12 mediates its effects on AR translocation.

IGF-IR signaling modulates AR nuclear translocation in LnCaP cells. In this study, we propose that the inhibition of IGF-IR signaling affects the translocation of the endogenous AR. Because the LuCaP xenograft does not grow *in vitro*, we have elected to use the LnCaP line because it is one of the few human prostate cancer cell lines with an endogenous AR. As seen in Fig. 6A to D, addition of dihydrotestosterone to the medium induces the nuclear translocation of the AR, with a further increase in nuclear AR density when IGF-I and dihydrotestosterone are added in combination, consistent with previous studies (24). When cells were treated with A12 before the addition of IGF-I, the level of nuclear AR was similar to the level seen with dihydrotestosterone alone (Fig. 6E and F). To further assess the effect of the IGF-IR on nuclear AR localization, we isolated the nuclear and cytoplasmic fractions of LnCaP cells treated as indicated with dihydrotestosterone and IGF (Fig. 6G). The purity of fractions was determined by Golgi and histone 2B Western blots for cytoplasmic or nuclear contamination, respectively. The Western blots were done in triplicate experiments, and AR bands were quantitated and controlled for

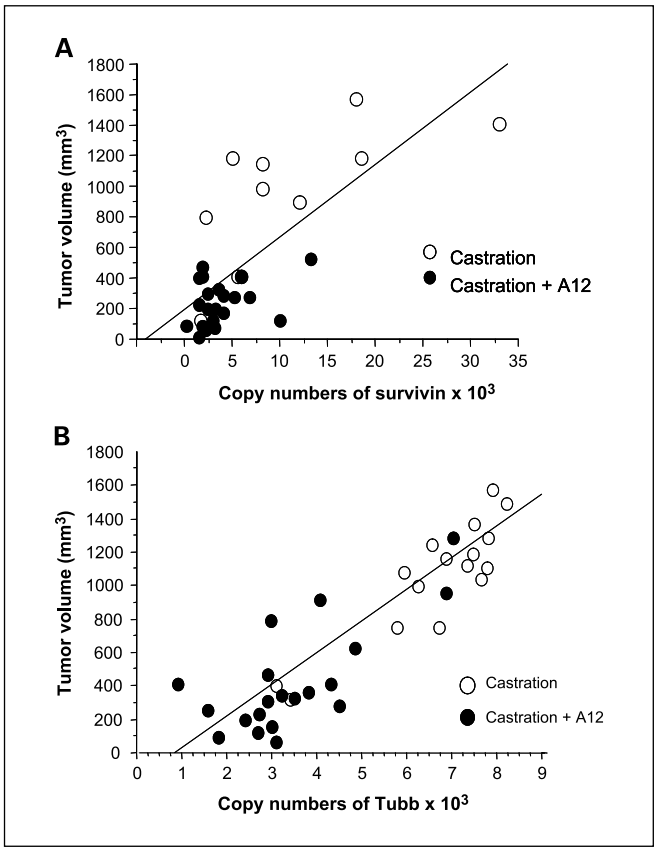

Fig. 4. *A,* correlation between survivin copy numbers and tumor volume. ○, castrate only, group 1, values; ●, castrate + A12 early and late values; $r = 0.66$, $P \leq 0.01$. Each value is the mean of three qRT-PCRs. *B,* correlation between tubulin-β peptide 3 copy numbers and tumor volume. ○, castrate only values; ●, castrate + A12 early and late values; $r = 0.59$, $P \leq 0.01$. Each value is the mean of three qRT-PCRs.

Table 1. Analysis of proliferation, apoptosis, and steroid levels in tumors

A. Apoptosis and BrdUrd uptake

Treatment group	Apoptosis (TUNEL; mean ± SE)	BrdUrd (mean ± SE)
Castrate	6.58 ± 1.41	27.74 ± 1.93
Castrate + A12 early	1.29 ± 0.49*	17.78 ∓ 2.74*
Castrate + A12 late	1.16 ∓ 0.37*	12.36 ± 1.75*

B. Serum testosterone levels and prostate xenograft levels of testosterone (60) and dihydrotestosterone (DHT)

Tissue	Serum testosterone (nmol ± SE)	Prostate testosterone (pg/mg ± SE)	Prostate DHT (pg/mg ± SE)
Non-castrate (n = 5)	15.00 ± 6.00	0.60 ± 0.21 †	1.07 ± 0.13 †
Castrate (n = 5)	0.70 ± 0.60	1. 72 ± 1.41	2.18 ± 0.81
Castrate + A12 (n = 5)	nd	1.16 ± 0.15	3.18 ± 1.68

NOTE: Note the decreased castrate levels of testosterone in the serum but increased levels of testosterone and dihydrotestosterone in prostate tissue compared with non-castrate tumors. Samples from groups 2 and 3 are included in the castrate + A12 category.
*P < 0.001 compared with castrate group.
†P < 0.001 versus serum testosterone.

loading by histone 2B protein. The nuclear/cytoplasmic AR (Nu/Cy) ratio increased significantly ($P < 0.01$) when cells were treated with IGF-I and returned to the level of dihydrotestosterone treatment alone when cells were treated with A12 before the treatment with IGF-I (Fig. 6I). These results were similar to those obtained by deconvolution microscopy, further confirming the effects of the IGF-IR on AR nuclear translocation. Associated with the decrease in nuclear AR, we have seen a decrease in PSA mRNA and protein (data not shown). The Western blots also indicate that in the absence of androgen, there is no effect of IGF or A12 because IGF-1R is not expressed in LnCaP cells without androgen (36).

Discussion

This study provides preclinical evidence that treatment with an IGF-IR inhibitory monoclonal antibody, A12, following castration significantly prolongs and accentuates the effect of androgen deprivation on prostate cancer response and time to recurrence in a human xenograft model of prostate cancer (23). A12 inhibits IGF-IR activity by interfering with IGF-ligand binding to the receptor, and A12 significantly decreases IGF-IR cell surface expression by lysosomal degradation (23, 28). In this study, a 2-week period of administration of A12 soon after castration was associated with a greater than 4-fold lengthening of the time of tumor regression in these mice. Because the study was stopped at 24 weeks, the entire length of time until tumor-related sacrifice in the A12-treated animals is not known. However, because SCID mice have a life span of approximate 52 weeks, the 2-week period of A12 treatment extended the tumor regression period by 40% of the animal's life span (The Jackson Laboratory).

Recent data in men as well as human prostate cancer xenografts in mice have shown that current methods of androgen ablation fail to decrease prostatic androgens below that expected to activate the AR (3, 6, 37, 38). Furthermore, it has been shown that AR expression is the most consistent factor associated with the progression of prostate cancer following androgen withdrawal (5, 39). AR expression increases in the LuCaP 35 human prostate cancer xenograft when regrowth occurred after castration (5). Despite these data indicating that current methods of androgen withdrawal fail to completely abrogate AR-driven tumor progression, castration remains the mainstay of treatment for recurrent prostate cancer with progression-free survival times between 12 and 36 months and time to death of 24 to 72 months.

The addition of A12 to androgen withdrawal has the potential to enhance the effects of castration through various pathways. One pathway would be blocking IGF-mediated recovery from apoptosis. The mechanisms by which the IGF-IR can abrogate apoptosis have been reviewed in several recent papers and are beyond the scope of this discussion, but may involve the Ras–extracellular signal-regulated kinase (Ras-ERK) and the phosphoinositide-3-kinase pathways (40, 41). This pathway is not unique to the prostate, but is one of the most common

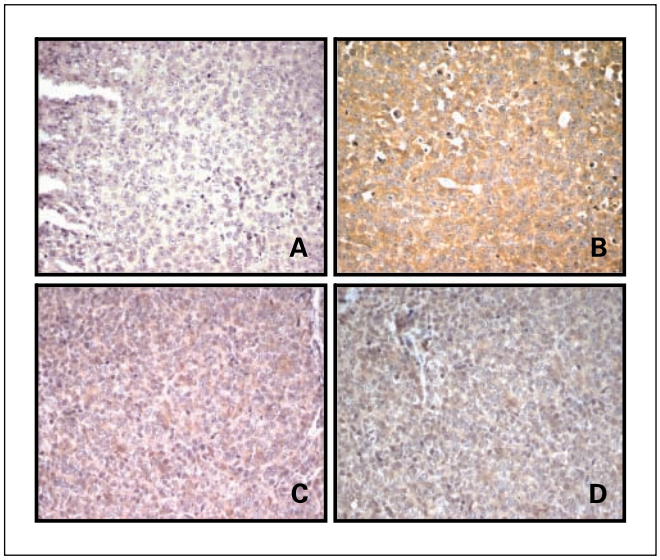

Fig. 5. IHC of IGF-IR. *A,* IgG control, *B,* castrate only, group 1. Note the well-defined IGF-IR expression on cell surface and in cytoplasm. *C* and *D,* representative tumors from groups 2 and 3, respectively. Note the decrease in overall IGF-IR staining in tumors from groups 2 and 3 compared with castrate only group 1.

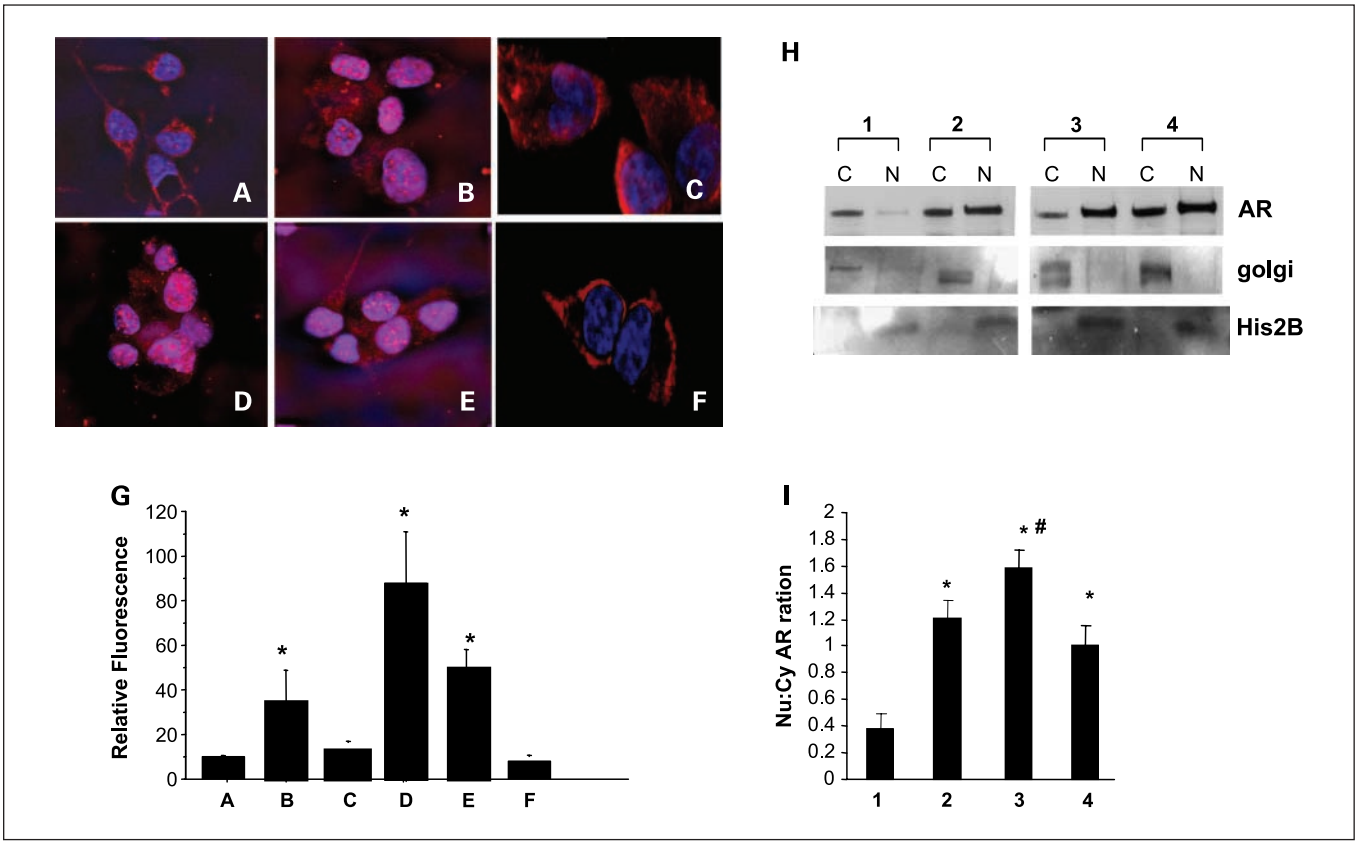

Fig. 6. IGF-I – induced AR translocation into the nucleus in LnCaP cells. *A* to *G,* data from deconvolution microscopy images. After treatment, cells were fixed and stained with an AR-specific antibody sc-7305 followed by a biotin-SP – conjugated goat anti-mouse IgG F(ab′)$_2$ and a streptavidin-Alexa^{594}. DAPI was used to stain for nucleus. *A,* LnCaP cells in CSS medium, AR is predominantly localized in the cytoplasmic compartment. *B,* with 10^{-8} mol/L of dihydrotestosterone treatment, most of the AR is localized in the nucleus. *C,* with 10 ng/mL IGF-I, the majority of AR is in the cytoplasm. *D,* with treatment of 10^{-8} mol/L dihydrotestosterone + 10 ng/mL IGF-I, nearly all AR is localized in the nucleus. *E,* with treatment of 10^{-8} mol/L dihydrotestosterone + 10 ng/mL IGF-I + 20 μg/mL A12, some AR moved from nucleus to the cytoplasm. *F,* treatment with 20 ng/mL A12 shows all AR in the cytoplasm. *A, B, D,* and *E,* magnification, 40×; *C* and *F,* magnification, 60×. *G,* relative quantitation of nuclear AR (*red*). *, $P < 0.01$, compared with (*A*). *H,* Western immunoblot of cytosol and nuclear fractions of LnCaP cells in T-Medium with CSS (*1*), Treated with 10^{-8} mol/L dihydrotestosterone (*2*), 10^{-8} mol/L dihydrotestosterone + 10 ng/mL IGF-I (*3*), 10^{-8} mol/L dihydrotestosterone + 10 ng/mL IGF-I + 20 μg/mL A12 (*4*). Cytosol and nuclear extractions controlled for loading and purity by ERK antibody. Further purity of separation is seen with all Golgi immunoreactivity, a cytoplasmic marker in the cytoplasm and histone 2B immunoreactivity, a nuclear marker, in the nucleus. Histone 2B and Golgi protein was affected by treatments and could not be used as a loading control. Each experiment was done in triplicate. *I,* nuclear/cytoplasmic ratio of AR based on the densitometry of triplicate Western blots from (*G*). #, $P < 0.01$, compared with 10^{-8} mol/L dihydrotestosterone (*2*) and 10^{-8} mol/L dihydrotestosterone + IGF-1 + 20 ng/mL A12 (*4*).

mechanisms involved in recovering from an apoptotic insult in multiple tissues (40, 42–51). In prostate cancer, there is clear clinical evidence that activation of IGF signaling occurs soon after castration, and IGF-IR expression increases in human prostate cancer as the time post-castration increases and with the development of androgen-independent disease (36). A second mechanism by which IGF-IR inhibition could prolong the effects of androgen withdrawal is by maintaining the tumor in cell cycle arrest following the initial apoptosis of androgen withdrawal. After the initial cell death induced by castration, the remaining prostate epithelial cells remain in a state of cell quiescence until tumor growth recurs. We and others have shown that IGF-IR inhibition can cause prostate cancer cells to undergo cell cycle arrest as well as enhance apoptosis (23). The BrdUrd uptake done on tumors harvested at the end of the study would suggest that this is one mechanism by which A12 has prolonged the effects of castration. A third potential mechanism for the activity of A12 in conjunction with castration would be to enhance the inhibition of signaling through the AR. Such a mechanism would be of interest because it would pose a specific reason for use of IGF-IR inhibition in prostate cancer.

We have looked at the expression of two genes that are regulated by the IGF-IR and associated with the development of resistance to castration, tubulin β-peptide (TUBB), and survivin (17, 34, 52). In this study, we noted that survivin and TUBB were suppressed by A12 in the castration-plus-A12 groups compared with the castrate-alone group. Because survivin has been shown as a pathway by which androgen-insensitive disease may arise following androgen deprivation and its expression is increased by IGF-IR activation, a decrease in survivin by the inhibition of IGF-IR may be an important mechanism and marker of A12 activity in prostate cancer. Likewise, TUBB is specifically increased in IGF-IR–mediated cell transformation, and its suppression by A12 may also be a specific biomarker and pathway for inhibition of prostate cancer by A12 (53).

Because the LuCaP 35 tumors used in this study are pTEN negative and because we have shown that A12 decreases AKT phosphorylation in these tumors, we would conclude that the loss of pTEN activity is not a mechanism of resistance to IGF-IR inhibition (27). The effectiveness of targeting the IGF-IR in the absence of pTEN has also been shown in other studies in the prostate as well as other tumors (54, 55).

Persistent signaling through the AR is a common feature of prostate cancer progression in all circumstances where it was examined. In fact, recent data from several groups suggest that not only is the AR continually expressed and active following androgen deprivation, but the prostate may be able to synthesize dihydrotestosterone from several precursor steroids and possibly acetate (3, 4, 39, 56, 57). If these data are correct, the activation of the AR in androgen-deprived prostate cancer patients has become an autocrine rather than endocrine function, and therapy needs to be directed at the AR. In this study, we present evidence that signaling through the IGF-IR enhances classic AR signaling by increasing the translocation to the nucleus. Furthermore, when IGF-IR signaling is blocked soon after castration, the effects of castration are augmented. Associated with the enhanced effects on tumor growth is a marked decrease in nuclear AR. Although marked decreases in serum PSA were noted with castration alone or castration plus A12, PSA began to increase within 4 weeks as tumor size increased in the animals treated with castration alone and was consistent with the regrowth of the tumor. In contrast, in the castration-plus-A12–treated animals, PSA remained suppressed significantly longer than those that received castration as the only treatment. When PSA did subsequently increase, tumor volume also began to increase. This suggests that in spite of being castrate, there was a return of androgen signaling. These differences between groups were confirmed by the cDNA array analysis. In the castration-only group, there were no differences in gene expression between tumors assayed at any of the time points noted. Although in the castration-plus-A12–treated animals, a significant increase in androgen-regulated genes was noted when the tumors recurred, suggesting a return to AR-driven tumor progression. When cDNA arrays were compared between those tumors that had recurred in the castrate group and those that had recurred in the castrate-plus-A12–treated groups, there were no differences, indicating that once the tumors had recurred, the same forces were driving tumor progression as determined by gene expression. We have also effectively ruled out the possibility that these changes in androgen-regulated genes are mediated by the modulation of tissue androgens. Therefore, other means by which AR-mediated signaling is abrogated must be invoked.

The finding most relevant to prostate cancer was the correlation between decreased nuclear AR and tumor volume. This suggests that the inhibition of IGF-IR signaling, in addition to its effects on antiapoptotic and proliferation pathways, may have a specific effect in prostate cancer by altering AR nuclear translocation and subsequent AR signaling. The mechanism by which A12 accomplishes this activity has yet to be defined. However, we do show that *in vitro* A12 decreases the nuclear/cytoplasmic ratio of AR, and that this change results in a decrease in androgen-regulated gene expression in LnCaP and M12 AR cells (27). We have previously reported that IGF treatment decreases AR phosphorylation (27), and Gioeli et al. have shown that phosphorylation of the AR at Ser^{650} is necessary for nuclear export of the AR (57). Therefore, a potential mechanism for the effect of A12 is to enhance AR phosphorylation at Ser^{650} and facilitate nuclear export. Lin has reported that signaling via the IGF-IR results in the phosphorylation of the AR in contrast with our studies (58). However, Gioeli has shown that there is no direct phosphorylation of the AR by IGF (59). Regardless, the decrease in phosphorylation of AR and increase in nuclear AR localization is consistent with the current study. The mechanism by which IGF induces dephosphorylation has not been defined.

Finally, as shown in the cDNA array data, the resumption of tumor growth in the castration-plus-A12 groups is associated with an increase in AR-regulated gene expression, consistent with the recurrence of AR-driven progression and the demonstration that A12 functions, at least in part, by the suppression of AR function.

In summary, we show in a preclinical study that the combination of castration plus IGF-IR inhibition significantly prolongs the time to the appearance of AI prostate cancer when compared with castration alone. If these data were confirmed in clinical trials, the addition of an IGF-IR monoclonal antibody in conjunction with castration would significantly increase the survival and symptom-free period of men with recurrent prostate cancer.

Acknowledgments

We thank Nicole Lavoie for her help in animal husbandry.

References

1. Scher H, Sawyers C. Biology of progressive, castration-resistant prostate cancer: directed therapies targeting the androgen-receptor signaling axis. J Clin Oncol 2005;23:8235–61.
2. Huggins C, Hodges C. Studies on prostate cancer: effect of castration, estrogen, and androgen injection on serum phosphatases in metastatic carcinoma of the prostate. Cancer Res 1941;1:293–7.
3. Titus M, Schell M, Lih F, Tomer K, Mohler J. Testosterone and dihydrotestosterone tissue levels in recurrent prostate cancer. Clin Cancer Res 2005;11:4653–7.
4. Mohler J, Gregory C, Ford O III, et al. The androgen axis in recurrent prostate cancer. Clinical Cancer Res 2004;10:440–8.
5. Chen C, Welsbie D, Tran C, et al. Molecular determinants of resistance to antiandrogen therapy. Nat Med 2004;10:33–9.
6. Page S, Lin D, Mostaghel E, et al. Persistent intraprostatic androgen concentrations after medical castration in healthy men. J Clin Endocrinol Metab 2006; 91:3850–6.
7. Kiyama S, Morrison K, Zellweger T, et al. Castration-induced increases in insulin-like growth factor-binding protein 2 promotes proliferation of androgen-independent human prostate LNCaP tumors. Cancer Res 2003; 63:3575–35.
8. Miyake H, Gleave M. Castration-induced up-regulation of insulin-like growth factor binding protein-5 (IGFBP-5) potentiates IGF-I action and accelerates progression to androgen-independence in prostate cancer xenograft models. Amer Assoc Cancer Res 2000;44:735.
9. Nickerson T, Miyake H, Gleave M, Pollak M. Castration-induced apoptosis of androgen-dependent shionogi carcinoma is associated with increased expression of genes encoding insulin-like growth factor binding proteins. Cancer Res 1999;59:3392–33.
10. Nickerson T, Pollak M, Huynh H. Castration-induced apoptosis in the rat ventral prostate is associated with increased expression of genes encoding IGFBP-2, -3, -4, and -5. Endocrinology 1998;139:807–10.
11. Miyake H, Nelson C, Rennie P, Gleave M. Overexpression of insulin-like growth factor binding protein-5 helps accelerate progression to androgen-independence in the human prostate LNCaP tumor model through activation of phosphatidylinositol 3-kinase pathway. Endocrinology 2000;141:2257–65.
12. Miyake H, Nelson C, Rennie P, Gleave M. Testosterone-repressed prostate message-2 is an antiapoptotic gene involved in progression to androgen independence in prostate cancer. Cancer Res 2000; 60:170–6.
13. Wright A, Douglas R, Thomas L, Lazier C, Rittmaster R. Androgen induced regrowth in the castrated rat ventral prostate: role of 5α-reductase. Endocrinology 1999;140:4509–15.
14. Huynh H, Yang X, Pollak M. A role of insulin like growth factor binding protein 5 in the antiproliferative action of the antiestrogen ICI 182780. Cell Growth Differ 1996;7:1501–6.
15. Ohlson N, Bergh A, Persson M, Wikström P. Castration rapidly decreases local insulin-like growth factor-1 levels and inhibits its effects in the ventral prostate in mice. Prostate 2006;66:1687–97.
16. Ai Z, Fischer A, Spray DC, Brown AM, Fishman GI. Wnt-1 regulation of connexin 43 in cardiac myocytes. J Clin Invest 2000;105:161–71.
17. Zhang M, Latham D, Delaney M, Chakravarti A. Survivin mediates resistance to antiandrogen therapy in prostate cancer. Oncogene 2005;24:2474–82.

18. Xin L, Teitell M, Lawson D, Kwon A, Mellinghoff I, Witte O. Progression of prostate cancer by synergy of AKT with genotropic and nongenotropic actions of the androgen receptor. Proc Natl Acad Sci U S A 2006;103:7789–94.

19. Abreu-Martin M, Chari A, Palladino A, Craft N, Sawyers C. Mitogen-activated protein kinase kinase kinase 1 activates androgen receptor-dependent transcription and apoptosis in prostate cancer. Mol Cell Biol 1999;19:5143–54.

20. Craft N, Shostak Y, Carey M, Sawyers C. A mechanism for hormone-independent prostate cancer through modulation of androgen receptor signaling by the HER-2/neu tyrosine kinase. Nat Med 1999;5:280–5.

21. Craft N, Chor C, Tran C, et al. Evidence for clonal outgrowth of androgen-independent prostate cancer cells from androgen-dependent tumors through a two-step process. Cancer Res 1999;59:5030–6.

22. Klein K, Reiter R, Redula J, et al. Progression of metastatic human prostate cancer to androgen independence in immunodeficient SCID mice. Nat Med 1997;3:402–8.

23. Wu JD, Odman A, Higgins LM, et al. *In vivo* effects of the human type I insulin-like growth factor receptor antibody A12 on androgen-dependent and androgen-independent xenograft human prostate tumors. Clin Cancer Res 2005;11:3065–74.

24. Wu J, Haugk K, Woodke L, Nelson P, Coleman I, Plymate S. Interaction of IGF signaling and the androgen receptor in prostate cancer progression. J Cell Biochem 2006;99:392–401.

25. Wu J, Corey E, Haugk K, et al. Targeting the type 1 insulin-like growth factor receptor with a monoclonal antibody enhances the activity of docetaxel against androgen-independent and osseous human prostate cancer *in vivo*. Clin Cancer Res 2006;12:6153–60.

26. Corey E, Quinn J, Buhler K, et al. LuCaP 35: A new model of prostate cancer progression to androgen independence. Prostate 2003;55:239–46.

27. Whang Y, Wu X, Suzuki H, et al. Inactivation of the tumor suppressor PTEN/MMAC1 in advanced human prostate cancer through loss of expression. Proc Natl Acad Sci U S A 1998;95:5246–50.

28. Burtrum D, Zhu Z, Lu D, et al. A fully human monoclonal antibody to the insulin-like growth factor I receptor blocks ligand-dependent signaling and inhibits human tumor growth *in vivo*. Cancer Res 2003;63:8912–21.

29. Tennant M, Vessella R, Sprenger C, et al. Insulin-like growth factor binding protein-related protein 1 (IGFBP-rP1/mac 25) is reduced in human prostate cancer and is inversely related to tumor volume and proliferation index in LuCaP 23.12 xenografts. Prostate 2003;56:115–22.

30. Hawkins V, Doll D, Bumgarner R, et al. PEDB: the prostate expression database. Nucleic Acids Res 1999;27:204–8.

31. Bonham M, Arnold H, Montgomery B, Nelson P. Molecular effects of the herbal compound PC-SPES: identification of activity pathways in prostate carcinoma. Cancer Res 2002;62:3920–4.

32. Tusher V, Tibshirani R, Chu C. Significance analysis of microarrays applied to ionizing radiation response. Proc Natl Acad Sci U S A 2001;98:5116–21.

33. Vaira V, Lee C, Goel H, Bosari S, Languino L, Altieri D. Regulation of survivin expression by IGF-1/mTOR signaling. Oncogene 2007;26:2678–84.

34. Shariat S, Lotan Y, Saboorian H, et al. Survivin expression is associated with features of biologically aggressive prostate carcinoma. Cancer 2005;100:751–7.

35. Loughran G, Huigsloot M, Kiely P, et al. Gene expression profiles in cells transformed by overexpression of the IGF-I receptor. Oncogene 2005;24:6185–93.

36. Krueckl S, Sikes R, Edlund N, et al. Increased insulin-like growth factor I receptor expression and signaling are components of androgen-independent progression in a lineage-derived prostate cancer progression model. Cancer Res 2004;64:8620–9.

37. Geller J, Albert GD, Nachsteim DA. Comparison of prostate cancer tissue dihydrotestosterone levels at the time of relapse following orchiectomy or estrogen therapy. J Urol 1984;132:693–700.

38. Gregory C, He B, Johnson R, et al. A mechanism for androgen receptor-mediated prostate cancer recurrence after androgen deprivation therapy. Cancer Res 2001;61:4315–9.

39. Yuan X, Li T, Wang H, et al. Androgen receptor remains critical for cell-cycle progression in androgen-independent CWR22 prostate cancer cells. Am J Pathol 2006;169:682–96.

40. Baserga R, Resnicoff M, D'Ambrosio C, Valentinis B. The role of the IGF-I receptor in apoptosis. Vitamins Horm 1997;53:55–98.

41. Baserga R. The IGF-I receptor in cancer research. Exp Cell Res 1999;253:1–6.

42. Baserga R, Hongo A, Rubini M, Prisco M, Valentinis B. The role of the IGF-I receptor in cell growth, transformation and apoptosis. Biochem Biophys Acta 1997;1332:F105–26.

43. Dews M, Nishimoto I, Baserga R. IGF-I receptor protection from apoptosis in cells lacking the IRS proteins. Receptors Signal Transduction 1998;7:231–40.

44. Davies M, Koul D, Dhesi H, et al. Regulation of Akt/PKB activity, cellular growth, and apoptosis in prostate carcinoma cells by MMAC/PTEN. Cancer Res 1999;59:2551–6.

45. Hongo A, Yumet G, Resnicoff M, Romano G, O'Connor R, Baserga R. Inhibition of tumorigenesis and induction of apoptosis in human tumor cells by the stable transfection of a myristylated COOH terminus of the insulin-like growth factor 1 receptor. Cancer Res 1998;58:2477–84.

46. London C, Kroeker A, Plymate S, Iverson P, Devi G. Induction of apoptosis and interference of IGF-1–mediated intracellular signaling by targeted inhibition of IGF-I receptor using morpholino antisense in prostate cancer cells. Proceedings of the 85th Annual Meeting, Endocrine Society, Washington, DC, 2004;69.

47. O'Connor R, Kauffmann-Zeh A, Liu Y, et al. Identification of domains of the insulin-like growth factor I receptor that are required for protection from apoptosis. Mol Cell Biol 1997;17:427–35.

48. O'Connor R, Fennelly C, Krause D. Cell survival and apoptosis. Biochemical Society Transactions 2000;99:47–51.

49. Parrizas M, Saltiel A, LeRoith D. Insulin-like growth factor 1 inhibits apoptosis using the phosphatidylinositol 3′-kinase and mitogen-activated protein kinase pathways. J Biol Chem 1997;272:154–61.

50. Resnicoff M, Baserga R. The role of IGF I receptor in transformation and apoptosis. Ann NY Acad Sci 1997;842:76–81.

51. Tenniswood M. Overview on Apoptosis. 1996 International Symposium on Biology of Prostate Growth, vol. 1. Washington, DC, 1996.

52. Stubbs A, Abel P, Golding M, et al. Differentially expressed genes in hormone refractory prostate cancer. Am J Pathol 1999;154:1335–43.

53. O'Connor R. Regulation of IGF-I receptor signaling in tumor cells. Horm Metab Res 2003;35:771–7.

54. Rochester M, Riedemann J, Hellawell G, Brewster S, Macaulay V. Silencing of the IGF1R gene enhances sensitivity to DNA-damaging agents in both PTEN wild-type and mutant human prostate cancer. Cancer Gene Ther 2005;12:90–100.

55. Burtrum D, Pytowski B, Ludwig D. Abrogation of PTEN does not confer resistance to anti–IGF-IR targeted therapy in IGF responsive tumor cells. AACR, 2007 Annual Meeting, Anaheim, CA 2007.

56. Labrie C, Be'langer A, Labrie F. Androgenic activity of dehydroepiandrosterone and androstenedione in the rat ventral prostate. Endocrinology 1988;123:1412–9.

57. Stanbrough M, Bubley G, Ross K, et al. Increased expression of genes converting adrenal androgens to testosterone in androgen-independent prostate cancer. Cancer Res 2006;66:2815–25.

58. Lin H, Yeh S, Kang H, Chang C. Akt suppresses androgen-induced apoptosis by phosphorylating and inhibiting androgen receptor. Proc Natl Acad Sci U S A 2001;98:7200–5.

59. Gioeli D, Ficarro S, Kwiek J, et al. Androgen receptor phosphorlyation: regulation and identification of the phosphorylation sites. J Biol Chem 2002;277:29304–14.

60. Ugi S, T I, Ricketts W, Olefsky J. Protein phosphatase 2A forms a molecular complex with Shc and regulates Shc tyrosine phosphorylation and downstream mitogenic signaling. Mol Cell Biol 2002;22:2375–87.

Tumor Suppressor BRCA1 Is Expressed in Prostate Cancer and Controls Insulin-like Growth Factor I Receptor (*IGF-IR*) Gene Transcription in an Androgen Receptor–Dependent Manner

Hagit Schayek,[1] Kathy Haugk,[2] Shihua Sun,[2] Lawrence D. True,[3] Stephen R. Plymate,[2,4] and Haim Werner[1]

Abstract

Purpose: The insulin-like growth factor (IGF) system plays an important role in prostate cancer. The *BRCA1* gene encodes a transcription factor with tumor suppressor activity. The involvement of BRCA1 in prostate cancer, however, has not yet been elucidated. The purpose of the present study was to examine the functional correlations between BRCA1 and the IGF system in prostate cancer.

Experimental Design: An immunohistochemical analysis of BRCA1 was done on tissue microarrays comprising 203 primary prostate cancer specimens. In addition, BRCA1 levels were measured in prostate cancer xenografts and in cell lines representing early stages (P69 cells) and advanced stages (M12 cells) of the disease. The ability of BRCA1 to regulate IGF-I receptor (IGF-IR) expression was studied by coexpression experiments using a BRCA1 expression vector along with an IGF-IR promoter-luciferase reporter.

Results: We found significantly elevated BRCA1 levels in prostate cancer in comparison with histologically normal prostate tissue ($P < 0.001$). In addition, an inverse correlation between BRCA1 and IGF-IR levels was observed in the androgen receptor (AR)–negative prostate cancer–derived P69 and M12 cell lines. Coexpression experiments in M12 cells revealed that BRCA1 was able to suppress IGF-IR promoter activity and endogenous IGF-IR levels. On the other hand, BRCA1 enhanced IGF-IR levels in LNCaP C4-2 cells expressing an endogenous AR.

Conclusions: We provide evidence that BRCA1 differentially regulates IGF-IR expression in AR-positive and AR-negative prostate cancer cells. The mechanism of action of BRCA1 involves modulation of *IGF-IR* gene transcription. In addition, immunohistochemical data are consistent with a potential survival role of BRCA1 in prostate cancer.

The insulin-like growth factors, IGF-I and IGF-II, are a family of mitogenic polypeptides with important roles in normal growth and differentiation as well as in tumor development and progression (1–3). In the specific context of prostate cancer, a significant amount of data has been accumulated over the last 20 years suggesting that the IGF axis plays an important role in the transformation of the prostate epithelium (4–7). The contribution of IGF action to prostate cancer development is further supported by epidemiologic studies showing a significant increase in serum IGF-I levels in patients who later developed prostate cancer (8). Acquisition of the malignant phenotype is initially IGF-I receptor (IGF-IR) dependent; however, the progression of prostate cancer from an organ-confined, androgen-sensitive disease to a metastatic one is associated with dysregulation of androgen receptor (AR)–regulated target genes and with a significant decrease in IGF-IR mRNA and protein levels (9, 10). Likewise, IGF-IR expression is extinguished in a majority of human prostate cancer bone marrow metastases (11). The molecular mechanisms that are responsible for regulation of the *IGF-IR* gene in prostate cancer, however, remain largely unidentified.

The familial breast and ovarian cancer susceptibility gene-1 (*BRCA1*) gene encodes a 220-kDa phosphorylated transcription factor with tumor suppressor activity (12). BRCA1 mutation was correlated with the appearance of breast and ovarian cancer at very young ages, although BRCA1 has been also implicated in the etiology of sporadic types of cancer (13–15). BRCA1 is normally targeted to the nucleus via two nuclear localization signals (16). The BRCA1 polypeptide participates in multiple biological pathways, including gene transcription, DNA damage repair, cell growth, and apoptosis (17). Both direct and indirect types of evidence support a tumor suppressor role of BRCA1. Direct evidence was provided by studies showing that transfer of BRCA1 protein arrested growth

Authors' Affiliations: [1]Department of Human Molecular Genetics and Biochemistry, Sackler School of Medicine, Tel Aviv University, Tel Aviv, Israel; [2]Geriatric Research and Education Clinical Center, Veterans Affairs Puget Sound Health Care System; and Departments of [3]Pathology and [4]Medicine, Gerontology and Geriatric Medicine, University of Washington, Seattle, Washington

Received 6/5/08; revised 10/13/08; accepted 11/10/08; published OnlineFirst 02/17/2009.

Grant support: Grant 2003341 from the United States-Israel Binational Science Foundation (H. Werner and S.R. Plymate) and grant CA97186-06 and Veterans Affairs Research Service (S.R. Plymate).

The costs of publication of this article were defrayed in part by the payment of page charges. This article must therefore be hereby marked *advertisement* in accordance with 18 U.S.C. Section 1734 solely to indicate this fact.

Requests for reprints: Haim Werner, Department of Human Molecular Genetics and Biochemistry, Sackler School of Medicine, Tel Aviv University, Tel Aviv 69978, Israel. Phone: 972-3-6408542; Fax: 972-3-6406087; E-mail: hwerner@post.tau.ac.il.

doi:10.1158/1078-0432.CCR-08-1440

Translational Relevance

The breast and ovarian cancer susceptibility gene-1 (BRCA1) was originally identified as a protein whose mutated form was associated with familial breast and/or ovarian cancer. However, it is clear that the nonmutated (wild-type) form of BRCA1 has distinct cellular functions, including activity as an androgen receptor (AR) coactivator as well as inhibition of insulin-like growth factor-I receptor (*IGF-IR*) gene expression. In this study, we were interested in determining the role BRCA1 may have in regulation of the *IGF-IR* gene in prostate cancer. We have shown that BRCA1 protein expression is increased in prostate cancer, but rather than suppressing IGF-IR expression, as we show in AR-negative prostate epithelial cell lines, we show that BRCA1 is positively correlated with IGF-IR. Further we show that the mechanism responsible for this correlation involves enhancing AR transactivation. These findings are of relevance because they show a new mechanism for IGF and AR stimulation of prostate cancer and further support the relevance of targeting AR and IGF-IR in prostate cancer with BRCA1 expression as a marker for defining the target activity.

of breast and ovarian cancer cells, whereas inactivation of the endogenous *BRCA1* gene induced cellular transformation (18). On the other hand, indirect evidence was provided by studies showing somatic allelic loss of 17q21 in breast and ovarian tumors (19).

The involvement of BRCA1 in prostate cancer etiology has been the focus of controversial debate. Previous studies have suggested that BRCA1 functions as an AR coregulator and plays a positive role in androgen-induced cell death (20, 21). Consistent with a potential tumor suppressor role, prostate cancer cells DU-145 transfected with a wild-type BRCA1 exhibited decreased proliferation rate, increased sensitivity to chemotherapy drugs, increased susceptibility to drug-induced apoptosis, and alterations in expression of key regulatory proteins (22). Furthermore, BRCA1 splice variant BRCA1a was recently shown to display antitumoral activity in triple-negative prostate cancer cells (23). Linkage studies have provided conflicting data about a potential correlation between *BRCA1/BRCA2* status and a familial history of prostate cancer. Thus, Struewing et al. (24) reported that by the age of 70 years, the estimated risk of prostate cancer in Ashkenazi Jewish men carrying mutations in the BRCA1 or BRCA2 genes was 16%. The hypothesis that deleterious mutations in BRCA2 are associated with an increased risk of prostate cancer was further substantiated by studies showing that this type of mutations is more likely to be found in unselected individuals with prostate cancer than in age-matched controls (25). In a recent study, the Icelandic BRCA2 999del5 founder mutation was strongly associated with rapidly progressing lethal prostate cancer (26). Specifically, patients carrying this mutation had a lower mean age of diagnosis, more advanced tumor stages, and shorter median survival times. On the other hand, a study by Vazina el al. (27) concluded that the rate of predominant Jewish BRCA1 and BRCA2 mutations in prostate cancer patients was not significantly different from that in the general population. Likewise, no strong evidence for a role of BRCA1 or BRCA2 mutations in the development of prostate cancer was provided by other reports (28, 29).

In view of the putative role of BRCA1 in prostate cancer, and to expand our previous studies on the interactions between BRCA1 and the IGF system, we evaluated in the present study (*a*) the potential correlation between BRCA1 expression and tumor status in a collection of prostate cancer specimens, and (*b*) the capacity of BRCA1 to control IGF-IR expression in prostate cancer cells with different AR status. Results obtained indicate that BRCA1 is expressed at relatively high levels in prostate cancer compared with a very low BRCA1 immunostaining in normal prostate epithelium. There is a significant negative relationship between IGF-IR and BRCA1 expression levels in AR-negative prostate cancer cell lines, whereas in cancer with an active AR this relationship is positive. In addition, we provide evidence that the *IGF-IR* gene is differentially regulated by BRCA1 in prostate cancer cells with different AR status.

Materials and Methods

Tissue acquisition. The tissue samples used in this study were tissue microarrays made from human radical prostatectomy specimens acquired and used in conformity with an Institutional Review Board–approved protocol at the University of Washington. Median patient age was 58 y (range, 48-74 y). The prostates ranged in weight from 21 to 123 g (median, 42 g). At presentation, 58% of patients were clinical stage *c*T1 and 42% *c*T2. The range of serum PSA was 2.2 to 24 ng/mL (median, 5.4 ng/mL).

Tissue microarrays. Two tissue microarrays were used for these studies. All samples in all arrays were provided in duplicate as 0.6-mm-diameter tissue cores. These arrays contained 203 prostate carcinomas exhibiting a range of Gleason grades (72% Gleason pattern 3, 27% Gleason pattern 4, 1% Gleason pattern 5) and 80 samples of nonmalignant prostate tissue of different biological states (normal, atrophy, and benign prostatic hyperplasia).

Immunohistochemistry. Antibodies recognizing BRCA1 (Santa Cruz Biotechnology, Inc.) and IGF-IR α-subunit (Santa Cruz Biotechnology) were used to stain the tissue microarrays. BRCA1 blocking peptide was purchased from Abcam. Specificity of staining was confirmed by omission of the primary antibody, by immunostaining the sections with a primary antibody against an irrelevant antigen, and by preincubating the anti-BRCA1 in a 5-fold molar excess concentration of BRCA1 peptide before incubating the sections with primary anti-BRCA1 antibody. In addition, specificity was determined by Western blot of a human prostate xenograft, LuCaP 35, which expresses BRCA1 protein. The Western blot was stained with BRCA1 antibody or a 10-fold excess of the BRCA1 blocking peptide plus BRCA1 antibody. Antigen was localized using a three-step avidin-biotin-peroxidase method. In brief, deparaffinized sections were rehydrated in PBS and subjected to antigen retrieval using a microwave (15 min in citrate buffer solution). Sections were then incubated sequentially in solutions of 5% albumin in PBS, 10% hydrogen peroxide in water, primary antibody, secondary antibody [biotinylated antirabbit IgG (BA-1000, Vector Labs)], and avidin-biotin-peroxidase solution (Vector Labs) with interval washes in PBS. Reaction product was detected by incubating the sections in an aqueous solution of 0.05% diaminobenzidine and 0.3% hydrogen peroxide. The sections were counterstained with hematoxylin. Nuclear BRCA1 localization was assessed by staining the tissue microarray without hematoxylin counterstain to more clearly show only BRCA1 staining in the nucleus.

Quantitation and statistical analysis. The immunohistochemical stains were evaluated in a blinded fashion by two independent

pathology reviewers using the following scale: 0, no expression; 1, faint/focal/equivocal staining; 2, <50% of the cells express the antigen; 3, >50% of cells express the antigen. The following cell types were evaluated: secretory and basal epithelial cells; high-grade prostate intraepithelial neoplasia; and Gleason pattern 3, Gleason pattern 4, and Gleason pattern 5 tumor cells. Statistical analysis was done using two-way ANOVA and Bonferonni correction for multiple comparisons. Statistics were done using the Statview statistical program.

Cell cultures. Derivation of the P69 and M12 cell lines has been previously described (30, 31). Briefly, the P69 cell line was obtained by immortalization of prostate epithelial cells with SV40 T antigen, and the M12 cell line was derived by injection of P69 cells into athymic nude mice and serial reimplantation of tumor nodules into nude mice. P69 and M12 cells were cultured in RPMI 1640 supplemented with 10 ng/mL epidermal growth factor, 0.1 nmol/L dexamethasone, 5 μg/mL insulin, 5 μg/mL transferrin, and 5 ng/mL selenium. P69 cells are responsive to IGF-I and are rarely tumorigenic, whereas M12 cells are highly tumorigenic and metastatic and exhibit a reduced IGF-I responsiveness (32). P69 and M12 cells express extremely low levels of AR. The LNCaP C4-2 cell line was maintained in T-Medium (Invitrogen) containing 5% fetal bovine serum.

Western immunoblots. Cells were harvested with ice-cold PBS containing 5 mmol/L EDTA and lysed in a buffer containing 150 mmol/L NaCl, 20 mmol/L HEPES (pH 7.5), 1% Triton X-100, 2 mmol/L EDTA, 2 mmol/L EGTA, 1 mmol/L phenylmethylsulfonyl fluoride, 2 μg/mL aprotinin, 1 mmol/L leupeptin, 1 mmol/L pyrophosphate, 1 mmol/L vanadate, and 1 mmol/L DTT. Protein content was determined using the Bradford reagent. Samples were electrophoresed through 10% SDS-PAGE, followed by blotting of the proteins onto nitrocellulose membranes. After blocking with 5% skim milk in T-TBS [20 mmol/L Tris-HCl (pH 7.5), 135 mmol/L NaCl, and 0.1% Tween 20], blots were incubated with a rabbit polyclonal anti-human IGF-IR β-subunit antibody (Santa Cruz Biotechnology), washed with T-TBS, and incubated with an horseradish peroxidase–conjugated secondary antibody. In addition, blots were incubated with antibodies against BRCA1 (C20, Santa Cruz Biotechnology), tubulin (T-5168, Sigma-Aldrich Co.), Akt and phospho-Akt (Ser473) (#9272 and #9271, respectively, Cell Signaling), extracellular signal–regulated kinase (Erk)-1 and phospho-Erk1/2 (Thr202/Tyr204) (SC-94, Santa Cruz Biotechnology, and #9101, Cell Signaling, respectively), and actin (A-5060, Sigma-Aldrich). Proteins were detected using the SuperSignal West Pico Chemiluminescent Substrate (Pierce).

Plasmids and DNA transfections. An expression vector encoding wild-type BRCA1 was constructed by cloning the BRCA1 cDNA into artificially engineered *Hin*dIII and *Not*I sites in the pcDNA3 vector (Invitrogen; ref. 33). The BRCA1 vector was kindly provided by Dr. Lawrence Brody (NIH, Bethesda, MD). For transient cotransfection experiments, an IGF-IR promoter luciferase reporter construct was used that includes 476 bp of 5′-flanking region and 640 bp of 5′-untranslated region of the *IGF-IR* gene [p(-476/+640)LUC]. The promoter activity of this genomic fragment has been previously described (34). P69 and M12 cells were transfected with 1 μg of the p(-476/+640)LUC reporter construct, along with 1 μg of the BRCA1 expression vector and 0.3 μg of a β-galactosidase expression plasmid (pCMV-β, Clontech), using the Jet-PEI (Polyplus) transfection reagent. Promoter activities were expressed as luciferase values normalized for β-galactosidase activity.

For stable transfections, parental P69 and M12 cells were plated in six-well plates and transfected with a wild-type BRCA1 expression vector (or pcDNA3 as a control) using the Jet-PEI reagent. After 24 h, selection by 500 μg/mL G418 (geneticin, A.G. Scientific, Inc.) was started. After 2 wk of G418 selection, independent colonies were picked up and BRCA1 expression was assessed by quantitative reverse transcription-PCR, as described below. Stable-transfected clones used in this study expressed at least 50% more BRCA1 mRNA than control cells.

Quantitative real-time PCR. Quantitative Real-time PCR was done using TaqMan Universal PCR MasterMix and Assay-on-Demand Gene Expression primers and probes (Applied Biosystems). An ABI Prism 7000 Sequence Detection System was used. The glyceraldehyde-3-phosphate dehydrogenase (GAPDH) mRNA levels were analyzed as an internal control and used to normalize the BRCA1 mRNA values. Amplification was carried out after an incubation of 2 min at 50°C and 10 min at 95°C, followed by 20 cycles at 95°C for 15 s, 1 min at 55°C, and 30 s at 72°C. The number of PCR cycles to reach the fluorescence threshold was the cycle threshold (C_t). Each cDNA sample was tested in triplicate and mean C_t values are reported. Furthermore, for each reaction, a "no template" sample was included as a negative control. Fold differences were calculated using the $2^{\Delta\Delta C}$t method.

Proliferation assays. Cells were plated in six-well plates (2×10^5 per well) in complete medium. After 24 h, the medium was changed to fresh, serum-containing medium. Cells were counted daily by trypsin treatment, followed by trypan blue staining and manual counting with a hemocytometer. At least four fields were counted at each time point and ligand dose. Proliferation experiments were replicated using 2,3-bis[2-methoxy-4-nitro-5-sulfophenyl]-2*H*-tetrazolium-5-carboxanilide inner salt staining (Biological Industries) with similar results.

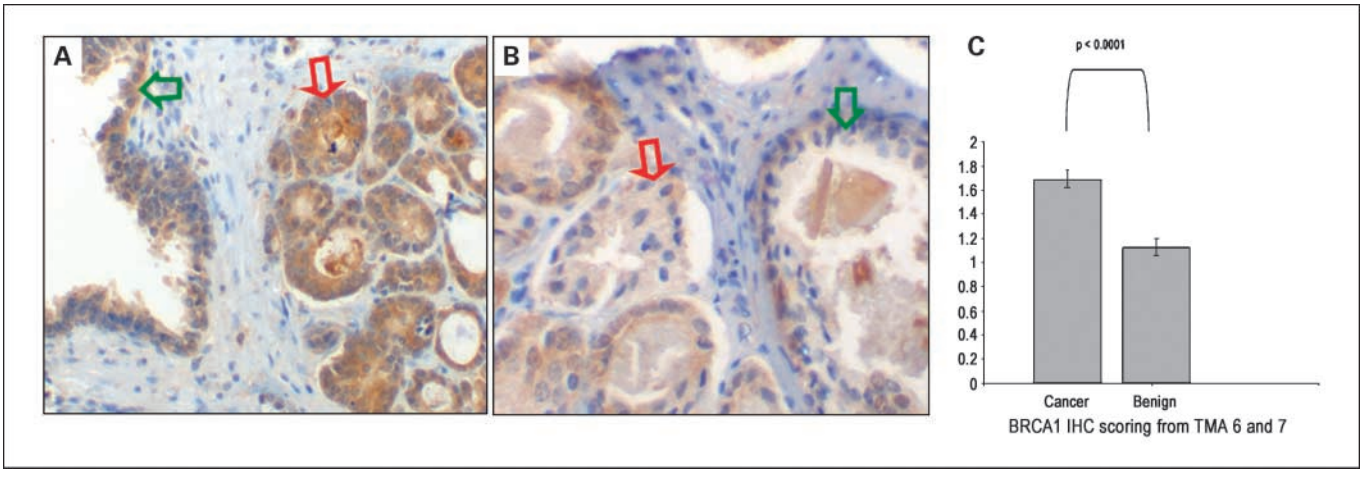

Fig. 1. Expression of BRCA1 in prostate cancer. Two tissue microarrays including 203 specimens were immunostained with BRCA1 antibody C20 as described in Materials and methods. *A,* Gleason score 6 cancer glands (*red arrows*) expressing intense immunoreactivity and a benign gland (*green arrow*) expressing faint immunoreactivity. *B,* Gleason score 6 cancer glands expressing faint immunoreactivity (*red arrow*) and adjacent normal gland (*green arrow*) with intraluminal crystalloid lacking immunoreactivity. *C,* statistical analysis of BRCA1 staining in prostate cancer versus normal adjacent prostate epithelium (average of the respective scores with SDs).

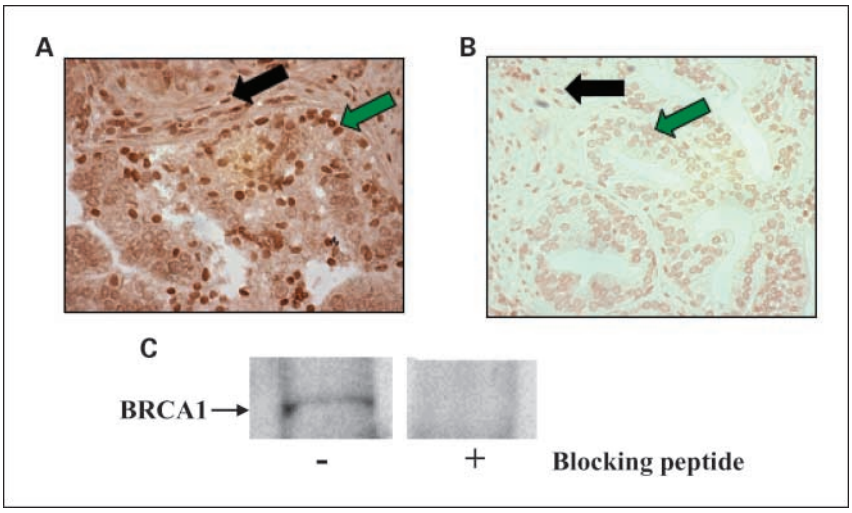

Fig. 2. Nuclear BRCA1 staining in prostate cancer. Nuclear staining by anti-BRCA1 of both benign epithelial (*green arrow*) and stromal (*black arrow*) cells in a section of prostate (*A*) was abolished when the primary anti-BRCA1 antibody was preincubated with a BRCA1 blocking peptide (*B*). *C,* tissue lysate from LuCaP 35 human prostate cancer xenograft was electrophoresed through SDS-PAGE and immunoblotted with anti-BRCA1 antibody in the absence or presence of a BRCA1 blocking peptide. Note loss of BRCA1 band with a 10-fold molar excess of the blocking peptide.

Results

Immunohistochemical analysis of BRCA1 expression in prostate cancer. The potential involvement of tumor suppressor BRCA1 in the etiology of prostate cancer has been the topic of controversial research. To investigate the expression of BRCA1 in primary prostate tumors, immunoreactive BRCA1 was measured in two tissue microarrays, which contained 203 prostate cancer specimens (Fig. 1). Only specimens including both tumor and normal prostate epithelium were included in our analysis. In general, no to very faint BRCA1 immunoreactivity was observed in benign glands, whereas variably intense staining was seen in prostate cancer. Statistical analysis of the data indicates a highly significant difference ($P < 0.001$) between BRCA1 expression levels in prostate cancer compared with normal adjacent tissue (Fig. 1C). IGF-IR immunostaining revealed no correlation between BRCA1 and IGF-IR staining in the benign luminal cells of the 203 specimens on the tissue microarrays that stained positively for both proteins ($r = -0.11$, $P > 0.05$). In contrast, in the malignant tissue from the same tissue microarrays, there was a significant positive correlation between IGF-IR and BRCA1 ($r = 0.21$, $P < 0.02$). IGF-IR levels were significantly higher in the malignant epithelium compared with normal luminal cells ($P < 0.01$). With respect to AR expression in the tissue samples by benign prostate luminal cells, 6% lacked AR immunoreactivity, 18% expressed AR at a level of 1, 31% at 2, and 45% at 3. All cancers expressed AR: 24% at 1, 34% at 2, and 42% at 3. BRCA1 was mainly localized to the nucleus, as shown by staining of the tissue microarray without hematoxylin counterstain (Fig. 2A). Furthermore, the specificity of the BRCA1 staining was addressed by preincubating the BRCA1 antibody in a 5-fold molar excess concentration of BRCA1 peptide before immunostaining. As shown in Fig. 2B, the intensity of the BRCA1 staining was significantly reduced in the presence of the peptide. Likewise, the intensity of the ~220-kDa BRCA1 band in a Western blot of a prostate cancer xenograft was largely reduced in the presence of a 10-fold molar excess of the BRCA1 blocking peptide (Fig. 2C).

BRCA1 expression in prostate cancer xenografts. To further examine BRCA1 levels in prostate cancer, protein expression was measured by Western blot in a collection of 27 human prostate cancer xenografts, kindly provided by Dr. Robert Vessella (University of Washington, Seattle, WA). Results obtained showed that BRCA1 was expressed in most of the xenografts; however, the levels varied over a wide range between xenografts. Likewise, large variations were seen in IGF-IR levels between xenografts. Equivalent amounts of protein were loaded in each lane and equal loading was confirmed by Erk loading (Fig. 3).

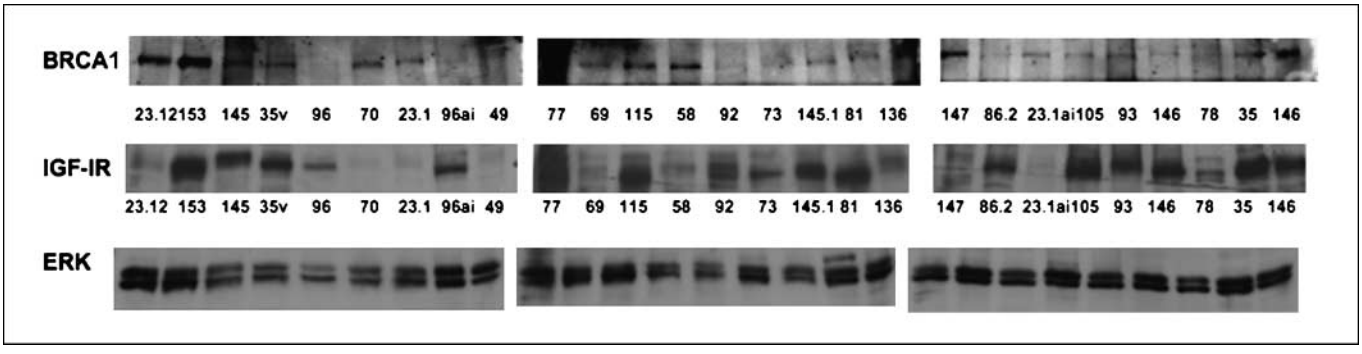

Fig. 3. Western immunoblots with BRCA1, IGF-IR, and Erk antibodies of cell extracts of 27 individual human prostate cancer xenografts grown in severe combined immunodeficient mice. Xenografts with a "v" or "ai" after the number are androgen-independent lines grown in castrated mice. All of the other lines were from intact mice. Tissue was kindly supplied by Dr. Robert Vessella.

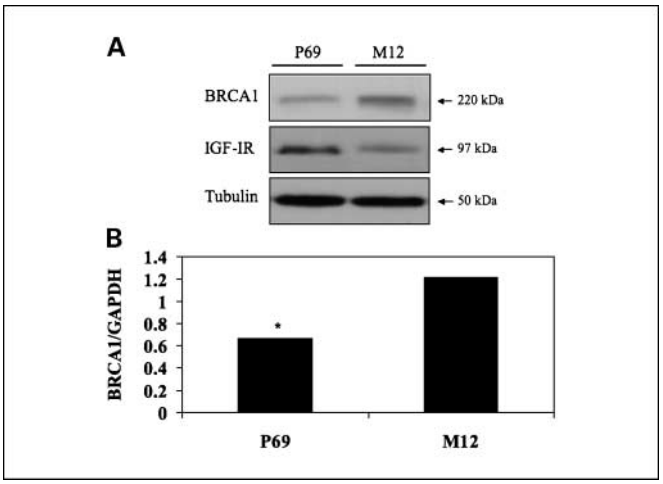

Fig. 4. Expression of endogenous IGF-IR and BRCA1 in P69 and M12 prostate cancer cells. *A,* Western blot analysis of IGF-IR and BRCA1 expression in prostate cancer cells. Untransfected M12 and P69 cells were lysed in the presence of protease inhibitors, as indicated in Materials and Methods. Equal amounts of protein (100 μg) were separated by 8% SDS-PAGE, transferred to nitrocellulose filters, and blotted with anti-BRCA1 (*top*), anti – IGF-IR (*middle*), and anti-tubulin (*bottom*) antibodies. The positions of the ~220-kDa BRCA1, ~97-kDa IGF-IR β-subunit, and ~50-kDa tubulin proteins are indicated. The figure shows a typical Western blot repeated at least thrice with similar results. *B,* quantitative real-time PCR of BRCA1 mRNA levels in prostate cancer cells. Total RNA was prepared from P69 and M12 cells, and BRCA1 mRNA and GAPDH mRNA values were measured using the TaqMan real-time PCR system. Analysis of the data was done as described in Materials and Methods. *, $P < 0.01$, versus M12 cells.

BRCA1 expression in prostate cancer cell lines. In view of the fact that progression to advanced stage disease is usually associated with a reduction in IGF-IR levels (9), and given that BRCA1 was previously shown to control IGF-IR levels in breast cancer cells in a negative fashion (35–37), we examined the pattern of expression of BRCA1 in two AR-negative prostate cancer–derived cell lines with different IGF-IR levels. As previously shown, the poorly tumorigenic P69 cell line expressed high IGF-IR levels, whereas the tumorigenic and metastatic M12 derivative exhibited significantly reduced IGF-IR values (32). Western blot analysis of BRCA1 revealed a diametrically opposite pattern of expression. Thus, BRCA1 levels were ~4-fold lower in P69 than in M12 cells (Fig. 4A). To assess whether the increased BRCA1 levels in M12 cells were associated with corresponding changes in mRNA levels, BRCA1 mRNA levels were measured in both prostate cell lines using quantitative real time-PCR. Results obtained showed that BRCA1 mRNA levels in M12 cells were ~1.5-fold higher than in P69 cells (Fig. 4B).

Regulation of IGF-IR promoter activity by BRCA1 in prostate cancer cells. To examine whether the reciprocal pattern of *BRCA1* and *IGF-IR* gene expression in prostate cancer cells could be due to transcriptional repression of the IGF-IR promoter by endogenous BRCA1, cotransfection experiments were done in M12 cells using a BRCA1 expression vector along with construct p(-476/+640)LUC, which contains most of the proximal region of the IGF-IR promoter fused to a luciferase gene. Forty-eight hours after transfection, cells were harvested and luciferase and β-galactosidase activities were measured. As shown in Fig. 5A, BRCA1 induced a significant reduction in IGF-IR promoter activity in comparison with pcDNA3-transfected cells (~50% suppression).

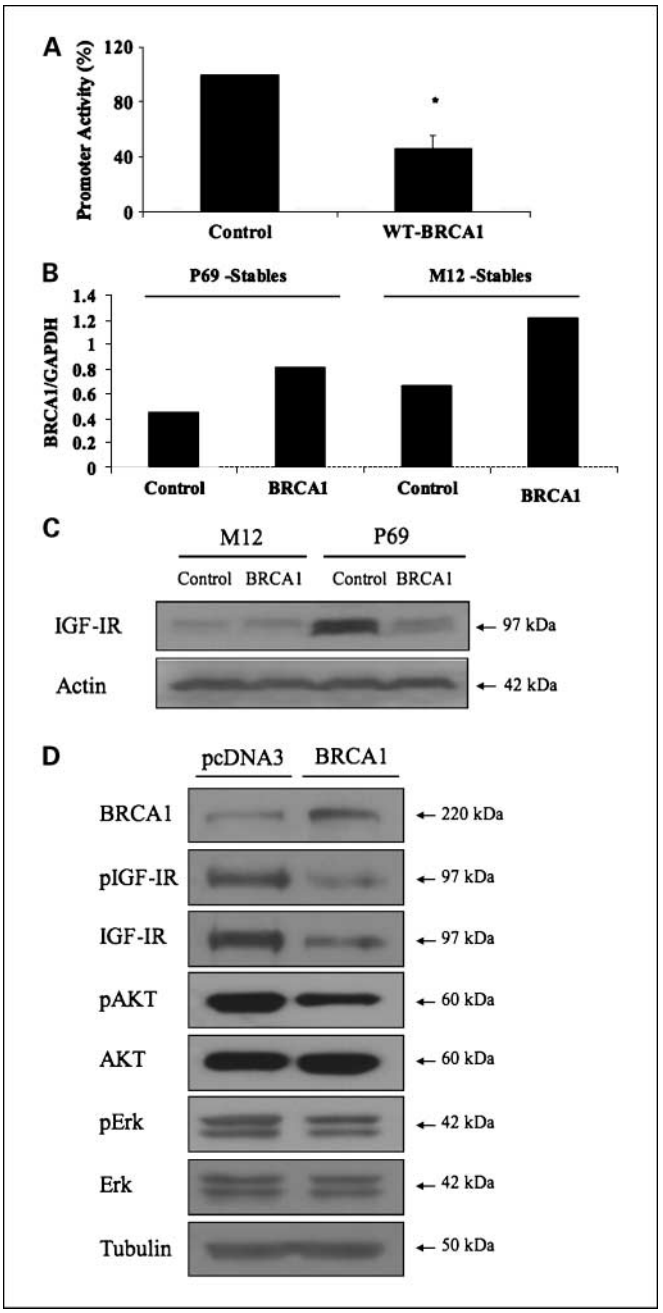

Fig. 5. Regulation of *IGF-IR* gene expression by BRCA1 in prostate cancer cells. *A,* regulation of IGF-IR promoter activity by BRCA1. M12 cells were transiently transfected with 1 μg of the p(-476/+640)LUC IGF-IR promoter-luciferase reporter construct, along with 1 μg of the BRCA1 expression vector (or empty pcDNA3) and 0.3 μg of the pCMVβ plasmid, using the Jet-PEI reagent. Forty hours after transfection, cells were harvested and the levels of luciferase and β-galactosidase were measured. Promoter activities are expressed as luciferase values normalized for β-galactosidase levels. Columns, mean of three independent experiments done in duplicate dishes; bars, SE. *, $P < 0.01$, versus pcDNA3-transfected cells. *B,* quantitative real time-PCR of BRCA1 mRNA in P69-derived and M12-derived stable BRCA1-overexpressing clones. BRCA1 mRNA levels were normalized to GAPDH mRNA levels and expressed in arbitrary units. Analyses were done as indicated in the legend to Fig. 4. Control, pcDNA3-transfected clones; BRCA1, full-length BRCA1-transfected clones. *C,* regulation of endogenous IGF-IR levels by BRCA1. Stable BRCA1-overexpressing (or pcDNA-3 transfected) P69 and M12 cells were lysed and endogenous IGF-IR levels were measured by Western blots. Blots were reprobed with anti-tubulin as a loading control. *D,* regulation of total and phosphorylated IGF-IR levels and downstream mediators by BRCA1. M12 cells were transfected with a BRCA1 expression vector (or empty pcDN3 vector), and after 48 h, cells were lysed and Western blots were done with antibodies against BRCA1, tubulin, and total and phospho-IGF-IR, Akt, and Erk.

Next we studied whether BRCA1 could suppress the expression of the endogenous *IGF-IR* gene. For this purpose, P69 and M12 cells were stably transfected with a BRCA1 expression vector followed by selection with G418. Total RNA was prepared from individual clones and BRCA1 mRNA levels were assessed by quantitative real-time PCR. Clones used in this study expressed at least 50% higher BRCA1 mRNA levels than control, pcDNA3-transfected P69 and M12 cells (Fig. 5B). Western blot analysis revealed that endogenous IGF-IR levels were largely reduced in BRCA1-overexpressing P69 cells in comparison with P69 control cells (Fig. 5C). On the other hand, no effect was seen on the already reduced endogenous IGF-IR levels in BRCA1-overexpressing M12 cells. An inhibitory effect of BRCA1 in M12 cells, however, was observed in cells that were transiently transfected with a BRCA1 vector. As shown in Fig. 5D, BRCA1 expression led to a reduction in total and phospho-IGF-IR, as well as in phospho-Akt, but not in total and phospho-Erk.

Effect of AR expression on BRCA1 action. Because most prostate cancer cells contain an AR and because BRCA1 is a recognized enhancing coregulator of the AR, we determined the response to BRCA1 in the AR-positive LNCaP C4-2 line, which expresses an endogenous AR, although mutated in the androgen-binding domain. The results of these studies are shown in Fig. 6. These studies show by both an AR reporter assay and measurement of the AR responsive gene TSC22 and IGF-IR mRNA by quantitative PCR that in the presence of a functional AR, enhancement of AR signaling by BRCA1 results in increased IGF-IR and TSC22 gene expression (Fig. 6A). In addition, BRCA1 expression enhanced AR transcriptional activity, as shown by cotransfection experiments using an AR-responsive luciferase reporter plasmid (AAR3; Fig. 6B).

Effect of BRCA1 expression on cell proliferation. To assess the potential effect of BRCA1 expression on cell proliferation, BRCA1-overexpressing P69 and M12 cells were plated in six-well plates at a density of 1×10^5 per well and counted after 24, 48, and 72 hours using a hemocytometer. Results obtained indicate that BRCA1-overexpressing P69 and M12 cells consistently displayed an enhanced proliferation rate in comparison with pcDNA3-transfected cells (~ 1.5-fold increase at 72 hours; $P < 0.05$, in three independent experiments; Fig. 6C).

Discussion

Tumor suppressor BRCA1 has been shown to be involved in the regulation of a number of biological processes in various cellular and animal models (17). A potential role for BRCA1 in prostate cancer was suggested by both epidemiologic and experimental studies (21, 38), although its mechanisms of action and potential targets have not yet been identified. The IGFs have been recognized as important regulators of prostate epithelial cell growth and differentiation as well as prostate

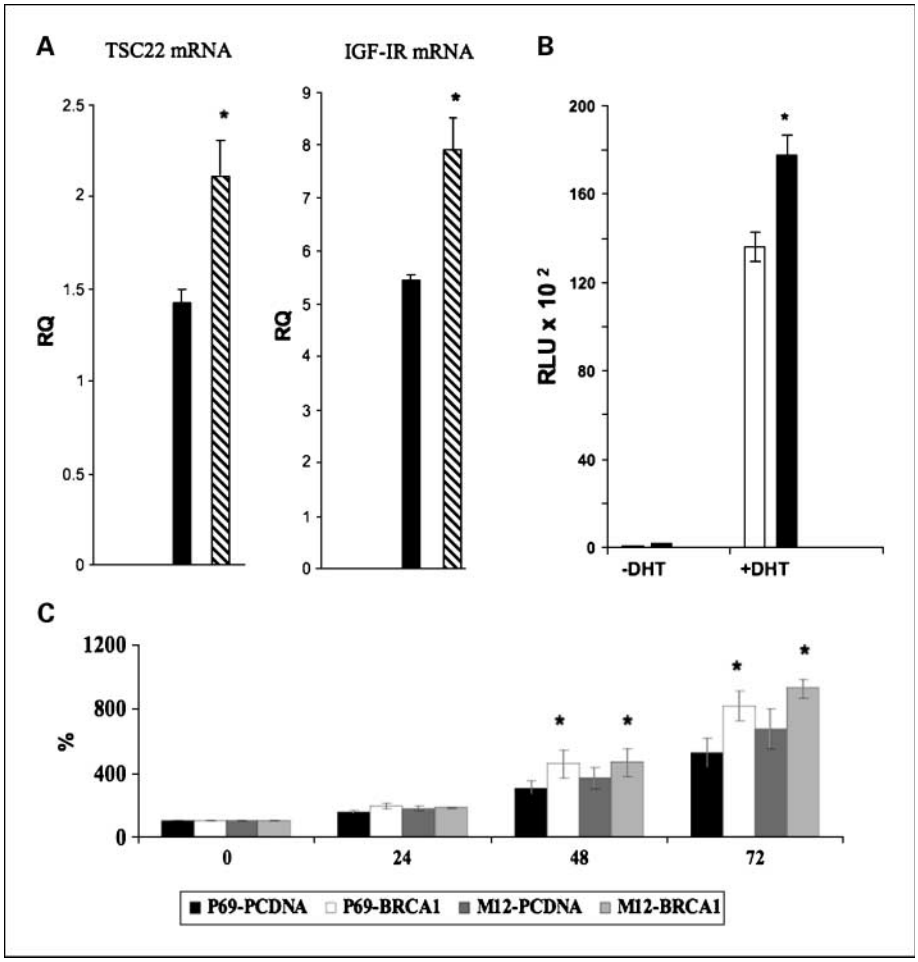

Fig. 6. Effect of AR status on BRCA1 action. *A,* LNCaP C4-2 cells were transfected with a BRCA1 expression vector (*hatched columns*) or an empty vector (*solid columns*) as described in Materials and Methods. Twenty-four hours after transfection, dihydrotestosterone 10^{-9} mol/L was added to the medium and total RNA was collected after an additional 3 h. Quantitative real-time PCR was run for the androgen-regulated gene TSC22 and IGF-IR mRNAs. *, $P < 0.01$, versus control. *B,* the AAR3 luciferase reporter construct was cotransfected onto LNCaP C4-2 cells along with a BRCA1 expression vector (*solid columns*) or an empty vector (*open columns*). Twenty-four hours after transfection, dihydrotestosterone 10^{-9} mol/L (or diluent) was added to the cells for an additional 3 h, after which luciferase activity was measured. Note the significant increase in reporter activity in the BRCA1-containing cells compared with control. RLU, relative luciferase units. *C,* effect of BRCA1 on cellular proliferation. BRCA1-expressing and control P69 and M12 cells were plated in six-well plates at a density of 2×10^5 per well in complete medium. Cells were trypsinized every 24 h, stained with trypan blue, and counted with a hemocytometer. The number of cells at time 0 was assigned a value of 100%. The *y*-axis denotes cell numbers (percentage of cells at time 0). Columns, mean ($n = 3$ independent experiments); bars, SD. Proliferation rates of BRCA1-expressing P69 and M12 cells at 72 h were significantly higher compared with control, pcDNA3-transfected cells ($P < 0.05$).

cancer development (39). The IGF-IR, which mediates the mitogenic and antiapoptotic actions of IGF-I and IGF-II, has been identified as a pivotal player in prostate cancer initiation and progression (10). The pattern of expression of the *IGF-IR* gene through the various stages of the disease, however, remains a controversial subject. Thus, whereas studies have shown that progression of prostate cancer xenografts to androgen independence is associated with a large increase in IGF-IR mRNA levels (compared with the original androgen-dependent tumors; ref. 40), other reports provided substantial evidence that IGF-IR levels were decreased in human prostate carcinoma compared with benign prostate epithelium (9). Consistent with this later study, and as shown in the present article, IGF-IR levels are much higher in the nonmetastatic prostate epithelial cell line P69 compared with its metastatic derivative, the M12 cell line (32). Furthermore, whereas IGF-IR mRNA levels were shown to be largely suppressed in bone marrow metastases (11), other studies reported a persistent expression of the *IGF-IR* gene in prostate metastases (41). Our data, showing a negative correlation between IGF-IR and BRCA1 levels in benign luminal cells and a positive correlation in the malignant tissues, suggest that in the transition from benign to malignant prostate epithelium, there is a potential enhancement of the IGF system with up-regulation of IGF-IR by BRCA1. Whether this is a direct interaction cannot be determined by this type of correlation analysis.

The present study identifies BRCA1 as a novel player in prostate cancer and establishes a functional link between BRCA1 and the IGF-IR with potentially relevant physiologic and pathologic implications in the prostate. Immunohistochemistry revealed that BRCA1 levels were ~60% higher in transformed epithelium in comparison with normal tissue ($P < 0.001$). This paradoxical pattern of expression is consistent with the results of assays showing that BRCA1-overexpressing cells exhibit an enhanced proliferation rate. In addition, data are also consistent with the results of ontogenetic analyses in rodents showing that BRCA1 is highly expressed in rapidly proliferating cells (42). BRCA1 expression is induced by positive growth signals at the cell cycle point where cells become committed to replicate their DNA and undergo cell division (17). Maximal BRCA1 expression was detected during the pre-replicative (G_1) phase of the cell cycle (43), and it was proved that BRCA1 is involved in the control of the G_1-S and G_2-M transition checkpoints (44). Furthermore, we have recently shown that IGF-II, whose levels are largely enhanced in prostate carcinoma, is a potent stimulator of BRCA1 expression (9, 45). On the other hand, BRCA1 overexpression in DU-145 prostate cancer cells was previously shown to cause a very small decrease in proliferation rate, as measured by [^{3}H]thymidine uptake (46). However, BRCA1 expression was associated with constitutive activation of STAT-3, a transcription factor with crucial roles in cell transformation and tumor formation. Moreover, the fact that reduction of STAT-3 levels with antisense oligomers inhibited cell proliferation suggests that BRCA1 expression may elicit a cell survival signal with importance in prostate cancer progression. Further support to the notion that BRCA1 may be involved in early (androgen-dependent) stages of the disease is provided by studies showing that BRCA1 directly interacts with AR and stimulates the activity of androgen response elements in prostate cancer cells (20). Of interest, a recent study has shown that the *BRCA1* gene is overexpressed in conjunction with a network of genes related to BRCA1 function in aggressive prostate, breast, and lung cancers in transgenic models associated with integrated SV40 T/t antigen expression (47). The apparent paradox between the increased BRCA1 levels in prostate cancer and a putative tumor suppressing activity may potentially stem from the multiple and often opposite cellular pathways elicited by BRCA1 (21).

Whereas the biological significance of IGF-IR reduction in prostate cancer is still unclear, the data presented here show that the *IGF-IR* gene is a downstream target for BRCA1 action in this organ. In prostate cancer cells not expressing an AR, BRCA1 expression resulted in an ~50% reduction in the activity of a cotransfected IGF-IR promoter construct, probably by a direct effect at the IGF-IR promoter. The physiologic relevance of these results is highlighted by the fact that the endogenous *IGF-IR* gene, as well as IGF-IR and Akt phosphorylation, was reduced in BRCA1-expressing M12 prostate cancer cells. However, in prostate epithelial cells that express an active AR, the effect of BRCA1 on *IGF-IR* gene expression is mediated through its enhancement of AR transcription and subsequent AR-mediated IGF-IR expression. These results are consistent with studies showing an interplay between BRCA1 and AR in transcriptional regulation (48). In terms of the mechanism of action of BRCA1, we have previously identified a proximal IGF-IR promoter region that mediated the effect of BRCA1 (35, 36). Specifically, this region included a cluster of four GC boxes, which are bona fide binding sites for zinc finger protein Sp1. Whereas we were unable to show direct binding of the *in vitro* translated BRCA1 protein to this promoter region, we identified a BRCA1 domain involved in Sp1 binding. Physical interaction between BRCA1 and Sp1 prevented binding of the zinc finger to *cis*-elements in the IGF-IR promoter, with ensuing reduction in promoter activity. A related mechanism of action was recently reported for the von Hippel-Lindau tumor suppressor in the specific context of IGF-IR regulation in clear cell renal carcinoma (49). Thus, similar to BRCA1, von Hippel-Lindau was shown to reduce IGF-IR promoter activity and mRNA levels via a mechanism that involves functional and physical interactions between von Hippel-Lindau and Sp1.

In summary, we have shown that BRCA1 regulates *IGF-IR* gene expression in prostate cancer cells via a mechanism that involves repression of *IGF-IR* gene transcription. In addition, immunohistochemical data are consistent with a potential survival role of BRCA1 in prostate cancer. Regulation of IGF-IR expression by BRCA1 may constitute a novel control mechanism that allows the IGF system to engage in both differentiative and proliferative types of actions.

Disclosure of Potential Conflicts of Interest

No potential conflicts of interest were disclosed.

Acknowledgments

We thank Dr. L. Brody for providing the BRCA1 expression vector, Dr. R. Vessella for prostate cancer xenografts, and Tal Ohayon for help with the manuscript. This work was done in partial fulfillment of the requirements for a Ph.D. degree by Hagit Schayek in the Sackler Faculty of Medicine, Tel Aviv University.

References

1. Samani AA, Yakar S, LeRoith D, Brodt P. The role of the IGF system in cancer growth and metastasis: overview and recent insights. Endocr Rev 2007;28: 20–47.
2. Khandwala HM, McCutcheon IE, Flyvbjerg A, Friend KE. The effects of insulin-like growth factors on tumorigenesis and neoplastic growth. Endocr Rev 2000;21: 215–44.
3. Werner H, Maor S. The insulin-like growth factor-I receptor gene: a downstream target for oncogene and tumor suppressor action. Trends Endocrinol Metab 2006;17:236–42.
4. Cohen P, Peehl DM, Lamson G, Rosenfeld RG. Insulin-like growth factors (IGFs), IGF receptors, and IGF-binding proteins in primary cultures of prostate epithelial cells. J Clin Endocrinol Metab 1991;73:401–7.
5. Kaplan PJ, Mohan S, Cohen P, Foster BA, Greenberg NM. The insulin-like growth factor axis and prostate cancer: lessons from the transgenic adenocarcinoma of mouse prostate (TRAMP) model. Cancer Res 1999;59:2203–9.
6. Ruan W, Powell-Braxton L, Kopchick JJ, Kleinberg DL. Evidence that insulin-like growth factor I and growth hormone are required for prostate gland development. Endocrinology 1999;140:1984–9.
7. DiGiovanni J, Kiguchi K, Frijhoff A, et al. Deregulated expression of insulin-like growth factor I in prostate epithelium leads to neoplasia in transgenic mice. Proc Natl Acad Sci U S A 2000;97:3455–60.
8. Chan JM, Stampfer MJ, Giovannucci E, et al. Plasma insulin-like growth factor-I and prostate cancer risk: a prospective study. Science 1998;279:563–6.
9. Tennant MK, Thrasher JB, Twomey PA, Drivdahl RH, Birnbaum RS, Plymate SR. Protein and mRNA for the type 1 insulin-like growth factor (IGF) receptor is decreased and IGF-II mRNA is increased in human prostate carcinoma compared with benign prostate epithelium. J Clin Endocrinol Metab 1996;81:3774–82.
10. Wu JD, Haugk K, Woodke L, Nelson P, Coleman I, Plymate SR. Interaction of IGF signaling and the androgen receptor in prostate cancer progression. J Cell Biochem 2006;99:392–401.
11. Chott A, Sun Z, Morganstern D, et al. Tyrosine kinases expressed *in vivo* by human prostate cancer bone marrow metastases and loss of type 1 insulin-like growth factor receptor. Am J Pathol 1999;155:1271–9.
12. Miki Y, Swensen J, Shattuck-Eidens D, et al. A strong candidate for the breast and ovarian cancer susceptibility gene BRCA1. Science 1994;266:66–71.
13. Futreal PA, Liu Q, Shattuck-Eidens D, et al. BRCA1 mutations in primary breast and ovarian carcinomas. Science 1994;266:120–2.
14. Merajver SD, Pham TM, Caduff RF, et al. Somatic mutations in the BRCA1 gene in sporadic ovarian tumours. Nat Genet 1995;9:439–43.
15. Turner NC, Reis-Filho JS, Russell AM, et al. BRCA1 dysfunction in sporadic basal-like breast cancer. Oncogene 2007;26:2126–32.
16. Chen CF, Li S, Chen Y, Chen PL, Sharp ZD, Lee WH. The nuclear localization sequences of the BRCA1 protein interact with the importin-α subunit of the nuclear transport signal receptor. J Biol Chem 1996;271: 32863–8.
17. Wang Q, Zhang H, Fishel R, Greene MI. BRCA1 and cell signaling. Oncogene 2000;19:6152–8.
18. Holt JT, Thompson ME, Szabo C, et al. Growth retardation and tumour inhibition by BRCA1. Nat Genet 1996;12:298–301.
19. Yang X, Lippman ME. BRCA1 and BRCA2 in breast cancer. Breast Cancer Res Treat 1999;54:1–10.
20. Yeh S, Hu YC, Rahman M, et al. Increase of androgen-induced cell death and androgen receptor transactivation by BRCA1 in prostate cancer cells. Proc Natl Acad Sci U S A 2000;97:11256–61.
21. Rosen EM, Fan S, Pestell RG, Goldberg ID. BRCA1 in hormone-responsive cancers. Trends Endocrinol Metab 2003;14:378–85.
22. Fan S, Wang J, Yuan RQ, et al. BRCA1 as a potential human prostate tumor suppressor: modulation of proliferation, damage responses and expression of cell regulatory proteins. Oncogene 1998;16:3069–82.
23. Yuli C, Shao N, Rao R, et al. BRCA1a has antitumor activity in TN breast, ovarian and prostate cancers. Oncogene 2007;26:6031–7.
24. Struewing JP, Hartge P, Wacholder S, et al. The risk of cancer associated with specific mutations of BRCA1 and BRCA2 among Ashkenazi Jews. N Engl J Med 1997;336:1401–8.
25. Kirchhoff T, Kauff ND, Mitra N, et al. BRCA mutations and risk of prostate cancer in Ashkenazi Jews. Clin Cancer Res 2004;10:2918–21.
26. Tryggvadottir L, Vidarsottir L, Thorgeirsson T, et al. Prostate cancer progression and survival in BRCA2 mutation carriers. J Natl Cancer Inst 2007; 99:929–35.
27. Vazina A, Baniel J, Yaacobi Y, et al. The rate of the founder Jewish mutations in BRCA1 and BRCA2 in prostate cancer patients in Israel. Br J Cancer 2000; 83:463–6.
28. Uchida T, Wang C, Sato T, et al. BRCA1 gene mutation and loss of heterozygosity on chromosome 17q21 in primary prostate cancer. Int J Cancer 1999; 84:19–23.
29. Sinclair CS, Berry R, Schaid D, Thibodeau SN, Couch FJ. BRCA1 and BRCA2 have a limited role in familial prostate cancer. Cancer Res 2000;60:1371–5.
30. Bae VL, Jackson-Cook CK, Brothman AR, Maygarden SJ, Ware JL. Tumorigenicity of SV40 T antigen immortalized human prostate epithelial cells: association with decreased epidermal growth factor receptor (EGFR) expression. Int J Cancer 1994;58: 721–9.
31. Bae VL, Jackson-Cook CK, Maygarden SJ, Plymate SR, Chen J, Ware JL. Metastatic sublines of an SV40 large T antigen immortalized human prostate epithelial cell line. Prostate 1998;34:275–82.
32. Damon SE, Plymate SR, Carroll JM, et al. Transcriptional regulation of insulin-like growth factor-I receptor gene expression in prostate cancer cells. Endocrinology 2001;142:21–7.
33. Fan S, Wang J-A, Yuan R, et al. BRCA1 inhibition of estrogen receptor signaling in transfected cells. Science 1999;284:1354–6.
34. Werner H, Rauscher FJ III, Sukhatme VP, Drummond IA, Roberts CT, Jr., LeRoith D. Transcriptional repression of the insulin-like growth factor I receptor (IGF-I-R) gene by the tumor suppressor WT1 involves binding to sequences both upstream and downstream of the IGF-I-R gene transcription start site. J Biol Chem 1994;269:12577–82.
35. Maor SB, Abramovitch S, Erdos MR, Brody LC, Werner H. BRCA1 suppresses insulin-like growth factor-I receptor promoter activity: potential interaction between BRCA1 and Sp1. Mol Genet Metab 2000; 69:130–6.
36. Abramovitch S, Glaser T, Ouchi T, Werner H. BRCA1–1 interactions in transcriptional regulation of the IGF-IR gene. FEBS Lett 2003;541:149–54.
37. Abramovitch S, Werner H. Functional and physical interactions between BRCA1 and p53 in transcriptional regulation of the IGF-IR gene. Horm Metab Res 2003;35:758–62.
38. Levy-Lahad E, Friedman E. Cancer risks among BRCA1 and BRCA2 mutation carriers. Br J Cancer 2007;96:11–5.
39. Roberts CT, Jr. IGF-1 and prostate cancer. Novartis Found Symp 2004;262:193–9.
40. Nickerson T, Chang F, Lorimer D, Smeekens SP, Sawyers CL, Pollak M. *In vivo* progression of LAPC-9 and LNCaP prostate cancer models to androgen independence is associated with increased expression of insulin-like growth factor I (IGF-I) and IGF-I receptor (IGF-IR). Cancer Res 2001;61:6276–80.
41. Hellawell GO, Turner GD, Davies DR, Poulsom R, Brewster SF, Macaulay VM. Expression of the type 1 insulin-like growth factor receptor is up-regulated in primary prostate cancer and commonly persists in metastatic disease. Cancer Res 2002;62:2942–50.
42. Marquis ST, Rajan JV, Wynshaw-Boris A, et al. The developmental pattern of BRCA1 expression implies a role in differentiation of the breast and other tissues. Nat Genet 1995;11:17–26.
43. Vaughn JP, Davis PL, Jarboe MD, et al. BRCA1 expression is induced before DNA synthesis in both normal and tumor-derived breast cells. Cell Growth Differ 1996;7:711–5.
44. Yarden RI, Pardo-Reoyo S, Sgagias M, Cowan KH, Brody LC. BRCA1 regulates the G_2/M checkpoint by activating Chk1 kinase upon DNA damage. Nat Genet 2002;30:285–9.
45. Maor S, Papa MZ, Yarden RI, et al. Insulin-like growth factor-I controls BRCA1 gene expression through activation of transcription factor Sp1. Horm Metab Res 2007;39:179–85.
46. Gao B, Shen X, Kunos G, et al. Constitutive activation of JAK-STAT3 signaling by BRCA1 in human prostate cancer cells. FEBS Lett 2001;488:179–84.
47. Deeb KK, Michalowska AM, Yoon C-Y, et al. Identification of an integrated SV40 T/t-antigen cancer signature in aggressive human breast, prostate, and lung carcinomas with poor prognosis. Cancer Res 2007; 67:8065–80.
48. Park JJ, Irvine RA, Buchanan G, et al. Breast cancer susceptibility gene 1 (BRCA1) is a coactivator of the androgen receptor. Cancer Res 2000;60:5946–9.
49. Yuen JSP, Cockman ME, Sullivan M, et al. The VHL tumor suppressor inhibits expression of the IGF1R and its loss induces IGF1R upregulation in human clear cell renal carcinoma. Oncogene 2007;26:6499–508.

Transforming Growth Factor-β–Stimulated Clone-22 Is an Androgen-Regulated Gene That Enhances Apoptosis in Prostate Cancer following Insulin-Like Growth Factor-I Receptor Inhibition

Cynthia C.T. Sprenger,[1,2] Kathleen Haugk,[3] Shihua Sun,[1] Ilsa Coleman,[4] Peter S. Nelson,[1,4] Robert L. Vessella,[2,3] Dale L. Ludwig,[5] Jennifer D. Wu,[1] and Stephen R. Plymate[1,3]

Abstract

Purpose: Inhibition of insulin-like growth factor (IGF) signaling using the human IGF-I receptor monoclonal antibody A12 is most effective at inducing apoptosis in prostate cancer xenografts in the presence of androgen. We undertook this study to determine mechanisms for increased apoptosis by A12 in the presence of androgens.

Experimental Methods: The castrate-resistant human xenograft LuCaP 35 V was implanted into intact or castrate severe combined immunodeficient mice and treated with A12 weekly. After 6 weeks of tumor growth, animals were sacrificed and tumors were removed and analyzed for cell cycle distribution/apoptosis and cDNA arrays were done.

Results: In castrate mice, the tumors were delayed in G_2 with no apoptosis; in contrast, tumors from intact mice underwent apoptosis with either G_1 or G_2 delay. Transforming growth factor-β–stimulated clone-22 (TSC-22) was significantly elevated in tumors from the intact mice compared with castrate mice, especially in those tumors with the highest levels of apoptosis. To further determine the function of TSC-22, we transfected various human prostate cancer cell lines with a plasmid expressing TSC-22. Cell lines overexpressing TSC-22 showed an increase in apoptosis and a delay in G_1. When these cell lines were placed subcutaneously in athymic nude mice, a decreased number of animals formed tumors and the rate of tumor growth was decreased compared with control tumors.

Conclusions: These data indicate that IGF-I receptor inhibition in the presence of androgen has an enhanced effect on decreasing tumor growth, in part, through increased expression of the tumor suppressor gene TSC-22. (Clin Cancer Res 2009;15(24):7634–41)

We have shown that inhibition of insulin-like growth factor-I receptor (IGF-IR) with the fully human monoclonal antibody A12 resulted in a decreased rate of tumor growth for both androgen-dependent and androgen-independent human prostate cancer xenografts (1, 2). However, depending on whether the xenograft was castration-resistant, we saw either apoptosis for androgen-dependent xenografts grown in intact mice or a slowing of tumor growth due to G_2 arrest without apoptosis for androgen-independent xenografts grown in castrate mice. Thus, inhibition of signaling through IGF-IR resulted in significant suppression of prostate tumor growth by both increased apoptosis and decreased proliferation (1). Furthermore, we showed that inhibition of IGF-IR signaling in androgen-dependent xenografts following castration significantly delayed progression to androgen-independent prostate cancer (3). A further suppression of androgen receptor transcriptional activity also occurred following A12 treatment (3). In this current study, we investigated whether the differences in apoptosis between androgen-dependent and androgen-independent human prostate cancer xenografts were due to the presence of androgen in the androgen-dependent animals or to a change in tumor phenotype.

We found an increase in transcript levels of several androgen-regulated genes when castrate-resistant LuCaP 35 V tumors were grown in intact mice. One androgen-regulated gene of particular interest was transforming growth factor-β (TGF-β)–stimulated clone-22 (TSC-22). TSC-22, which is regulated by androgens, TGF-β_1, and PPAR-γ, has been associated with decreased tumor formation and thus is a putative tumor suppressor gene (4–10).

Authors' Affiliations: Departments of [1]Medicine and [2]Urology, University of Washington; [3]Puget Sound Veterans Affairs Health Care System; [4]Fred Hutchinson Cancer Research Center, Seattle, Washington and [5]Imclone Systems, Inc., New York, New York

Received 2/2/09; revised 8/4/09; accepted 8/31/09; published OnlineFirst 12/8/09.

Grant support: NIH grants CA085859 and CA97186, Department of Defense grant W81XWH-04-1-0912, and Veterans Affairs Merit Award (S.R. Plymate) and NIH Institutional Training grant T32 DK07779-08 (C.C.T. Sprenger).

The costs of publication of this article were defrayed in part by the payment of page charges. This article must therefore be hereby marked *advertisement* in accordance with 18 U.S.C. Section 1734 solely to indicate this fact.

Requests for reprints: Stephen R. Plymate, Box 359625, 325 9th Avenue, Seattle, WA 98104. Phone: 206-857-4275; Fax: 206-897-5396; E-mail: splymate@u.washington.edu.

doi:10.1158/1078-0432.CCR-09-0264

Translational Relevance

In this study, we show that androgen-regulated genes such as transforming growth factor-β–stimulated clone-22 (TSC-22) may be responsible for the induction of apoptosis following inhibition of the insulin-like growth factor-I receptor (IGF-IR) in androgen-dependent prostate cancer. The induction of TSC-22 by androgen in castrate-resistant prostate cancer xenografts that are placed in an intact host may reinitiate an apoptotic response to IGF-IR inhibition that is lost when the same xenografts are placed in castrate hosts. Clinically, both fully human monoclonal antibodies, such as A12, and small molecules are in trial for prostate as well as other epithelial malignancies. The timing for the best effects of IGF-IR–targeted therapy is important to achieve optimal tumor regression. In this study, we have identified one factor, TSC-22, the expression of which in androgen-dependent disease could indicate a favorable response to early IGF-IR inhibition in prostate cancer.

In this study, we show that TSC-22 is an androgen-regulated tumor suppressor gene and that inhibition of IGF-IR signaling increased TSC-22 expression in a human xenograft model of prostate cancer. We further show that expression of TSC-22 in three human prostate cancer cell lines increased the apoptotic response, which may account, in part, for our previous observation of an apoptotic response to IGF-IR inhibition in androgen-dependent prostate tumor xenografts (1).

Materials and Methods

Xenografts and cell lines. The LuCaP 35 V androgen-independent human prostate xenograft, which only grows *in vivo*, was originally described by Corey et al. (11). The generation and characterization of the M12 cell line has been described previously (12–14). The PC-3 cell line was obtained from the American Type Culture Collection. Both cell lines were cultured in RPMI 1640 supplemented with 5% FCS, 10 ng/mL epithelial growth factor, 0.02 mmol/L dexamethasone, 5 μg/mL insulin, 5 μg/mL transferrin, 5 ng/mL selenium, fungizone, and gentamicin at 37°C with 5% CO_2. The androgen receptor–positive LNCaP C4-2 subline was a gift from Dr. Robert Sikes (University of Delaware). These cells were grown in T-medium (Invitrogen) supplemented with 10% fetal bovine serum, 100 units/mL penicillin, and 100 μg/mL streptomycin at 37°C with 5% CO_2.

Cell transfection. A human full-length cDNA clone of TSC-22 (NM_006022) was obtained from Origene Technologies and subcloned into pcDNA 3.1 with a G418 resistance gene. M12, PC-3, and the LNCaP C4-2 human prostate cancer cells were transfected with either control pcDNA 3.1 vector or pcDNA-TSC-22 plasmid. Transfections were done with Lipofectin 2000 (Promega) according to the manufacturer's protocol. Stable clones were obtained with G418 selection (400 μg/mL) and the expression of TSC-22 was confirmed by Western blotting.

RNA interference. Small hairpin RNAs targeting TSC-22 mRNA were designed and purchased from Origene. The small hairpin RNA sequence resulting in the most inhibition was shTSC22D1: 5′-CCTCATTTGCCTCACCTTCCACAACAGAA-3′. shTSC22D1 was transfected into LNCaP C4-2 cells using Lipofectamine (Invitrogen). Levels of TSC-22 were measured 3 days post-transfection. For apoptosis studies, transfected cells were treated 72 h post-transfection with A12, IGF, and dihydrotestosterone (DHT) for 6 to 48 h.

Animal studies. The growth of LuCaP 35 V in castrate mice and the responses to A12 treatment have been reported previously from our laboratory (1). The RNA used for microarray analysis in this study was collected immediately after the tumor was removed and was preserved in DEPC H_2O at -80°C. For studies of LuCaP 35 V growth and response to A12 in noncastrate (intact) animals, tumor bits (20-30 mm^3) of LuCaP 35 V were implanted subcutaneously into ten 6- to 8-week-old intact severe combined immunodeficient mice as described previously for the LuCaP 35 xenografts (1). When the implanted tumor reached a volume of 100 mm^3, half the animals received A12 antibody intraperitoneally at a dose of 40 mg/kg body weight three times a week for up to 5 weeks and the other half received human IgG as a control. Animals were weighed twice a week. Blood samples were collected from orbital sinus weekly. Plasma was separated and prostate-specific antigen level was determined using the IMx Total PSA Assay (Abbott Laboratories). Tumors were measured twice weekly and tumor volume was estimated by the formula: volume = $(l \times w^2) / 2$. After euthanization, tumors were collected, quartered, and treated as follows: (*a*) fixed in 10% neutral buffered formalin and embedded in paraffin, and sections (5 μm) were prepared for immunohistochemistry; (*b*) separated into single cells mechanically by mincing and filtering through 70 μm nylon sieves for flow cytometry; (*c*) minced and extracted for protein blots; and (*d*) RNA extracted and cDNA prepared for microarrays as described previously (1, 15). For TSC-22 studies, groups of 10 male athymic nude mice were subcutaneously injected with 1 million cells each of either empty vector control cells (M12pc) or TSC-22–overexpressing cells (M12 TSC-22). Mice were monitored weekly for tumor formation; tumors were measured and tumor volume was estimated as described above. Animals were euthanized after 7 weeks and tumors were removed. All animal studies performed followed a University of Washington–approved Institutional Animal Care and Use Committee animal protocol.

cDNA microarray analyses. Custom PEDB cDNA microarrays were constructed as described previously using clones derived from the Prostate Expression Database (16), a sequence repository of human prostate expressed sequence tag data available to the public.[6] The inserts of individual cDNA clones were amplified by PCR, purified, and spotted in duplicate onto glass microscope slides (Gold Seal; Becton Dickinson) with a robotic spotting tool (GeneMachine OmniGrid 100). Labeling with Cy3 and Cy5 fluorescent dyes and hybridization to the microarray slides were essentially as described (17). Fluorescent array images were collected for both Cy3 and Cy5 using a GenePix 4000B fluorescent scanner (Molecular Devices). The image intensity data were gridded and extracted using GenePix PRO 4.1 software, and spots of poor quality determined by visual inspection were removed from further analysis. RNA from tumors from A12-treated castrate mice was pooled into two groups: (*a*) tumors that exhibited G_2 arrest (8 tumors) and (*b*) tumors that exhibited no G_2 arrest (10 tumors). These two pools were hybridized against a pool of 18 tumors from untreated castrate tumor controls. RNA from tumors from A12-treated intact mice was pooled into three groups: (*a*) G_1 arrest with apoptosis (2 tumors), (*b*) G_2 arrest with apoptosis (2 tumors), and (*c*) G_1 arrest with no apoptosis (2 tumors). These three pools were hybridized against a pool of 4 untreated noncastrate tumor controls. RNA also was collected from laser-captured microdissections from 37 human prostate cancer tissue samples. Each sample yielded RNA from two areas: benign and cancer. Each of these experiments (LuCaP 35 V RNA and human prostate cancer RNA) was repeated with a switch in fluorescent labels to account for dye effects. Normalization of the Cy3 and Cy5 fluorescent signal on each array was done using GeneSpring 7.3 software (Agilent Technologies). A print-tip specific Lowess curve was fit to the log-intensity versus log-ratio plot and 20.0% of the data was used to calculate the Lowess fit at each point. This curve was used to adjust the control value for each measurement. If the control channel

[6] http://www.pedb.org

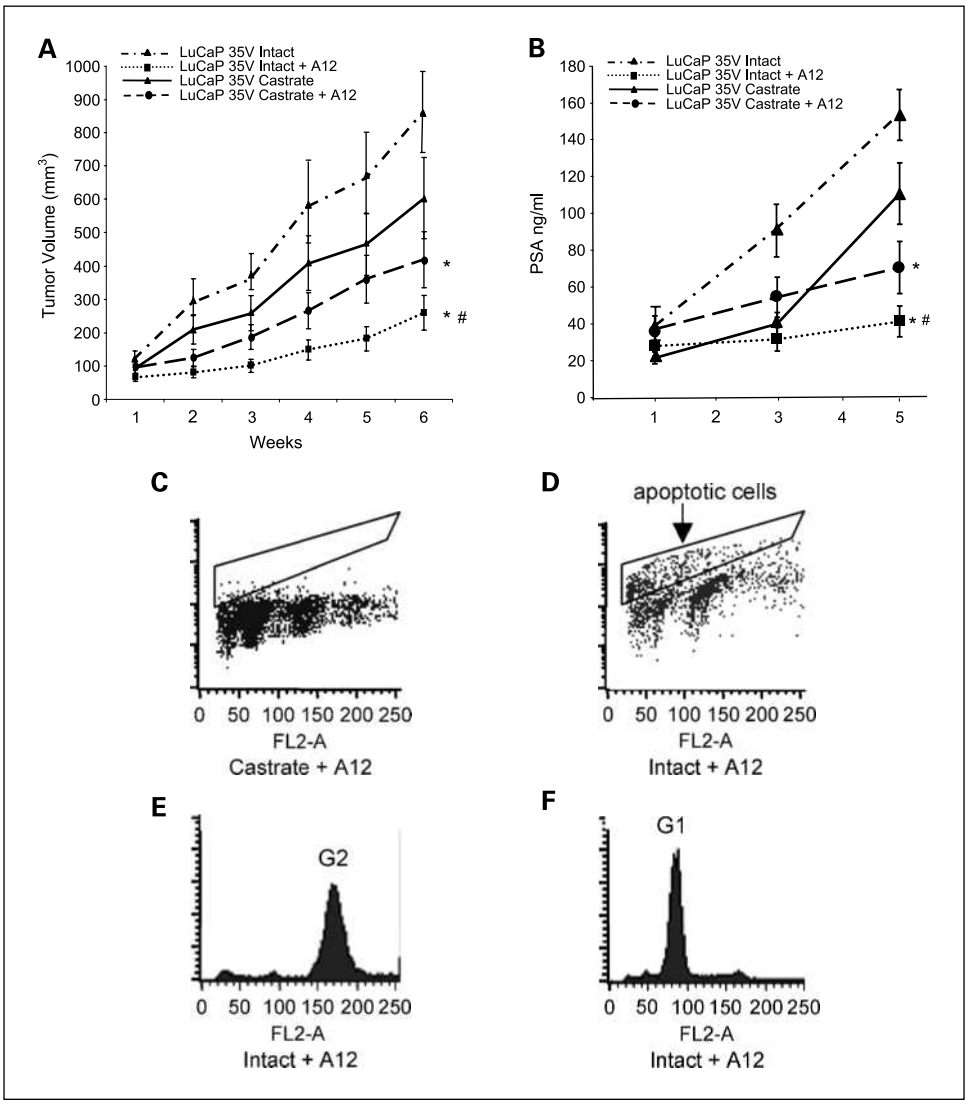

Fig. 1. *A,* tumor volume of LuCaP 35 V tumors grown in castrate mice compared with growth in noncastrate mice. In both groups, half of the animals were treated with A12, 40 mg/kg per body weight, once the tumor reached 100 mm^3. Changes in tumor volume after first injection are shown. Note the significant decrease in growth rate of LuCaP 35 V tumors grown in noncastrate animals treated with A12 compared with castrate mice (both treated and untreated). *B,* serum prostate-specific antigen (*PSA*) levels from the various animal groups. *, $P < 0.01$, each A12-treated group versus appropriate nontreated group; #, $P < 0.05$, intact + A12 versus castrate + A12. *C* and *D,* examples of flow cytometry measuring apoptosis of A12-treated LuCaP 35 V tumors from a castrate host (*C*) and an intact host (*D*). Apoptosis is shown as events above and to the left of the horizontal line. *E* and *F,* flow cytometry showing the G_2 (*E*) and G_1 (*F*) delay of the A12-treated LuCaP 35 V tumors grown in noncastrate animals.

was <10, then 10 was used instead. Data were filtered to remove values from poorly hybridized cDNAs with average foreground minus background intensity levels <300. Data from the two duplicate cDNAs spots on each PEDB chip were combined and the average ratios were used for comparative analyses. Ratios were filtered to include only clones whose expression was measurable in at least 75% of the samples. Differences in gene expression were determined using the SAM procedure (18).[7] Gene expression differences with a false discovery rate of ≤1% were considered significant.

Immunohistochemistry. Tumor samples were fixed in 10% neutral buffered formalin, embedded in paraffin, and sectioned at 5 μm onto slides. After deparaffinization and rehydration, antigens were retrieved with 0.01 mol/L citric acid (pH 6.0) at 95°C for 2 to 5 min. Slides were allowed to cool for 30 min followed by sequential rinsing with PBS. Endogenous peroxidase activity was quenched by an incubation with 0.3% H_2O_2 in methanol for 15 min. After blocking with 1.5% normal goat serum in PBS containing 0.05% Tween 20 for 1 h, slides were incubated with TSC-22 antibody (1 μg/mL) for 1 h followed by sequential incubation with biotinylated goat anti-mouse IgG for 30 min, peroxidase-labeled avidin for 30 min (Santa Cruz Biotechnology), and diaminobenzidine/hydrogen peroxide chromogen substrate (Vector Laboratories) for 5 to 10 min. Negative controls were done with TSC-22 antibody preabsorbed with TSC-22 protein (Abnova). All incubation steps were done at room temperature. Slides were counterstained with hematoxylin (Sigma) and mounted with Permount (Fisher Scientific).

Western blotting. For cells in culture, cells were washed with PBS and lysed with cold lysis buffer [50 mmol/L HEPES (pH 7.5), 150 mmol/L NaCl, 1.5 mmol/L $MgCl_2$, 1 mmol/L EGTA, and 10% Triton X-100] containing Phosphatase Inhibitor Cocktail II (Sigma) and protease inhibitors (Complete Mini Tablets; Roche). For assaying *in vivo* effects of A12, freshly prepared xenografts were minced and then washed with PBS and lysed as described for cell culture. Twenty-five micrograms of protein were resolved on 4% to 15% SDS-PAGE gels, transferred onto a nitrocellulose membranes, and probed with a 1:400 dilution of a rabbit polyclonal TSC-22 antibody (ProteinTech Group). The blot was washed and incubated with a horseradish peroxidase–conjugated secondary antibody (Pharmacia Biotech) for 1 h. Immunoreactive proteins were detected by enhanced chemiluminescence (Pharmacia Biotech). The membranes were stripped for 30 min in stripping buffer (Pierce) and reprobed with anti–β-actin antibody (Chemicon) as described above. Independent experiments validated that this stripping procedure did not lead to loss of signal.

Apoptosis and cell cycle assay. Apoptosis was measured by terminal deoxynucleotidyl transferase–mediated nick end labeling assay using the Apop-Direct kit (BD BioScience) as described previously (19). Briefly,

[7] http://www-stat.stanford.edu/_tibs/SAM/

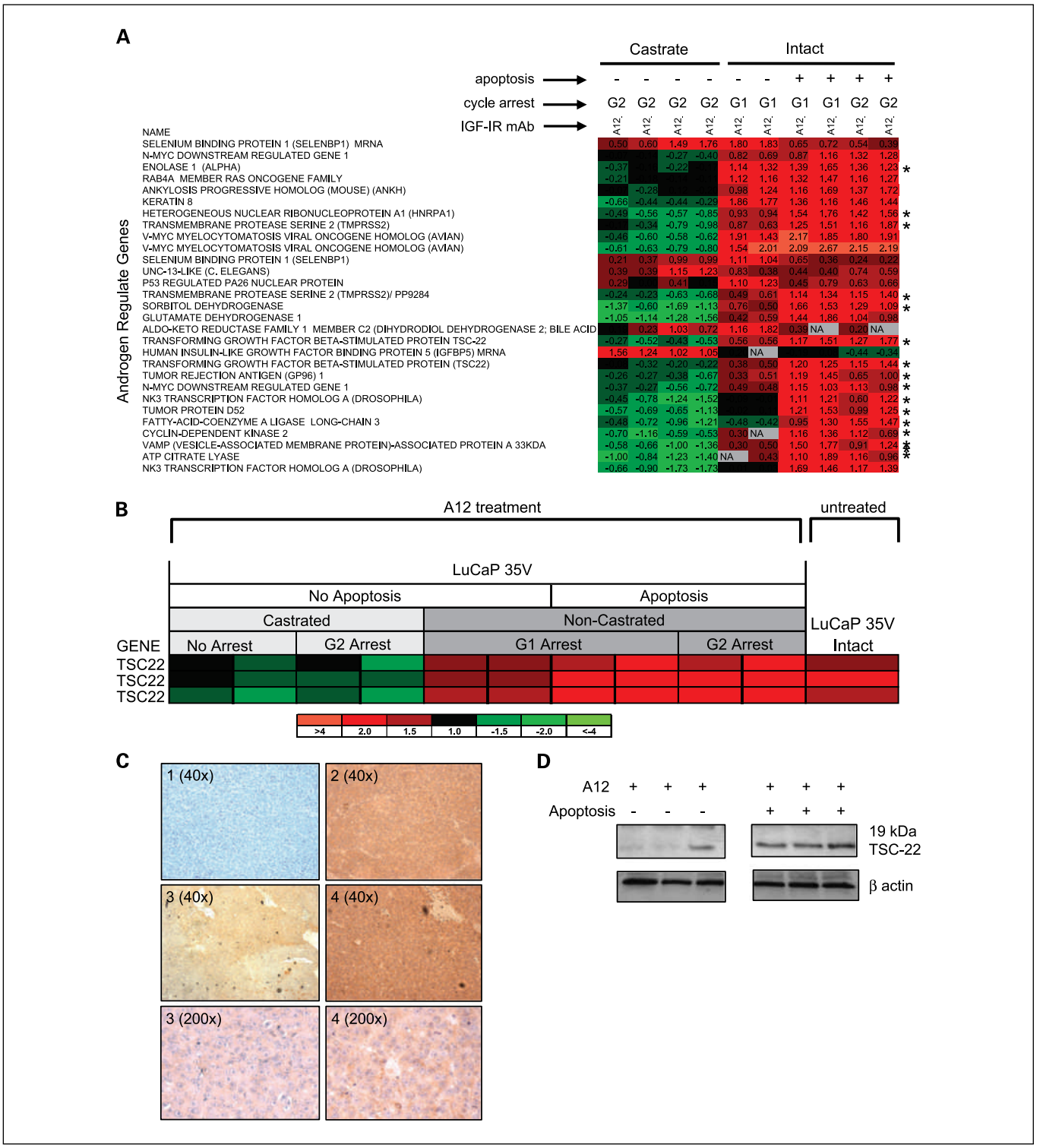

Fig. 2. *A,* cDNA microarray expression values of androgen-regulated genes differentially expressed in apoptotic LuCaP 35 V tumors relative to nonapoptotic tumors from both intact and castrate animals. There were 28 genes that changed in the same direction in each pool that were significantly different from each nonapoptotic pool as well as had a false discovery rate of <1%. Identical gene listings (such as TSC-22) indicate that different areas of the sequence were spotted on the array. As expected, most androgen-regulated genes were increased in the intact versus castrate tumors; however, an additional set was increased in those tumors treated with A12 in which apoptosis occurred. *, $P < 0.05$, apoptosis versus no apoptosis. *B,* results of microarray data for TSC-22 including LuCaP 35 V xenografts grown in intact mice. TSC-22 is increased in the xenografts grown in intact mice when compared with castrate mice and TSC-22 expression is increased even further when A12 is added ($P < 0.05$). *C,* immunohistochemistry for TSC-22 protein in representative LuCaP 35 V xenografts. 1, negative control with TSC-22 antibody preabsorbed with TSC-22 protein; 2, untreated intact mouse; 3, A12-treated castrate mouse; 4, A12-treated intact mouse. Note the increase in staining for TSC-22 in tumors from intact mice (*2* and *4*) compared with castrate mice (*3*; magnification, ×40). A representative higher-magnification image (×200) is shown for the tumors from intact mice showing positive cytoplasmic staining for TSC-22 compared with castrate host tumors, which have weak staining. *D,* Western blot of levels of TSC-22 in apoptotic LuCaP 35 V tumors versus nonapoptotic LuCaP 35 V tumors from intact mice. β-Actin was used as a loading control.

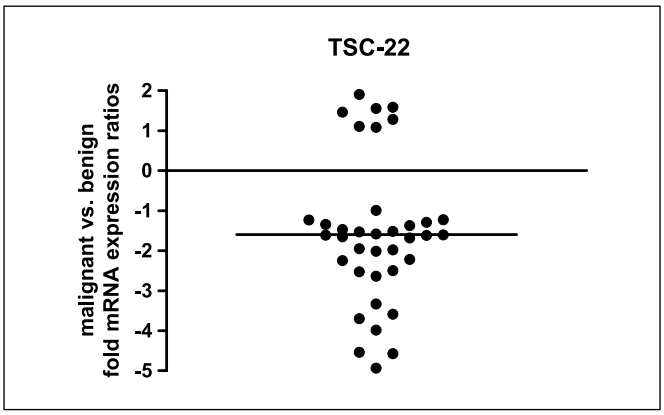

Fig. 3. TSC-22 expression in malignant human prostate glands. Matched benign and malignant glands were laser capture–microdissected from 37 prostate cancer patients and analyzed by cDNA microarray analysis for TSC-22 expression. TSC-22 was significantly downregulated in 30 of 37 glands ($P < 0.0001$).

1×10^6 cells from the single-cell suspension were fixed with 10% neutral buffered formalin followed by 70% ethanol alcohol at -20°C for 30 min. After several washes, cells were permeabilized with 0.1% Triton X-100 and incubated with FITC-conjugated dUTP and terminal deoxynucleotidyl transferase enzyme at 37°C for 1 h followed by an incubation with a propidium iodide/RNase buffer (100 μg/mL propidium iodide and 50 μg/mL RNase) at room temperature for 60 min. Cell cycle was determined by staining separate cell aliquots with propidium iodide as described previously (1). Samples were analyzed by flow cytometry using a BD FACScan (BD Bioscience). Data were analyzed with CellQuest^{PRO} software. Apoptosis was also measured via Western blots using antibodies against the intact and cleaved forms of poly(ADP-ribose) polymerase and caspase-3 and -7 (Cell Signaling Technology). The presence of cleavage products with a concomitant decrease in levels of intact protein for any of these three proteins indicates apoptosis has occurred.

Cell proliferation assay. Cells were seeded in a 96-well plate at 2,500 per well in RPMI T&S for 24 h before addition of 1 or 5 ng/mL TGF-β, 10^{-8} DHT, 20 ng/mL IGF-I, 40 μg/mL A12, DHT + IGF, DHT + A12, IGF + A12, or DHT + IGF + A12. When A12 was used, it was added 1 h before addition of other factors. Proliferation was quantified after 72 h by a colormetric MTS tetrazolium (MTT) assay using the Cell Titer 96 AQ_{queous} kit (Promega) according to the manufacturer's protocol. Eight replicates were done in each experiment and each experiment was done three times.

Real-time PCR. M12, PC3, and LNCaP C4-2 cells were treated with IGF-I (1, 10, and 50 ng/mL), DHT, and A12 (40 μg/mL) for 3 h. Then, RNA was collected and real-time PCR was done on an Applied Biosystems 7900HT Fast Real-time PR System using ABI SYBR Green 2× MasterMix (ABI). Primers used were IGF-IR forward (5′-GAAGTGGAACCCTCCCTCTC-3′), IGF-IR reverse (5′-CTTCTCGGCTTCAGTTTTGG-3′), TSC-22 forward (5′-GAAATGTTGTCCACAAGAGTGTC-3′), and TSC-22 reverse (5′-TGCTGAGGAGACATTCGGCTG-3′).

Results

Growth and prostate-specific antigen levels of LuCaP 35 V tumors in castrate and noncastrate mice. A12 treatment significantly reduced tumor volume and prostate-specific antigen levels of LuCaP 35 V tumors grown in noncastrate animals

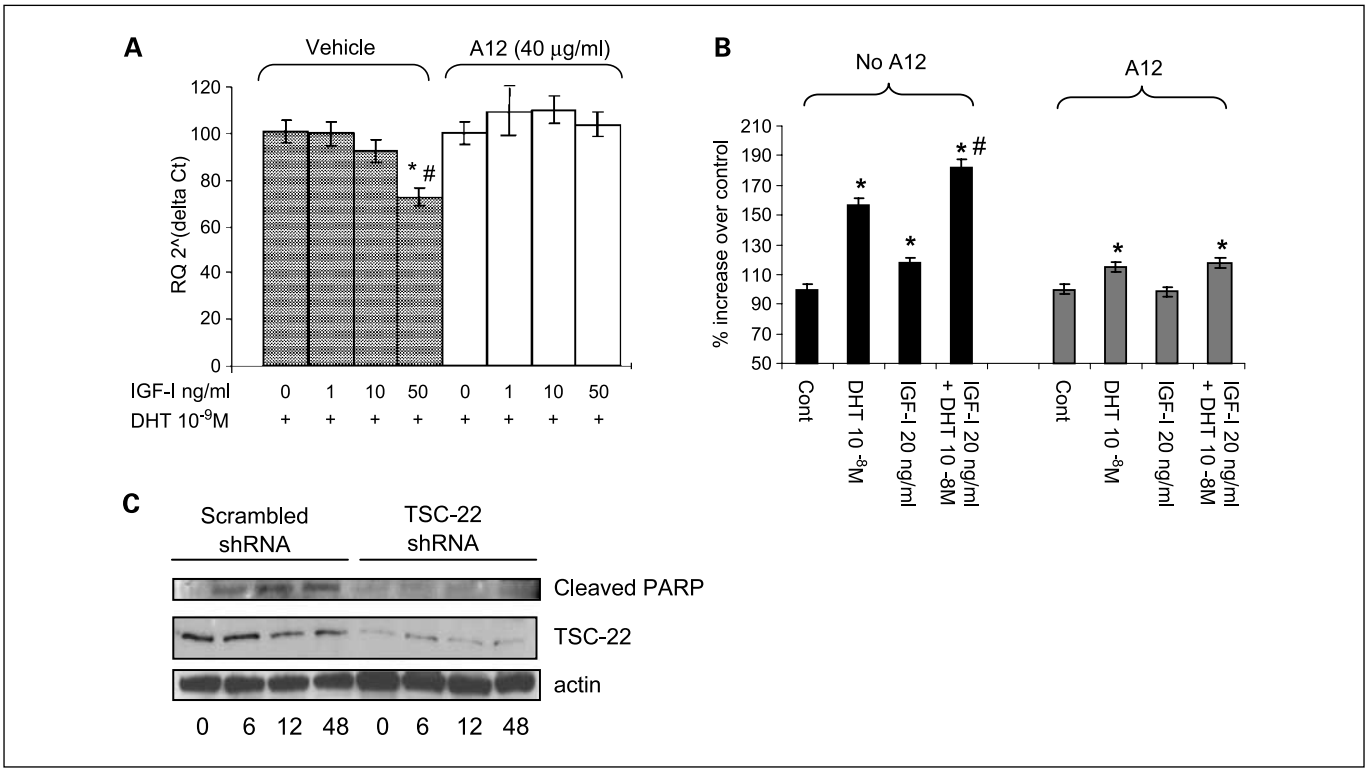

Fig. 4. *A,* quantitative real-time PCR of TSC-22 in LNCaP C4-2 cells treated with IGF-I and DHT and A12. Note that IGF-I decreases TSC-22 mRNA levels (*, $P < 0.05$ versus 0 or 1 ng IGF-I) and the addition of A12 inhibits this decrease (#, $P < 0.01$ versus non–A12-treated cells ± SE). *B,* proliferation assay on LNCaP cells treated as indicated in medium containing 5% charcoal-stripped serum. Note the marked enhancement of proliferation with IGF-I and DHT consistent with DHT increasing IGF-IR expression. Effects of DHT and IGF-I are blocked by A12. *, $P < 0.05$, compared with control; #, $P < 0.05$, IGF + DHT compared with DHT or IGF alone. *C,* knockdown of TSC-22 with RNA interference inhibits A12 induced apoptosis. Significant poly(ADP-ribose) polymerase (*PARP*) cleavage occurred in the control (scrambled RNA interference) but occurred minimally in the TSC-22 RNA interference–transfected cells following A12 treatment.

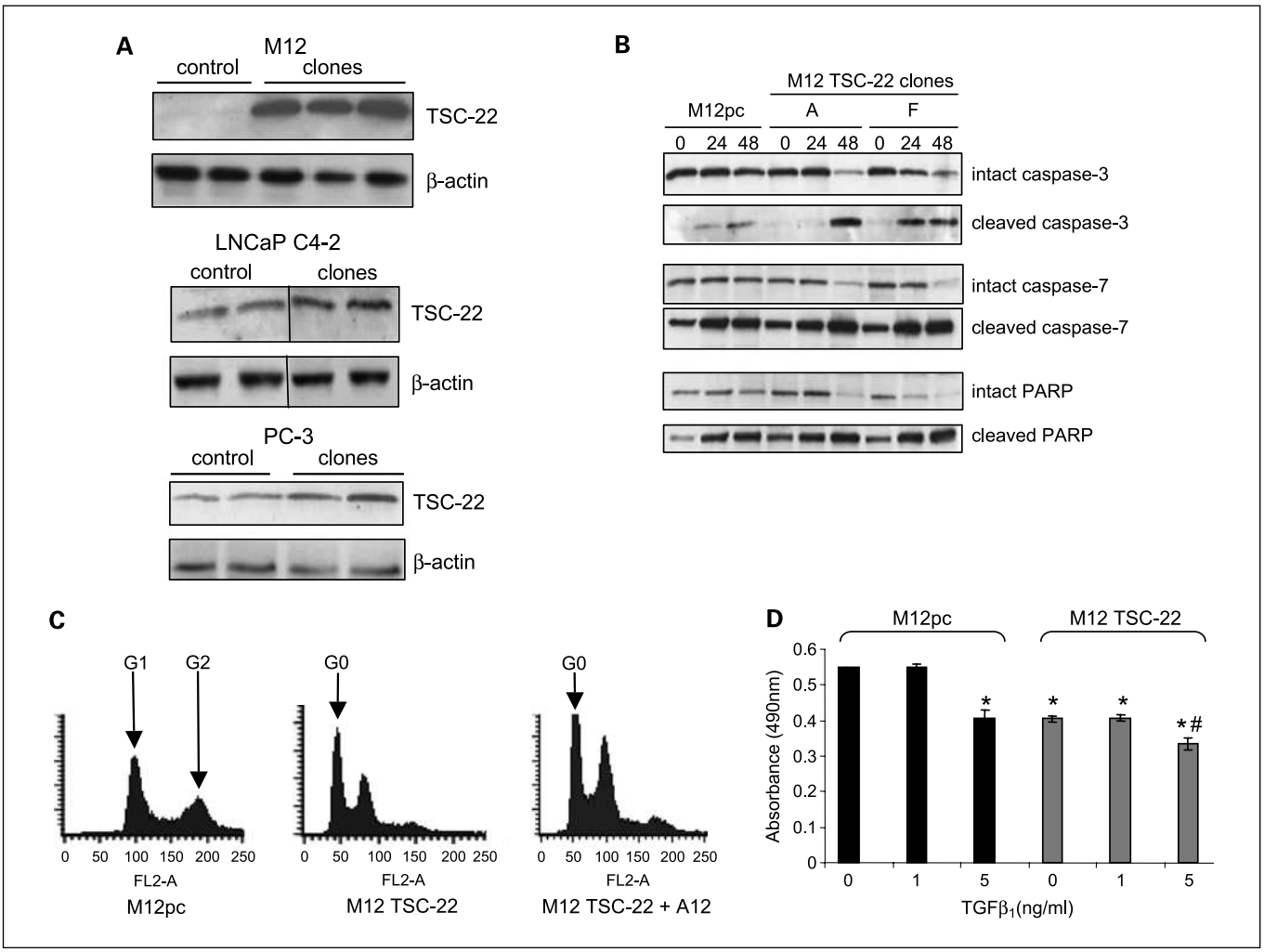

Fig. 5. *A,* Western blot of TSC-22 expression in M12, LNCaP C4-2, and PC-3 cells transfected with TSC-22 compared with empty vector controls. Clones of the indicated cell lines expressing TSC-22 are shown. β-Actin is the loading control. *B,* representative Western blots of caspase-3 and -7 and poly(ADP-ribose) polymerase showing increased cleavage of all three proteins over a 48-h period of culture treatment with TGF-β. Note that an increase in cleavage of these proteins with a concomitant decrease in intact protein is associated with apoptosis. *C,* flow cytometry showing a sub-G_0 peak, indicating apoptosis, in the cells overexpressing TSC-22 (± A12). *D,* MTT assay showing the decreased proliferation of cells overexpressing TSC-22 compared with control cells as well as in response to TGF-β. *, $P < 0.01$ versus M12pc control; #, $P < 0.05$ versus M12 TSC-22 control.

($P < 0.01$; Fig. 1A and B). Further, LuCaP 35 V tumor volumes were significantly lower in the A12-treated intact mice than in the A12-treated castrate mice ($P < 0.05$; Fig. 1A). This decrease in tumor volume was accompanied by a significant decrease in serum prostate-specific antigen in the treated intact mice compared with the treated castrate mice ($P < 0.05$; Fig. 1B).

Cell cycle and apoptosis in xenografts. In contrast to the studies in castrate animals in which LuCaP 35 V animals treated with A12 had smaller tumors due to an arrest in G_2, 60% of the LuCaP 35 V tumors treated with A12 in intact animals underwent both apoptosis and cell cycle arrest, either G_1 or G_2 (Fig. 1C-F).

Transcriptional program of LuCaP 35 V tumors treated with A12. To identify factors that may be responsible for apoptosis, we examined those androgen-regulated genes that were differentially regulated in tumors undergoing apoptosis versus non-apoptotic tumors from either intact or castrate mice and their regulation in each set of animals by A12 (Fig. 2A). In the intact group that underwent apoptosis, A12 elicited a significant increase in several androgen-regulated genes, including TSC-22, which is of particular interest because it has been associated with the induction of apoptosis and it is a potential tumor suppressor gene for salivary, glial, and prostate cancers (4–7, 9, 20, 21). As would be expected for an androgen-induced gene, TSC-22 mRNA levels were significantly higher in xenografts grown in intact mice (both treated and untreated) compared with xenografts grown in treated castrate mice ($P < 0.01$); mean mRNA levels of TSC-22 in xenografts from treated intact mice were also higher than those from the untreated intact mice ($P < 0.05$; Fig. 2B). Immunohistochemistry on tumors showed a decrease in TSC-22 levels in the castrate hosts compared with intact hosts (Fig. 2C). Using Western blot, we then showed an increase in TSC-22 protein levels for tumors that underwent apoptosis following A12 treatment (Fig. 2D).

TSC-22 expression in benign and malignant human prostate glands. To determine the clinical relevance of TSC-22 in prostate cancer, we examined laser capture–dissected prostate RNA from 37 patients with prostate cancer (Gleason 6-10; ref. 22). Benign and malignant glands were dissected from each individual, so each gland served as its own control. Amplified cDNA made from the RNA was then examined by cDNA microarray analysis

as described in Materials and Methods. Analysis of TSC-22 showed a significant decrease in mRNA expression compared with normal tissue in 30 of 37 glands ($P < 0.0001$; Fig. 3). This finding is consistent with a recent report using immunohistochemistry showing that TSC-22 protein was also significantly decreased in malignant versus benign prostate epithelium (10).

In vitro *effects of TSC-22 in the M12, LNCaP C4-2, and PC-3 human prostate cancer cell lines.* Because TSC-22 is an androgen-regulated and potentially an IGF-IR negatively regulated gene, we treated the androgen receptor–positive LNCaP C4-2 cell line with both DHT and IGF-I and then exposed the cells to either A12 or IgG. DHT exposure significantly increases levels of IGF-IR in androgen receptor–positive prostate cancer cells, including the LNCaP cell lines, but has no effect in androgen receptor–negative lines such as PC3 (23, 24). In LNCaP C4-2 cells grown in the absence of androgen, TSC-22 is detectable, but levels are markedly lower than in cells grown in the presence of androgen. Real-time PCR showed a significant decrease in the mRNA levels of TSC-22 following IGF-I treatment and this decrease was blocked by the addition of A12 (Fig. 4A). Proliferation assays on these cells following treatment with DHT and A12 showed that A12 blocked the DHT and DHT + IGF-I induced increase in proliferation (Fig. 4B). Finally, when we used small hairpin RNAs to knockdown TSC-22 levels in the LNCaP C4-2 cells, we saw decreased apoptosis following DHT + A12 treatment (Fig. 4C). Thus, the *in vitro* data with the androgen receptor–positive LNCaP C4-2 line reflected what we observed with the LuCaP 35 V xenografts *in vivo*. For the two lines that do not express an androgen receptor, M12 and PC3, no TSC-22 to very little was detected with PCR or Western blot and levels were not altered by exposure to DHT, IGF-I, or A12 (data not shown); because both of these lines are androgen receptor–negative and are poorly responsive to exogenous IGF-I, these results were expected.

Because TSC-22 expression has been associated with increased apoptosis in other cancers, we overexpressed TSC-22 in the M12, LNCaP C4-2, and PC-3 cell lines (Fig. 5A) and then evaluated the effect of increased expression of TSC-22 on response to A12 and TGF-β treatment. Elevated expression of TSC-22 increased apoptosis in response to A12 and TGF-β treatment as shown by the significantly increased amount of cleaved caspase-3 and -7 and poly(ADP-ribose) polymerase and decreased levels of intact protein ($P \leq 0.01$; Fig. 5B) and by flow cytometry (Fig. 5C). Further, all of the cell lines overexpressing TSC-22 had significantly decreased cell proliferation ($P < 0.05$; Fig. 5D).

In vivo *tumorigenicity of the M12 TSC-22 cells.* To assess the effect of TSC-22 expression on tumorigenicity of prostate cancer cells, we injected male athymic nude mice subcutaneously with either 1×10^6 empty vector control M12 cells (M12pc) or the stably transfected M12 TSC-22 cells. Seven weeks post-injection, 4 of 10 animals (40%) injected with M12 TSC-22 cells had developed tumors compared with 8 of 10 animals (80%) injected with M12pc cells. Further, the tumors in the TSC-22–injected animals were significantly smaller than those in the animals injected with the control cells ($P < 0.001$; Fig. 6).

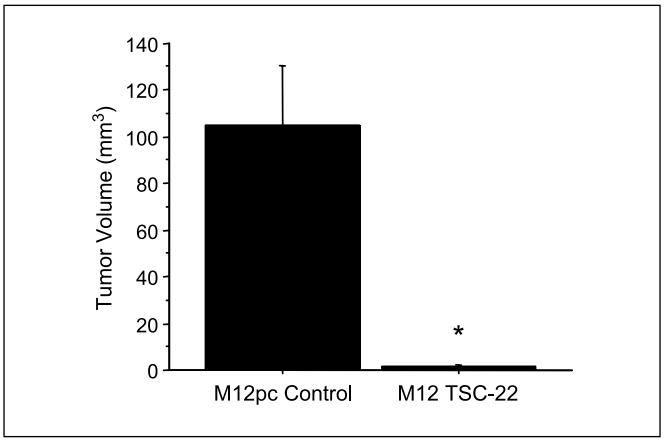

Fig. 6. Comparison of average tumor volume 7 wk after subcutaneous injection of either M12pc control cells or M12 TSC-22 cells into male athymic nude mice ($P < 0.001$).

Discussion

Therapy directed toward inhibition of IGF-IR is currently in clinical trials for several malignancies. Preclinical data suggest that it may be a successful adjunctive therapy for solid tumors, including prostate cancer (1–3). In preclinical prostate xenograft studies, we have shown that when the fully human monoclonal IGF-IR antibody A12 is used as a single-agent therapy, the response to IGF-IR inhibition differs depending on whether the tumor is androgen-dependent (grown in an intact host) or androgen-independent (grown in a castrate host; refs. 1, 3). In this study, to determine if it was the innate change in the tumor as it proceeded from androgen-dependent to androgen-independent or the decrease in androgens resulting from castration that accounted for the difference in response to A12, we grew the castrate-resistant LuCaP 35 V xenograft in an intact host and showed that the xenograft underwent apoptosis when exposed to A12. These data suggest that genes regulated by the androgen receptor–driven transcription program, in some fashion, sensitize the cells to undergo apoptosis after inhibition of the IGF-IR.

The first of these potential genes is the IGF-IR itself. Others and we have shown that the IGF-IR is increased in prostate cancer cells by activation of the androgen receptor (1, 23, 24). However, there is no evidence that the level of androgen receptor in and of itself determines whether a cell will undergo apoptosis versus cell cycle arrest. Rather, these data suggest that the presence of higher levels of androgen in the intact mice makes the cells more sensitive to IGF-IR inhibition and thus to apoptosis. Based on the results of the microarray data, several candidate genes that are known to be associated with tumor suppression, including TSC-22, were upregulated in the tumors undergoing apoptosis (8). Thus, TSC-22 is likely part of a group of factors responsible for the effects described in this article.

TSC-22 has been associated with cellular differentiation, shown to be associated with apoptosis in head and neck epithelial cancers, and to act as a transcription repressor in hepatocellular and lymphoid tumors (5, 20, 25–27). TSC-22 was first identified in prostate cancer as a gene that was upregulated in response to thiazolidinediones in primary prostate cancer cultures (9). Rentsch et al. then showed a decrease in TSC-22 protein expression in human prostate cancer (10). In this study, we have shown a decrease in TSC-22 transcripts in laser capture–microdissected prostate cancer compared with normal epithelium from the same gland.

Nelson et al. first showed that TSC-22 was a gene that was significantly increased by androgens in the prostate epithelium (8). In this study, we show that TSC-22 is increased in the LuCaP 35 V xenografts by androgen and further increased by the addition of the human monoclonal IGF-IR antibody A12. Further, we present *in vitro* data showing that TSC-22 is negatively regulated by IGF-I at the mRNA level and that addition of A12 blocks this decrease. *In vivo*, the increase in TSC-22 was greatest in those xenografts where apoptosis was clearly evident, suggesting that TSC-22 can induce an apoptotic response in prostate cancer similar to that seen in other tumors. We confirmed this finding *in vitro* by showing a decrease in apoptosis in LNCaP cells expressing a TSC-22 small hairpin RNA and an increase in apoptosis following A12 treatment in three human prostate cancer cell lines transfected with TSC-22 expression plasmids. TSC-22 expression also decreased *in vitro* proliferation of these prostate cancer cell lines and decreased *in vivo* tumorigenicity of the M12 TSC-22 cells compared with the M12pc control cells. These results support the role of TSC-22 as an androgen and potentially IGF-IR–regulated tumor suppressor in prostate.

This study shows that an increase in TSC-22 expression is part of the mechanism by which IGF-IR inhibition in prostate cancer xenografts induces apoptosis. It further indicates that inhibition of IGF-IR as a therapeutic strategy may be more effective in the presence of androgen or in androgen-dependent disease rather than in the castrate patient with androgen-independent disease.

Disclosure of Potential Conflicts of Interest

No potential conflicts of interest were disclosed.

Acknowledgments

We thank Holly Nguyen for her assistance with the animal work.

References

1. Wu JD, Odman A, Higgins LM, et al. *In vivo* effects of the human type I insulin-like growth factor receptor antibody A12 on androgen-dependent and androgen-independent xenograft human prostate tumors. Clin Cancer Res 2005;11:3065–74.
2. Rowinsky EK, Youssoufian H, Tonra JR, Solomon P, Burtrum D, Ludwig DL. IMC-A12, a human IgG1 monoclonal antibody to the insulin-like growth factor I receptor. Clin Cancer Res 2007; 13:5549–55s.
3. Plymate SR, Haugk K, Coleman I, et al. An antibody targeting the type I insulin-like growth factor receptor enhances the castration-induced response in androgen-dependent prostate cancer. Clin Cancer Res 2007;13:6429–39.
4. Choi SJ, Moon JH, Ahn YW, Ahn JH, Kim DU, Han TH. Tsc-22 enhances TGF-β signaling by associating with Smad4 and induces erythroid cell differentiation. Mol Cell Biochem 2005;271:23–8.
5. Shostak KO, Dmitrenko VV, Garifulin OM, et al. Downregulation of putative tumor suppressor gene TSC-22 in human brain tumors. J Surg Oncol 2003;82:57–64.
6. Gupta RA, Sarraf P, Brockman JA, et al. Peroxisome proliferator-activated receptor γ and transforming growth factor-β pathways inhibit intestinal epithelial cell growth by regulating levels of TSC-22. J Biol Chem 2003;278:7431–8.
7. Nakashiro K, Kawamata H, Hino S, et al. Down-regulation of TSC-22 (transforming growth factor β-stimulated clone 22) markedly enhances the growth of a human salivary gland cancer cell line *in vitro* and *in vivo*. Cancer Res 1998;58:549–55.
8. Nelson P, Clegg N, Arnold H, et al. The program of androgen-responsive genes in neoplastic prostate epithelium. Proc Natl Acad Sci U S A 2002;99:11890–5.
9. Xu Y, Iyengar S, Roberts R, Shappell S, Peehl D. Primary culture model of peroxisome proliferator-activated receptor γ activity in prostate cancer cells. J Cell Physiol 2003;196:131–43.
10. Rentsch C, Cecchini M, Schwaninger R, et al. Differential expression of TGF β-stimulated clone 22 in normal prostate and prostate cancer. Int J Cancer 2006;118:899–906.
11. Corey E, Quinn J, Buhler K, et al. LuCaP 35: a new model of prostate cancer progression to androgen independence. Prostate 2003;55: 239–46.
12. Bae V, Jackson-Cook C, Maygarden S, Chen J, Plymate S, Ware J. Metastatic sublines of an SV40 large T antigen immortalized human prostate epithelial cell line. Prostate 1998;34: 275–82.
13. Plymate S, Tennant M, Birnbaum R, Thrasher J, Chatta G, Ware J. The effect of IGF system in human prostate epithelial cells of immortalization and transformation by simian virus-40 T antigen. J Clin Endocrinol Metab 1996;81:3709–16.
14. York T, Plymate S, Nelson P, Eaves L, Webb H, Ware J. cDNA microarray analysis identifies genes induced in common by peptide growth factors and androgen in human prostate epithelial cells. Mol Carcinog 2005;44:242–51.
15. Plymate S, Haugk K, Sprenger C, et al. Increased manganese superoxide dismutase (SOD-2) is part of the mechanism for prostate tumor suppression by mac25/insulin-like growth factor binding-protein-related protein-1. Oncogene 2003;22:1024–34.
16. Nelson P, Pritchard C, Abbott D, Clegg N. The human (PEDB) and mouse (mPEDB) prostate expression databases. Nucleic Acids Res 2002;30: 218–220.
17. Bonham M, Arnold H, Montgomery B, Nelson PS. Molecular effects of the herbal compound PC-SPES: identification of activity pathways in prostate carcinoma. Cancer Res 2002;62:3920–4.
18. Tusher VG, Tibshirani R, Chu G. Significance analysis of microarrays applied to the ionizing radiation response. Proc Natl Acad Sci U S A 2001;98:5116–21.
19. Oh Y, Muller H, Ng L, et al. Transforming growth factor-β-induced cell growth inhibition in human breast cancer cells is mediated through insulin-like growth factor-binding protein-3 action. J Biol Chem 1995;270:13589–92.
20. Kawamata H, Fujimori T, Imai Y. TSC-22 (TGF-β stimulated clone-22): a novel molecular target for differentiation-inducing therapy in salivary gland cancer. Curr Cancer Drug Targets 2004;4:521–9.
21. Uchida D, Kawamata H, Omotehara F, et al. Over-expression of TSC-22 (TGF-β stimulated clone-22) markedly enhances 5-fluorouracil-induced apoptosis in a human salivary gland cancer cell line. Lab Invest 2000;80:955–63.
22. True L, Coleman I, Hawley S, et al. A molecular correlate to the Gleason grading system for prostate adenocarcinoma. Proc Natl Acad Sci U S A 2006;103:10991–6.
23. Pandini G, Mineo R, Frasca F, et al. Androgens up-regulate the insulin-like growth factor-I receptor in prostate cancer cells. Cancer Res 2005;65: 1849–57.
24. Plymate S, Tennant M, Culp S, et al. Androgen receptor (AR) expression in AR-negative prostate cancer cells results in differential effects of DHT and IGF-I on proliferation and AR activity between localized and metastatic tumors. Prostate 2004;61:276–90.
25. Lu Y, Kitaura J, Oki T, et al. Identification of TSC-22 as a potential tumor suppressor that is upregulated by Flt3-835V but not Flt3-ITD. Leukemia 2007;21:2246–57.
26. Iida M, Anna CH, Gaskin ND, Walker NJ, Devereux TR. The putative tumor suppressor TSC-22 is downregulated early in chemically induced hepatocarcinogenesis and may be a suppressor of Gadd45b. Toxicol Sci 2007;99: 43–50.
27. Hino S, Kawamata H, Uchida D, et al. Nuclear translocation of TSC-22 (TGF-β-stimulated clone-22) concomitant with apoptosis: TSC-22 as a putative transcriptional regulator. Biochem Biophys Res Commun 2000;278: 659–64.